UNIVERSITÀ POLITECNICA DELLE MARCHE

ENGINEERING FACULTY

PhD Course in Information Engineering

Curriculum: Biomedical, Electronic and Telecommunication Engineering

ELECTROCARDIOGRAPHIC ALTERNANS: AUTOMATIC IDENTIFICATION AND CLINICAL SIGNIFICANCE

ALTERNANZA ELETTROCARDIOGRAFICA: IDENTIFICAZIONE AUTOMATICA E SIGNIFICATO CLINICO

Supervisor:
Prof. Laura Burattini

PhD Student:
Ilaria Marcantoni

Academic Year: 2019-2020

Abstract

Sudden cardiac death (SCD) is a serious public health problem, annually causing more than 4 million deaths in the world. Availability of reliable risk indexes of vulnerability to develop malignant cardiac events is fundamental, since they are among the principal causes of SCD. The electrocardiogram (ECG) is a noninvasive clinical measurement to evaluate heart health status. ECG alternans (ECGA) reflects an electrophysiological phenomenon manifesting as the ABAB fluctuation in morphology of one or more ECG waves, and thus it can manifest as P-wave alternans (PWA), QRS-complex alternans (QRSA), T-wave alternans (TWA). Aim of this PhD thesis is to provide insights on ECGA clinical role, evaluating its applicability as a cardiac risk index. The specific objective is to present the first automatic method to reliably identify and measure all ECGA forms. Many automatic methods detecting TWA exist. They investigated TWA in several cardiac diseases and define it as an index of ventricular electrical instabilities. TWA still lacks to be deeply investigated in non-cardiac pathologies and existent methods did not focus on all ECGA forms, but almost only on TWA. In this thesis work, two methods, the correlation method (CM) and the heart-rate adaptive match filter method (AMFM), have been updated for their application in ECGA analysis. CM relies on a non-conventional correlation index and AMFM relies on a strictly filtering around ECGA frequency. They were applied in several scenarios, also non-cardiac pathologies or non-pathologic conditions. A study performed by CM on TWA association with dofetilide drug assumption found out that TWA increases 6 h, 7 h and 8 h after administration, with values 6 times greater than before on average, suggesting a higher predisposition to dofetilide-induced arrhythmias. A study performed by AMFM on TWA association with epileptic seizures found out high TWA in proximity of them (before: 31 μV; during: 46 μV; after: 30 μV), suggesting a higher electrical instability that rises arrhythmia vulnerability. Other studies performed by AMFM analyzed TWA in the non-pathological fetal and preterm conditions. All non-pathological fetuses and preterm infants showed TWA (direct fetal ECG: 9 μV; indirect fetal ECG: 11 μV; preterm ECG: 26 μV). Also, in preterm infants, TWA appeared higher in very small infants and was related to the ratio of gestational age over birth weight (0.76, $p = 0.02$), suggesting that TWA is probably related to the state of incomplete development, as an indirect index of cardiac immaturity. Two case reports on patients with myocardial bridging and undergoing hemodialysis, respectively, analyzed all ECGA forms by the updated AMFM. In both cases, TWA was identified as the prevalent one. ECGA highly correlated with heart rate (0.72, $p<0.01$) in the patient with myocardial bridging, suggesting a higher risk condition, especially while practicing physical activity. ECGA was high before (51 μV) and during (53 μV) hemodialysis and decreased (28 μV) after the dialytic session, suggesting a lower risk condition after the treatment. In order to simultaneously identify and measure all forms of ECGA, avoiding their reciprocal influence, the enhanced AMFM (EAMFM) was developed. Thanks to the introduction of a signal enhancement procedure and of an ECGA area parameter, EAMFM provided reliable ECGA measurements in both simulated and experimental conditions: the highest error in simulation was 2%, while TWA was prevalent in heart failure patients with implanted cardioverter defibrillator for primary prevention (PWA area: 545 μV·ms; QRSA area: 762 μV·ms; TWA area: 1382 μV·ms). Thus, EAMFM may help determine incremental clinical utility of PWA and QRSA with respect to only TWA. Future studies are intended to fill in the gap between these scientific research findings and routine clinical care, possibly validating ECGA prognostic role in the prevention of SCD.

CONTENTS

INTRODUCTION

One of the most serious public health problems is sudden cardiac death (SCD) (*Chugh, 2017*). Annually, it accounts for an estimated 350,000 deaths in the United States, 700,000 deaths in Europe and more than 4 million deaths around the world (*Chugh, 2017*).

Sudden death is defined as the natural unexpected demise of a person not showing a prior condition that would seem fatal; the demise occurs within a short period of time, usually within one hour of the appearance of symptoms, if the person is assisted, or within one day of having been observed alive, if the person is not assisted. Sudden death usually has cardiac causes and, in case, is defined as SCD (*Gimeno-Blanes, 2016*).

SCD is mainly due to arrhythmias occurrence (e.g. ventricular tachycardia, ventricular fibrillation, or asystole); structural heart disease (e.g. congenital heart disease); dysfunction of the autonomic nervous system, which does not represent the primary death cause itself, but it can favor causes, like arrhythmias (*Gimeno-Blanes, 2016*). In order to prevent SCD, paradigms and methods have been implemented to stratify subjects in terms of their predisposition to develop malignant cardiac events. The prevention is made more difficult considering that not only patients suffering from coronary disease or cardiomyopathy experience SCD, but also people apparently healthy, without previous evident cardiac symptoms or without evident symptoms at all (*Gimeno-Blanes, 2016*).

Left ventricular ejection fraction is widely used to identify patients at high cardiac risk, but other noninvasive parameters have been proposed. Most of these noninvasive parameters are derived from the surface electrocardiogram (ECG). ECG is widely used in clinical applications to monitor the heart health status, for its noninvasiveness and reliability in reveling electrical cardiac functionality. Nevertheless, these parameters are often poorly used in clinical routine and the underlying reasons can be many. First of all, a unified opinion on the best parameter or on the best computational method still lack, secondly several of the proposed parameters depend on electrophysiological mechanism that are not completely known to permit an objective and reliable interpretation, and mostly, their prediction ability is not general. There is no universal cardiac risk index and the best choice may heavily depend on the specific pathology under study (*Gimeno-Blanes, 2016*).

In this scenario, aim of this PhD thesis is to provide more insights on an ECG risk marker that is the alternans. ECG alternans (ECGA) is an anomaly that can manifest on any wave of the ECG. Until now, existent methods are designed to investigate almost only ECGA manifesting on the ECG T wave. Nevertheless, it is not deeply understood still; so, its actual role should be investigated in a wide variety of scenarios, including also non-cardiac pathologies, in order to test its generalization of applicability as risk index. Therefore, in the thesis, ECGA is analyzed also in contexts that seem to be far from the strictly cardiac pertinence, e.g. in case of hemodialysis for kidney disfunctions, in case of epileptic seizures due to neurologic dysfunctions, in association with drug assumption and also in conditions that are non-pathologic, but in the same time tricky, specifically in case of prematurity or during birth.

Moreover, the specific objective of this PhD thesis is presenting a new automatic method for the evaluation of cardiac electrical instability through the ECGA, with a broad spectrum of

investigation on the heart in all its parts and in all its electric functional phases. This new method of analysis is specially designed to reliably identify and measure ECGA in all its possible forms (i.e. when affecting the ECG P wave, QRS complex or T wave). The method has the final purpose to strengthen the prognostic value of ECGA as an index of cardiac risk.

1

HEART: ELECTRICAL ACTIVITY

The heart is a specialized muscular organ, the central motor organ of the blood circulatory system, inside which it pushes blood throughout the blood vessels by its involuntary rhythmic contractions. The heart is placed in the central part of thoracic cavity, between the lungs; it is contained within a large sac, which is called pericardium. The heart has the shape of a cone, the base of which faces backwards and to the right and the apex of which looks forward and to the left, reaching the 5th intercostal space [a] in the adult, approximately 9 cm from the median sagittal plane [b]. Being a little flattened in an antero-posterior direction, the heart has both an anterior face, which is called sterno-costal face, and a posterior face, which is called diaphragmatic face; it also has a right margin, called acute margin, and a left margin, called obtuse margin. Internally, the heart is divided into two parts: the right one and the left one (*Castellucci, 2009; Klabunde, 2011*).

The cardiac cycle is the single period of the iterative activity of the heart. It consists of two phases: one during which the heart muscle relaxes and refills with blood, called diastole, the other following period during which the heart muscle contracts and pumps blood, called systole. The left heart rhythmically contracts pumping blood into the aorta (**Fig. 1.1**); then, the aorta branches repeatedly until it resolves into very small caliber and extremely thin-walled vessels, called blood capillaries. In correspondence with the blood capillaries, nutritional and gaseous exchanges with the tissues take place: blood releases oxygen to the surrounding tissues and charges itself with carbon dioxide. Then, from the blood capillaries, the veins originate. The veins converge gradually until they reach the right heart through the superior vena cava and the inferior vena cava (**Fig. 1.1**). The right heart rhythmically contracts pumping blood into the pulmonary artery (**Fig. 1.1**) that carries blood to the two lungs and within them gives rise to blood capillaries, where blood is

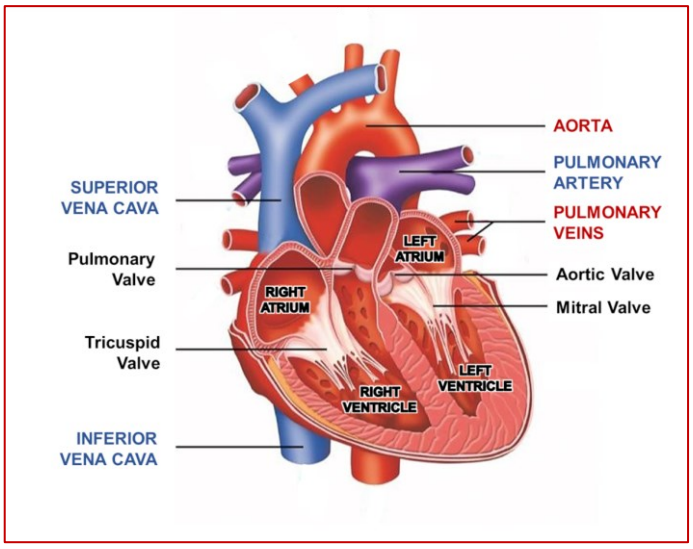

Figure 1.1. *The heart anatomy.*

a) 5th intercostal space: space between the 5th and 6th ribs.

b) median sagittal plane: in anatomy, plane through the midline of the body that divides the body or any of its parts into right and left halves. The others are the frontal plane (orthogonal to the median one, dividing the body into anterior and posterior halves) and the transversal plane (orthogonal to the other two planes, dividing the body into superior and inferior halves).

oxygenated. Blood returns to the left heart via the pulmonary veins (**Fig. 1.1**) and the cycle starts again (*Castellucci, 2009*).

Both the right and the left sides of the heart are divided in two cavities: an upper cavity, called atrium and a lower cavity, called ventricle (**Fig. 1.1**). The boundary between the two atria and the two ventricles is marked on the outer surface of the heart by a circular groove, called the coronary sulcus. The border between the two ventricles is also evident on the external surface of the heart by means of the anterior longitudinal (or interventricular) sulcus and the posterior longitudinal (or interventricular) sulcus, which run from the coronary sulcus to the apex of the heart on the sterno-costal face and on the diaphragmatic face, respectively (*Castellucci, 2009*). The right atrium and right ventricle are intercommunicating with each other through the right atrioventricular orifice, which is provided with the right atrioventricular valve, also called tricuspid valve (**Fig. 1.1**); the left atrium and left ventricle are also intercommunicating through the left atrioventricular orifice, which is provided with the left atrioventricular valve, also called bicuspid valve or mitral valve (**Fig. 1.1**). The two atrioventricular valves are open during the diastole of the ventricles to allow the flow of blood from the atria into the ventricles, but they close during the systole of the ventricles to prevent the reflux of blood into the atria.

The veins arrive at the atria, the arteries depart from the ventricles, in particular the pulmonary artery from the right ventricle and the aorta from the left ventricle. The orifices of the veins in the atria lack valves or, if they exist, they are insufficient, while each of the two arterial orifices is provided with the so-called semilunar valves. Each of these two valves (one for the pulmonary artery and one for the aorta) consists of three valve flaps (**Fig. 1.1**). The semilunar valves open during systole of the ventricles to allow the passage of blood from the ventricles into the arteries, while they close in the diastole of the ventricles to prevent the reflux of blood from the arteries into the ventricles (*Castellucci, 2009*).

Between the two right cavities and the two left cavities of the heart there is no way of communication with the impossibility of blood exchange. In fact, the two right cavities are separated from the two left cavities by means of the so-called partition of the heart, constituted above by the interatrial septum, which separates the two atria, and below by the interventricular septum, which separates the two ventricles from each other (*Castellucci, 2009*). In the right cavities of the heart there is venous blood (i.e. rich in carbon dioxide) while the left cavities contain arterial blood (i.e. rich in oxygen) (*Castellucci, 2009*).

Mechanical contraction of the heart occurs thanks to the cardiac electrical system. It is a tissue that creates and conducts an electrical impulse from the atria to the ventricles, thus creating the contraction suitable for perfusing the entire body with blood. It consists of the sinoatrial node, which is an autonomous pacemaker, the atrioventricular node, which slows electrical conduction, and the bundle of His, which spreads the impulse to the ventricles. In turn, electrical function of the heart is regulated by a system of autonomic innervation. The heart is innervated by parasympathetic and sympathetic efferent fibers. The right vagus nerve innervates the sinoatrial node and the left vagus nerve innervates the atrioventricular node. Vagal efferent nerves innervate atrial myocardium and slightly ventricular myocardium. Vagal action consists in decreasing the heart rate, of the conduction velocity and of cardiac inotropy [c].

c) cardiac inotropy: cardiac contractility.

Indeed, increased activity of the parasympathetic nervous system reduces sinoatrial nodal firing and slows atrioventricular nodal conduction. Under normal resting conditions, the neurons afferent to the parasympathetic nervous system are active, producing the so-called "vagal tone" on the cardiac muscle, resulting in resting heart rates. Sympathetic efferent nerves innervate both the atria, especially the sinoatrial node, and the ventricles, together with the conduction system of the heart. Sympathetic action consists in the increasing of the heart rate, of the conduction velocity and of inotropy. Indeed, increased activity of the sympathetic nervous system produces cardiac stimulation and systemic vasoconstriction. Sympathetic denervation of the heart and systemic blood vessels usually results in cardiac slowing and systemic vasodilation. At low resting heart rates, the effects of sympathetic denervation on the heart rate are relatively low because the heart is under a high level of vagal tone and relatively weak sympathetic tone. Normally, there is reciprocal activation of the sympathetic and parasympathetic systems: from their synergic interaction depends the heart rate variability that in a healthy heart allows to respond to the physiological needs related to the person's condition (e.g. rest, exercise, psychology attention, anxiety). Thus, a balance between sympathetic and parasympathetic systems is essential for the regulation of cardiac electrical function. The heart and the arteries departing from it have vagal and sympathetic afferent nerve fibers. They carry information from stretch and pain receptors. The former act in feedback regulation of blood volume and arterial pressure, while the last cause chest pain when activated during myocardial ischemia (*Klabunde, 2011*).

1.1 Cardiac Electrical System: From the Cell Membrane Potential to the Conduction System

The heart pumping action is triggered and controlled by electrical changes within the cardiac myocytes across cell membrane; these changes generate an electrical signal that is called action potential. The action potential is generated by the cells of the sinoatrial node, located in the right atrium (posterior wall), spreads across the atria and reaches the conduction system. The conduction system (formed by the His bundle, the bundle branches and the Purkinje fibers), in turn, triggers the ventricles.

Cell membrane potentials

Cardiac cells, commonly to the other living body cells, are characterized by an electrical potential across the cell membrane. Conventionally, the potential of the outside of the cell is assumed 0 mV. The resting membrane potential is the electrical potential inside the cell relative to the outside of a resting cell. It is caused by the concentration of positively and negatively charged ions across the cell membrane, by the relative permeability of the cell membrane to the ions and by the ionic pumps transporting ions across the cell membrane. In case of a ventricular myocyte, the resting membrane potential is about -90 mV (*Klabunde, 2011*).

The myocyte membrane potential is mostly determined by concentrations of sodium (Na^+), potassium (K^+) and calcium (Ca^{++}), **Table 1.1.1**. Chloride ions are also present inside and outside the cell, but their influence on the resting membrane potential is quite negligible; whereas, among Na^+, K^+ and Ca^{++}, K^+ is the ion that most affects it. In heart cells, K^+ concentration is high inside and low outside. Therefore, the chemical gradient [(d)] of K^+ drives it to diffuse out of the cell. On the

Table 1.1.1. *Concentrations of K^+, Na^+, and Ca^{++} inside and outside a cardiac myocyte at a resting membrane potential of −90 mV.*

Ion	Inside (mM)	Outside (mM)
K^+	150	4
Na^+	20	145
Ca^{++}	0.0001	2.5

opposite, Na^+ and Ca^{++} concentrations are low inside and high outside the cell and their chemical gradients drive them to diffuse inside the cell. The chemical gradient across the cell membrane for the ions are regulated by the activity of energy-dependent ionic pumps, the sodium-calcium exchanger and the presence of negatively charged proteins within the cell that influences the passive distribution of cations and anions (*Klabunde, 2011*).

Considering the simplified model in which K^+ is the only ion across the membrane but the negatively charged proteins inside the cell, K^+ diffuses outside the cell following its chemical gradient, leaving negative charge inside. In this situation, a separation of charges (negative inside and positive outside the cell) happens determining a potential difference across the cell membrane. The membrane potential to oppose the K^+ outward diffusion is called equilibrium [e] or Nernst potential for K^+ (E_K) and at 37 °C it is as follows:

$$E_K = -61 \log \frac{[K^+]_i}{[K^+]_o} = -96\ mV \qquad (1)$$

where $[K^+]_i$ is the K^+ concentration inside, $[K^+]_o$ is the K^+ concentration outside (**Table 1.1.1**) and -61 is given by RT/zF, where R is the gas constant, z is the number of ion charges [f], F is Faraday constant and T is the temperature expressed in °K. Therefore, if the outside K^+ concentration increased, E_K would be lower, i.e. less negative. The resting membrane potential for a ventricular myocyte is less negative than E_K, but near E_K. Thus, a small net electrochemical force (resulting in +6 mV) drives the diffusion of K^+ out of the cell. Moreover, at rest, the permeability of the membrane to K^+ is finite, so the diffusion of K^+ out of the cell is slow (*Klabunde, 2011*).

K^+ is not the only ion to determine the heart-cell membrane potential: Na^+ ions have an important role. Contrary to K^+, Na^+ concentration is lower inside the cell than outside and its diffusion is driven inward the cell. In order to balance Na^+ inward diffusion, a large positive charge inside the cell is necessary. The membrane potential to oppose the Na^+ inward diffusion is the equilibrium or Nernst potential for Na^+ (E_{Na}) and at 37°C it is as follows:

$$E_{Na} = -61 \log \frac{[Na^+]_i}{[Na^+]_o} = +52\ mV \qquad (2)$$

where $[Na^+]_i$ is the Na^+ concentration inside, $[Na^+]_o$ is the Na^+ concentration outside (**Table 1.1.1**). The resting membrane potential for a ventricular myocyte is very negative, far from E_{Na}. Thus, a large net electrochemical force (resulting in -142 mV) drives the diffusion of Na^+ into the cell. However, at rest, the permeability of the membrane to Na^+ is so low that the diffusion of Na^+ into the cell is limited (*Klabunde, 2011*).

The resting membrane potential is near to E_K and quite far from E_{Na} and from the equilibrium or Nernst potential for Ca^{++} (E_{Ca}). This reflects not only the concentration gradients of ions across the cell (i.e. their equilibrium potentials), but also the selective

d) chemical gradient: concentration difference.

e) equilibrium potential: potential difference across the membrane required to keep the concentration gradient across the membrane.

f) z: 1 for monovalent ions (e.g. K^+, Na^+), 2 for divalent ions (e.g. Ca^{++}).

permeability of the membrane to these ions. Indeed, the cell membrane, at rest, is much more permeable to K^+ than Na^+ or Ca^{++}. Consequently, Na^+ and Ca^{++} have reduced contributions to determining the resting membrane potential (*Klabunde, 2011*).

Membrane potential is determined by the balance of ionic concentration gradients across the membrane. The maintenance of this balance involves energy expenditure, through adenosine triphosphate (ATP) hydrolysis, together with ionic pumps: an energy-dependent pump system in the sarcolemma [g] pumps Na^+ and Ca^{++} out and K^+ into the cardiac cell. Regular activity of these pumps is fundamental to maintain Na^+ and K^+ concentrations inside the cell. If the pump activity stops or is inhibited, Na^+ concentration rises and K^+ concentration decreases inside the cell, resulting in a more depolarized resting membrane potential. Moreover, the pumps are electrogenic, since they force out three Na^+ for every K^+ getting in the cell. Thus, more positive charges come out than those that enter the cell and the energy-dependent pump system determines a negative potential in the cardiac cell, termed electrogenic potential that may be up to -10 mV, according to the activity level of the pump. Ca^{++} concentration gradient, like Na^+ and K^+ ones, needs to be maintained. This is possible thanks to: an ATP-dependent Ca^{++} pump that actively pumps Ca^{++} outside the cell, generating a slight negative electrogenic potential, and the sodium-calcium exchanger, through which Na^+ and Ca^{++} are carried in opposite directions across the membrane. This exchanger can act in either direction across the sarcolemma according to the membrane potential. In resting cardiac cells, the negative membrane potential provokes three Na^+ ions to get in the cell for each Ca^{++} ion getting out the cell. This results in a slight electrogenic potential (few millivolts) inside the cell. The contrary occurs if the cardiac cell depolarizes. This exchanger is also affected by Na^+ concentration changes, as in case the function of the pump system is decreased by drug assumption (*Klabunde, 2011*).

The movement of ions across the cell membrane occurs through specialized ion channels (**Table 1.1.2**) present in the phospholipid bilayer of the cell membrane. These channels are made up of large polypeptide chains that create an aperture passing through the cell membrane. Ions are enabled or inhibited to transverse according to conformational changes in the proteins of the ion channel that alter its shape. Ion channels are selective for several cations and anions, as K^+, Na^+, Ca^{++}. Moreover, an ion may have different types of channels managing its movement across the cell membrane. Two types of ion channels exist: voltage-gated and receptor-gated ones. The voltage-gated channels enable and inhibit following changes in membrane potential. Several Na^+, K^+ and Ca^{++} channels involved in cardiac electrical function are voltage gated. The receptor-gated channels enable and inhibit following chemical signals acting through membrane receptors. An example of these chemical signals is acetylcholine, a neurotransmitter released by the vagus nerves innervating the heart: acetylcholine binds to a receptor of the cell membrane and in turn the receptor enables particular types of K^+ channels. An example of voltage-gated channels is the fast Na^+ channel. At a normal resting membrane potential, Na^+ channel inhibits the passing of ions. Particularly, in this configuration, the Na^+ activation gate is closed, while the inactivation gate is open. These gates are polypeptides present in the

g) sarcolemma: membrane that surrounds the muscle cells.

Table 1.1.2. *Ion channels of cardiac cells (Klabunde, 2011).*

Ion	Channel	Gating	Characteristics/Interested Cells
Na^+	Fast Na^+	Voltage	myocytes
	Fast Na^+	Voltage and receptor	sinoatrial and atrioventricular nodal cells
Ca^{++}	L-type	Voltage	Slow inward, long-lasting current; myocytes and sinoatrial and atrioventricular nodal cells
	T-type	Voltage	Transient current; sinoatrial and atrioventricular nodal cells
K^+	Inward rectifier	Voltage	closes with depolarization
	Transient outward	Voltage	myocytes
	Delayed rectifier	Voltage	repolarization
	ATP-sensitive	Receptor	Inhibited by ATP; opens when ATP decreases during cellular hypoxia
	Acetylcoline activated	Receptor	Activated by acetylcholine and adenosine; slows sinoatrial nodal firing
	Calcium activated	Receptor	Activated by high cytosolic calcium; accelerates repolarization

transmembrane protein channel having conformational changes following changes in membrane potential. When the cell membrane is depolarized, the activation gate is open and Na^+ gets in the cell. As the activation gate opens, the inactivation gate starts to close. The rate with which this happens is different, since the activation gate is more rapid than the inactivation one; so, Na^+ rapidly gets in the cell. After few milliseconds, the inactivation gate closes and Na^+ stops getting in. The inactivation state lasts the repolarization phase of the membrane cell, during which it recovers to the resting state. In proximity of end of repolarization, the negative membrane potential leads the activation gate closing and the inactivation gate opening. At this point, the ion channel returns to its initial resting state. After the restoring of the resting membrane potential, the inactivation gate may spend 0.1 s (or longer) to recover. The mechanism just described occurs if the resting membrane potential is normal, i.e. about -90 mV, and the membrane quickly depolarizes, for example if a normal depolarization current diffuses from a cardiac cell to another during electrical cardiac activation. If the resting membrane potential is partially depolarized or the cell is slowly depolarized, the reaction of the fast Na^+ channel is different. In case the resting membrane potential is less negative, as when cardiac cell is in a hypoxic state, the partially depolarized state leads to inactivation of Na^+ gate. The more a cardiac cell is depolarized, the more numerous are the inactivated Na^+ channels (if the membrane

potential was about -55 mV, all Na^+ channels would be inactivated). In case the cell is slowly depolarized, inactivation gates have more time to close meanwhile the activation gates open. As a result, Na^+ channel passes from the resting closed state directly to the inactivated closed state: fast Na^+ currents are inhibited to transit through channels and the channel cannot resume its resting closed state. For the single cardiac cell not only one Na^+ channel is present, and each present channel has a slightly different voltage of activation and a slightly different timing to open (i.e., time of activated state). Thus, Na^+ current relies on the amount of Na^+ channels, the time of activated state, and the electrochemical gradient that drives Na^+ getting into the cell. The mechanism of enabling and inhibiting channels described for Na^+ is analogous for the other ions. Moreover, this is a conceptual model that needs to be more detailed through further studies (*Klabunde, 2011*).

Action potential

Cardiac action potential occurs when the membrane potential rapidly depolarizes and repolarizes, coming back to the resting state. There are two principal types of cardiac action potentials: the non-pacemaker one and the pacemaker one. The fundamental difference between them is that the non-pacemaker action potential is triggered by depolarizing ion currents coming from adjacent cells, while the pacemaker action potential is able of spontaneous automaticity. The action potential of cardiac myocytes differs from the action potential of nervous or skeleton muscular cells (**Fig. 1.1.1**). One of the differences relates to the timing: the action potential of nervous cell lasts about 1 ms to 2 ms; the skeletal muscular action potential lasts about 2 ms to 5 ms. In contrast, the non-pacemaker action potential of cardiac myocytes lasts 200 to 400 ms. These timing

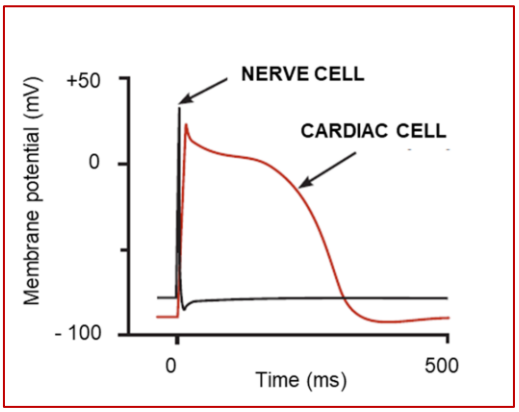

Figure 1.1.1. *Non-pacemaker action potential, longer in duration than nerve cell one* (*Klabunde, 2011*).

differences are due to the net electrochemical force acting on the ions, defined as the ratio between the ion current and the net voltage (a high membrane permeability for an ion corresponds to a high net electrochemical force).

Non-pacemaker action potential is found in atrial, ventricular cardiac cells and Purkinje fibers (see "*Conduction System*" section). Conventionally, the non-pacemaker action potential is considered as composed by five phases (**Fig. 1.1.1**).

- Phase 4 represents the initial resting membrane potential, to which the cardiac cell comes back at the end of the action potential (so they assume the same phase numbering). The resting membrane potential stays near the equilibrium potential for K^+, since the membrane conductivity for K^+ is much larger than for Na^+ or Ca^{++} in a resting cardiac cell.
- Phase 0 involves a rapid depolarization, when cardiac cells are rapidly depolarized from -90 mV to –70 mV by a transient increasing in the net electrochemical force of voltage-gated, fast Na^+ channels and decreasing in the net electrochemical force of K^+ channels. As a result, the membrane potential approaches the Na^+ equilibrium potential.

- Phase 1 involves an initial depolarization, due to the activation of a particular type of K^+ channels and inactivation of Na^+ channels.
- Phase 2 represents the plateau phase or delayed depolarization, due to activation of long-lasting (L-type) Ca^{++} channels that favor slow Ca^{++} currents getting in cardiac cell. Long-lasting Ca^{++} channels are activated when the membrane potential is about -40 mV (L-type channels are the most present Ca^{++} channels in cardiac muscle, are voltage-operated, stay open for a long time and can be inhibited by classical L-type Ca^{++} channel blocker, as verapamil or diltiazem).
- Phase 3 represents the repolarization, due to increasing in the net electrochemical force of K^+ channels through rectifier K^+ channels and decreasing in the net electrochemical force of Ca^{++} channels.

During phases 0, 1, 2 and partially phase 3 the cardiac cell is refractory, this means that it cannot be excited to initiate a new action potential, since the inactivation gates are closed. This period is termed effective or absolute refractory period and represents a protective mechanism through which the action potential rate is limited. The action potential rate mechanically reflects in the heart contraction rate. At the end of effective refractory period the cell is in relative refractory period. In this period a suprathreshold depolarization stimulus is necessary to initiate an action potential, since not all Na^+ channels have recovered to the resting phase and the generated action potentials are characterized by a decreased slope and lower amplitude of phase 0.

Pacemaker action potential is not characterized by a true resting phase and is generated regularly and spontaneously. The rate of depolarization in pacemaker cells is slower than non-pacemaker ones, so pacemaker action potentials are called slow response action potentials. The primary pacemaker site of the heart is constituted by the sinoatrial node. Secondary pacemaker sites are in the atrioventricular node and ventricular conduction system. The sinoatrial node drives the other pacemaker cell sites through an intrinsic higher excitatory rate, since the intrinsic activity of the secondary pacemaker sites is cancelled by a mechanism termed overdrive suppression, which causes the hyperpolarization of secondary pacemakers when driven by a rate higher than its intrinsic one. Hyperpolarization is due to the stimulation of the energy ATP-dependent pump system, consequent to the higher incoming of Na^+ in the cell. If the sinoatrial node is not able to elicit action potentials or they fail to reach the secondary pacemaker sites, the overdrive suppression mechanism stops its role and the new primary pacemaker site is outside the sinoatrial node: it is called ectopic focus. Sinoatrial node action potential is considered as composed by three phases (**Fig. 1.1.2**).

- Phase 0 represents the depolarization, mostly due to increasing of the net electrochemical force for Ca^{++} through L-type Ca^{++} channels. The incoming of Ca^{++} is lower than Na^+ channels, so the phase 0 slope (indicating depolarization rate) is slower than non-pacemaker cells. The membrane potential approaches the

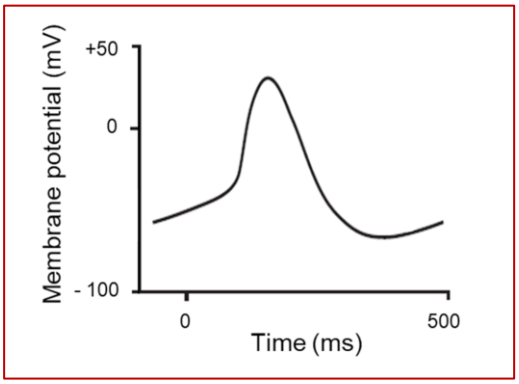

Figure 1.1.2. *Pacemaker action potential*.

equilibrium potential of Ca^{++} and a decrease of the net electrochemical force for K^+ favors the depolarization.

- Phase 3 represents the repolarization, due to the opening of voltage-operated, delayed K^+ channels (consequent to depolarization) that increases the net electrochemical force for K^+. The membrane potential approaches the equilibrium potential of K^+. In the meantime, the slow incoming of Ca^{++} decreases. Repolarization is self-limited, through the closing of K^+ channels, and stops when the membrane potential is -65 mV.
- Phase 4 represents the depolarization, due to multiple ionic currents: a decreasing in the net electrochemical force for K^+, a pacemaker current, partially composed by a slow incoming of Na^+, a slight increasing of the net electrochemical force for Ca^{++}, through T-type channels (they differ from L-type because they open at very negative voltage and cannot be blocked by the classical L-type Ca^{++} channel blockers) and L-type channels. This happens until threshold is reached and phase 0 is elicited.

Conduction system

After being generated by the sinoatrial node (**Fig. 1.1.3**), action potential diffuses through the atria mostly by cell-to-cell conduction. When a cardiac cell depolarizes, ionic currents are able to flow between adjoining cells across the gap junction that join together cardiac cells. If these ionic currents are sufficient to overcome the threshold potential of the adjoining cell, they rapidly depolarize the cell, eliciting an action potential in it. Being this mechanism repeatedly performed in all the cardiac cells, the action potential spreads throughout the atria. The velocity of action potential conduction in atria is about 0.5 m/s.

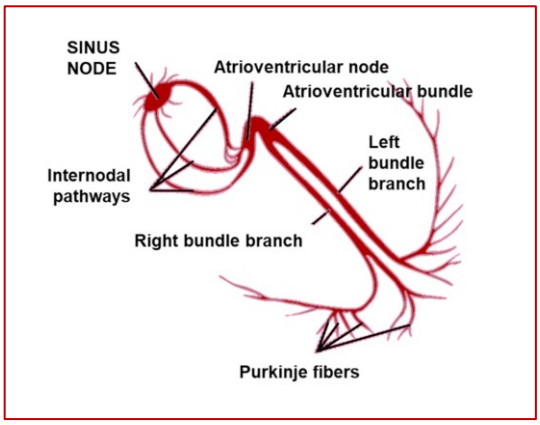

Figure 1.1.3. *Conduction system of the heart.*

Some functional characteristics lead to hypothesize the probable existence of specialized cardiac cells that operates as favored conducting pathways in the atria, called internodal pathways (**Fig. 1.1.3**). This conduction of action potential through the atria elicits excitation-contraction coupling to allow the mechanical function of the atria.

Atria and ventricles are reciprocally electrically separated, so action potentials have only one available pathway to get into the ventricles: a specialized site located in the inferior-posterior site of the interatrial septum, termed atrioventricular node (**Fig. 1.1.3**). The atrioventricular node is a specialized conducting tissue that slows down the velocity of action potentials to about 0.05 m/s. This causes a delay in the conduction between atria and ventricles that is physiologically particularly important. Indeed, it leaves the necessary time to atria to depolarize (so to mechanically contract, filling ventricles of blood coming from atria, before their depolarization and consequent contraction) and limits the rate of action potentials arriving to ventricles, so they have adequate time to be filled by blood and guarantee cardiac output. After reaching atrioventricular node, action potentials enter the ventricles (at the base) at the bundle of His and then run through the left and right bundle branches, located along the interventricular septum (**Fig. 1.1.3**). Bundles of His are

composed by specialized fibers able to conduct action potentials at about 2 m/s, so at high velocity. Then, the bundle branches split into a system of fibers called Purkinje fibers (**Fig. 1.1.3**) able to conduct action potentials at about 4 m/s. Eventually, these fibers connect with ventricular cardiac cells driving the action potentials throughout the ventricles via a cell-to-cell conduction system.

The conduction system is fundamental to regulate the efficient mechanical function of the heart. Depolarization and consequent contraction have to be well-organized to generate the right blood pressures. If it is compromised, as in case of ischemia or myocardial infarction, pathways and velocities of conduction are altered, and so also generated blood pressure. These anomalous conditions may fall to arrhythmias (*Klabunde, 2011*).

1.2 Systems of Regulation of Automaticity and Conduction System

Many factors can affect the firing rate of the sinoatrial node and the conduction velocity (**Table 1.2.1**).

Regulation of automaticity

Intrinsic automaticity of the sinoatrial node has a rate of 100 to 110 triggers per minute, which correspond to 100 to 110 bpm, so to heart rate. This rate can vary between low resting values of 50 to 60 bpm and high values of 200 bpm. Possible changes are regulated by autonomic nerves acting on the sinoatrial node, determining increased heart rate (positive chronotropic response) or reduced heart rate (negative chronotropic response). At low resting heart rates, vagal influences are dominant with respect sympathetic influences (vagal tone). At high heart rates, sympathetic influences are dominant with respect vagal tone. Heart rate can be altered by autonomic influences through prolonging or reducing the time to reach threshold voltage. This can occur by: changing the slope of phase 4; changing the threshold voltage for triggering phase 0; changing the hyperpolarization entity at the end of phase 3. Sympathetic influence on sinoatrial node increases phase 4 slope and reduce the threshold, resulting in an increased pacemaker rate. This effect is mainly due to norepinephrine release by sympathetic nerves; norepinephrine is a neurotransmitter whose final consequence is the increasing of pacemaker current and earlier opening of L-type Ca^{++} channels. Vagal influence decreases phase 4 slope, hyperpolarizes the cardiac cell and increases the threshold voltage to trigger phase 0, resulting in a reduced pacemaker rate. Non-neural influences also affect pacemaker

Table 1.2.1. *Factors increasing/decreasing firing rate of the sinoatrial node and the conduction velocity; those on white background have effects on both sinoatrial node and conduction velocity, while those on grey background have effects only on sinoatrial node (Klabunde, 2011).*

Increasing	Decreasing
Sympathetic stimulation	Parasympathetic stimulation
Muscarinic receptor antagonist	Muscarinic receptor agonist
β-Adrenoceptor agonist	β-Blockers
Circulating catecholamines	Ischemia/Hypoxia
Hypokalemia	Hyperkalemia
Hyperthyroidism	Sodium and calcium channel blockers
Hyperthermia	Hypothermia

activity (**Table 1.2.1**). Moreover, several drugs treating anomalous heart rhythm (i.e., antiarrhythmic drugs) influence sinoatrial node rhythm. Ca^{++} channel blockers induce bradycardia, because they inhibit L-type Ca^{++} channels decreasing Ca^{++} currents getting inside the cardiac cell during phase 0 and phase 4. Drugs influencing autonomic control or receptors compromise regular pacemaker activity (*Klabunde, 2011*).

Regulation of conduction system

Cell-to-cell conduction rate is affected by intrinsic and extrinsic factors. Intrinsic factors comprehend electrical resistance between adjacent cells and action potential nature. The high and rapid slope of non-pacemaker action potential is mainly due to fast Na^+ channels. If the number of activated fast Na^+ channels increases, the rate of depolarization is higher. If cardiac cells depolarize more rapidly, adjoining cells will depolarize at higher rate. Thus, conditions that decrease the enabling of fast Na^+ channels, as hypoxia, decrease the rate and magnitude of phase 0, and consequently conduction velocity throughout the heart. Analogously, since in the atrioventricular node the phase 0 of action potential is mainly due to slow Ca^{++} channels, changes in the enabled Ca^{++} channels alter the rate of depolarization, and consequently conduction velocity between atrioventricular node cells. Extrinsic factors comprehend autonomic nerves, circulating hormones and several drugs (**Table 1.2.1**). Autonomic nerve activity particularly influences the conduction velocity in the specialized conduction system. An increased sympathetic eliciting or an increase in the circulation of particular hormones, increases conduction velocity, while activation of parasympathetic nerves decreases conduction velocity, especially in the atrioventricular node that is highly innervated by the parasympathetic nerves. Many drugs alter autonomic action or intercellular conduction, e.g. in non-nodal tissue, antiarrhythmic drugs block fast Na^+ channels decreasing conduction velocity or in the atrioventricular node, digoxin stimulates parasympathetic influences on the conduction system (*Klabunde, 2011*).

1.3 Arrhythmias: Mechanisms of Genesis

If electrical function of the heart cannot follow the regular pathways, the efficiency of mechanical heart action is compromised, and arrhythmias can occur. If an ischemic damage or excessive parasympathetic stimulation block the atrioventricular node, electric signals generated and propagated in the atria cannot reach the ventricles. Ventricles have latent pacemakers able to activate ventricles independently from signals coming from atria, but their eliciting frequency is lower. This situation results in ventricular bradycardia and lower cardiac output. If one of the bundle branches is blocked, ventricular depolarization occurs following altered pathways. This situation leads to a delay in ventricular activation and a lower contraction efficiency. If an ectopic heartbeat occurs, it can compromise ventricular depolarization (*Klabunde, 2011*).

A particular abnormal conduction situation is represented by the mechanism of reentry (**Fig. 1.3.1**). Reentry is a cyclical rapid reactivation of a conducting pathway, caused by an early stimulus coming from the previous action potential. When a Purkinje fiber forms two branches, the action potential will divide between the two. If these branches go into the same common pathway, the action potentials will cancel each other. A possible reentry occurs if one of the two branches is partially depolarized and so the action potential can travel through it only in retrograde direction.

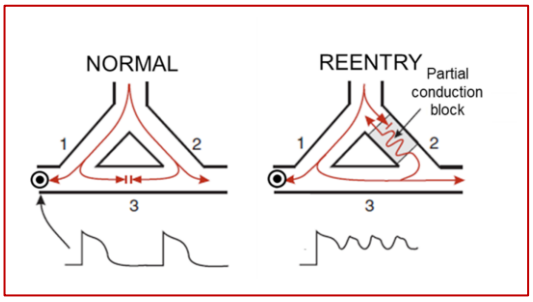

Figure 1.3.1. *Reentry mechanism. In normal conduction of action potentials, impulses travel throughout branches 1 and 2, reciprocally cancelling in branch 3. Under reentry condition, one of the two branches (branch 2) is partially depolarized and impulses can slowly travel only in retrograde direction. If an impulse travel in retrograde way, reaching excitable tissue, an action potential can be conducted prematurely throughout branch 1 and tachycardia can occur. In the lower part of the figure the action potential morphology that can be revealed by an electrode placed between branch 1 and 3* (*Klabunde, 2011*).

The action potential running through the other branch after entering the common pathway travel through the second one in retrograde way. There, the conduction velocity is reduced because the depolarized branch. When the action potential gets out of the branch and finds excitable tissue, it is conducted again through the first branch. On the other hand, if the action potential finds unexcitable tissue, it stops to propagate. In this condition, timing (depending on conduction velocity and refractory state) is crucial, since only if the action potential find excitable tissue, a reentry circuit can be established. Arrhythmias provoked by reentry can be paroxysmal: in this case the conditions that suddenly elicit reentry are canceled thanks to the influence of autonomic nerve or other factors. Reentry mechanisms can happen globally, if they involve both atria and ventricles, or locally, if they involve a localized site of atria or ventricles. The first ones can result in supraventricular tachyarrhythmias, as the Wolff-Parkinson-White syndrome, while the second ones can result in ventricular or atrial tachyarrhythmias, according to the localization of reentry (*Klabunde, 2011*).

2

ELECTROCARDIOGRAM

ECG (in German, and also often in English EKG, from Elektrocardiogram) has had an incalculable impact on cardiology field. It has provided and still provides an important insight into the structural and functional characteristics of both healthy and diseased hearts. Nowadays, the use of the ECG is a standard of care in cardiology and still now new improvements in the field are constantly being reached thanks to new technologies. Other ECG advantages make it one of the most widespread and used measurement in clinical tests: one of them is its ability to map cardiac electrical activity in a completely noninvasive but reliable way. There are no risks for the person, since during the measurement, the source of the energy that is recorded by the acquisition tool comes from the subject himself. Ultimately, the ECG is the simplest, fastest, safe and inexpensive measurement from which the clinician can get a lot of information about the condition of a person's heart.

Practically, the ECG[ξ] is a graph of voltage versus time of the electrical activity of the heart obtained by electrodes placed on the skin. These electrodes detect the small electrical changes that are a consequence of heart depolarization followed by repolarization during each cardiac cycle (heartbeat). Many ways to record the ECG were introduced along the decades, evolving in a powerful diagnostic tool for several kinds of heart diseases, including cardiac rhythm disturbances (e.g. atrial fibrillation and ventricular tachycardia), inadequate coronary artery blood flow (e.g. myocardial ischemia and myocardial infarction), and electrolyte disturbances (e.g. hypokalemia and hyperkalemia). For example, the standard ECG, detecting cardiac activity only for a few seconds, is unable to identify pathologies that occur only occasionally, such as some arrhythmias. In these cases, it may be appropriate to use a 24-hour dynamic Holter ECG. Furthermore, the ECG is not able to highlight those cardiac pathologies, which are not detectable in conditions of rest; in these cases, an exercise ECG may be useful.

Historically, the discovery of intrinsic electrical activity of the heart dated back to 1840s. Indeed, in 1842, the Italian physicist Carlo Matteucci first observed that an electrical current is associated to each heartbeat. In 1856, Heinrich Miller and Rudolph von Koelliker recorded firstly the cardiac action potential using a galvanometer. In 1870s the capillary electrometer was invented and Augustus D. Waller recorded firstly the human ECG, showing that the heart electrical activity precedes the mechanical one and, furthermore, that it can be acquired by applying electrodes to both hands and one hand and one foot. A wider breakthrough in cardiac electrocardiography was performed in 1901, when Willem Einthoven invented the string galvanometer. Willem Einthoven was also the first to label the deflections consequent to the cardiac electrical activity as P, Q, R, S, T. In 1912, Willem Einthoven was able to derive mathematical relationship linking the direction and the size of deflections recordable by the

ξ in this thesis, the electrocardiogram is always referred to as surface electrocardiogram, otherwise explicitly specified.

three limb leads, known also now as the Einthoven's Triangle (**Fig. 2.1**). About thirty years later, Frank Wilson introduced the unipolar leads, together with the precordial lead configuration. The standard limb leads, the unipolar limb leads, and the precordial leads compose the 12-lead ECG configuration, in use also nowadays. ECG equipment changed a lot during the years. The first instrument was manufactured in 1905 and it was massive and heavy. By the years the instrument became less heavy and in 1920s bedsides machines arrived. "Portable" versions of the machine were manufactured later, but the possibility to record the ECG even in non-clinical settings was made possible in 1949, thanks to Norman Jeff Holter through the Holter monitor. Further miniaturized versions have been made available. Now, digital ECG recordings are used, and people can be monitored for long periods of time (*Iaizzo, 2009*).

Figure 2.1. *Early commercial ECG machine, built in 1911 by the Cambridge Scientific Instrument Company (Christoph Zywietz, A Brief History of Electrocardiography - Progress through Technology; S. L. Barron, The development of the electrocardiograph in Great Britain, British Medical Journal 1:720, 25 March 1950) to measure the human electrocardiogram according to the standards developed by Einthoven.*

2.1 Genesis: The Electric Dipole

The ECG measures changes of heart electrical activity over time, when action potentials spread throughout all the cells of the heart during each cardiac cycle. Specifically, it does not represent a direct measure of depolarization and repolarization at the cellular level, but rather a relative measure of the cumulative electrical activity of populations of cardiac cells in time (*Iaizzo, 2009*).

Basically, from the ECG view, the human body can be considered as filled with tissues immersed in a conductive ionic fluid, so, ultimately, as a large-volume conductive medium, in which the heart is present. During a cardiac cycle one part of the heart is depolarized, while the other is at rest or polarized. The result is a charge separation, reflected in the equivalent electric dipole, by which the heart can be modeled (**Fig. 2.1.1**). This dipole is composed by two opposite electric poles: they create a current flow spreading across the surrounding body fluid, resulting in a fluctuating electric field throughout the body. Indeed, an electric wave

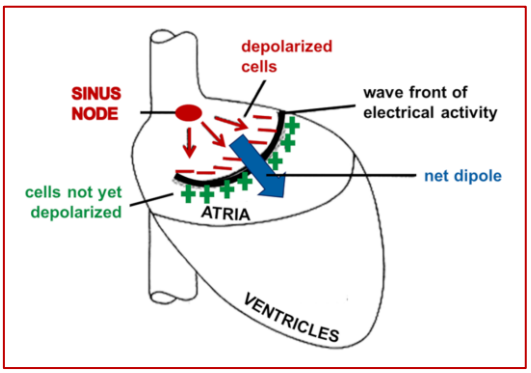

Figure 2.1.1. *The cardiac electric dipole (Iaizzo, 2009).*

front moving cycling from atria to ventricles, with polarized cells beyond and depolarized cells behind it, causes a current flow changing in time that can be detected by electrodes placed on the skin surface. The intensity and direction of the voltage depends on the orientation of the electrodes with respect to the electric dipole. Particularly, voltage amplitude is proportional to the mass of tissue creating the dipole, but also to its configuration, during the acquisition. Detection of the electric currents by an array of electrodes attached on the thoracic skin provides a recorded ECG tracing. It is express in voltage vs time and generally displayed in millivolts (mV) vs seconds (s) on paper (in clinical set up) running at 25 mm/s and with vertical calibration of 1 mV/cm (*Iaizzo, 2009; Klabunde, 2011*).

2.2 Typical Morphology

The ECG is composed by a pattern of typical waves that repeats in a pseudo-periodic way. A typical waveform, conventionally used to represent the ECG morphology is that from one of the standard limb leads, usually that obtained placing the negative electrode on the right wrist and the positive one on the left ankle (*Iaizzo, 2009*). The repeating waves and segments, visible from the recording (**Fig. 2.2.1**), reflect the sequence of depolarization and repolarization of atria and ventricles, so in general a different event associated with the cardiac cycle.

Actually, the cardiac cycle starts with the sinoatrial node firing, but it cannot be detected by the surface ECG, since the sinoatrial node is composed by a too small amount of cells, so the electric potential is low in amplitude and dissipates throughout the body fluids before reaching the body surface, where the detecting electrodes are placed. On the contrary, the following coordinated depolarization of right and left atria can be detected and is visible on the ECG (*Iaizzo, 2009*). Indeed, the P wave represents the wave of depolarization spreading from the sinoatrial node throughout the atrial tissue. It usually lasts 0.08 s to 0.10 s. The isoelectric [h] period following the P wave represents the time in which all the atrial cells are depolarized and the electric impulse is travelling in the atrioventricular node (also in this case the amount of cells involved is not enough to cause an electric potential with an amplitude that can be detectable by surface electrodes and so visible on the ECG); there, the conduction velocity is reduced. The first negative deflection is the Q wave, the large positive deflection is the R wave and the following negative deflection is the S wave (*Iaizzo, 2009; Klabunde, 2011*).

The time interval between the onset of P wave to the onset of QRS complex is called PR interval. It usually lasts 0.12 s to 0.20 s. It reflects the time interval between the starting of atrial depolarization and the starting of ventricular depolarization. The QRS complex represents the ventricular depolarization.

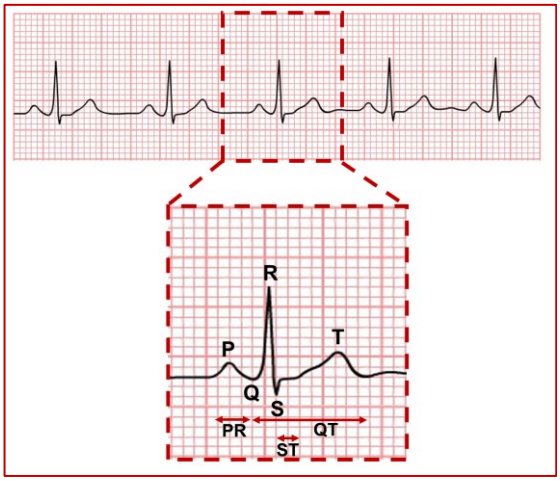

Figure 2.2.1. *The normal morphology of ECG tracing.*

h) isoelectric: electrocardiogram baseline.

Ventricular depolarization masks atrial repolarization: so, the wave representing atrial repolarization, very low in amplitude (involving a reduced amount of cells), results not visible in the ECG. The QRS complex lasts 0.06 to 0.10 s (ventricular depolarization is faster than atrial depolarization). The isoelectric period following the QRS complex represents the time in which all the ventricular cells are depolarized, and it is called ST segment. The T wave represents ventricular repolarization. It lasts longer than ventricular depolarization. The time interval between the onset of QRS complex and the offset of T wave is called QT interval. During the QT interval both ventricular depolarization and ventricular repolarization occur. It lasts 0.20 s to 0.40 s, depending on the heart rate: at increased heart rate, QT interval is shorter (*Klabunde, 2011*).

2.3 Leads of Acquisition

The ECG is recorded through an array of electrodes placed on the surface skin in standardized locations. By convention, electrodes are placed on both arms and legs and on the chest. By these electrodes, the three basic types of ECG leads can be recorded:

- the bipolar standard limb leads;
- the unipolar augmented limb leads;
- the unipolar precordial chest leads.

These electrode leads are conveniently connected to a device capable of detecting and acquiring the potential differences between certain leads to produce the characteristic ECG tracings. The bipolar leads are defined between pairs of positive/negative electrodes, while the unipolar leads are defined between a single positive electrode and the other electrodes electrically joined together to act as a common negative electrode (*Klabunde, 2011*).

In the standard limb leads (**Fig. 2.3.1**), lead I configuration is defined between the positive

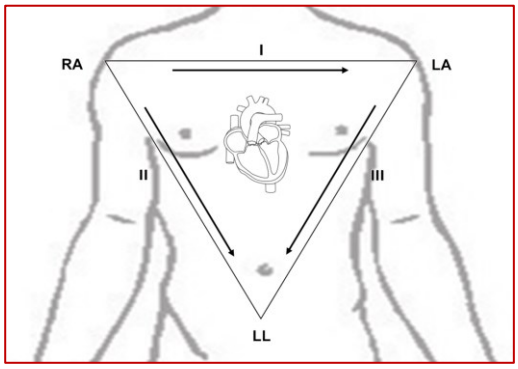

Figure 2.3.1. T*he bipolar standard limb leads.*

electrode placed on the left arm and the negative electrode placed on the right arm; lead II configuration is defined between the positive electrode placed on the left leg and the negative electrode placed on the right arm; lead III configuration is defined between the positive electrode placed on the left leg and the negative electrode placed on the left arm. In all standard limb leads, an electrode placed on the right leg serves as reference electrode. The three standard limb leads roughly form an equilateral triangle around the heart that is in the barycenter, the Einthoven's Triangle. Ideally, no difference for the recording purpose comes out if the limb leads are placed at the end or at the origin of the limbs, so wrists or shoulders for the arms and ankles or upper thighs for the legs. Usually, proximal limb lead positions are preferred in case of activity-compatible electrocardiographic monitoring. Nevertheless, Pahlm et al. has demonstrated that arm electrodes cannot be placed higher than halfway the upper arms without changing the ECG recorded through the standard electrode configuration (*Pahlm, 1992*). Therefore, it is important that ECG recordings made with electrode configurations at alternative sites are tagged accordingly so that their ECG output cannot be confused with the ECG output obtained from electrode configurations at standard sites.

Supposing the three standard limb leads collapsing on the heart, the axial reference system is defined. In it, the positive electrode for lead I is at 0° with respect to the heart; the positive electrode for lead II is at +60° with respect to the heart; the positive electrode for lead III is at +120° with respect to the heart (*Klabunde, 2011*).

The augmented limb leads (**Fig. 2.3.2**) have single positive electrodes that are referenced against a combination of the others. In other words, the other leads are joined to create the negative electrode. The positive electrodes are placed on the left arm, aVL, the right arm, aVR, and the left leg, aVF. Practically, they are the same positive electrodes for the standard limb leads; it is the ECG recording instrument to do the rearranging of the electrode definition. The lead aVL is at -30° respect to lead I axis; aVR is at -150° respect to lead I axis; aVF is at +90° respect to lead I axis. The standard limb leads and the augmented limb leads record electrical activity on a single body plane, i.e. the frontal one (*Klabunde, 2011*).

The precordial chest leads (**Fig. 2.3.3**) have six electrodes placed on the chest surface in correspondence of the heart. The right arm, the left arm, and left leg electrodes are used combined to serve as neutral reference lead, in the center of the chest. The six leads are termed as V1, V2, V3, V4, V5, V6. The positive "exploring" electrodes are placed to the right of the sternal border (for V1), to the left of the sternal border (for V2), in the midway between V2 and V4 (for V3), in the fifth intercostal space in the midclavicular line (for V4), in the fifth intercostal space in correspondence of beginning of the axilla (for V5), in the fifth intercostal space at the mid-axillary line (for V6). The precordial chest leads record electrical activity on a single body plane, i.e. the transverse plane (*Klabunde, 2011*).

2.4 Reading of the Tracing

The ECG waveforms depend on the location of recording electrodes, on the conduction pathways, on the conduction velocity and on the changes in the cardiac tissue.

The wave front of heart electrical activity causes a current flow changing in time and electrodes placed on the skin surface can detect it. The orientation of the electric wave front between positive and negative recording electrodes influence the polarity and the magnitude of the voltage acquired, i.e. of the ECG morphology. Particularly:

- if the instantaneous electric wave front reflects depolarization and is travelling toward a positive electrode, the deflection in the ECG is positive; on the contrary if it is travelling away from a positive electrode, the deflection is negative;
- if the instantaneous electric wave front reflects repolarization and is travelling

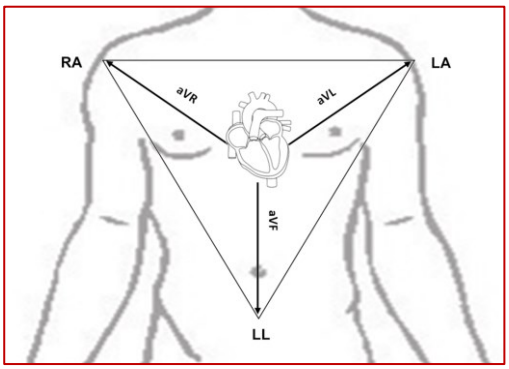

Figure 2.3.2. *The unipolar augmented limb leads.*

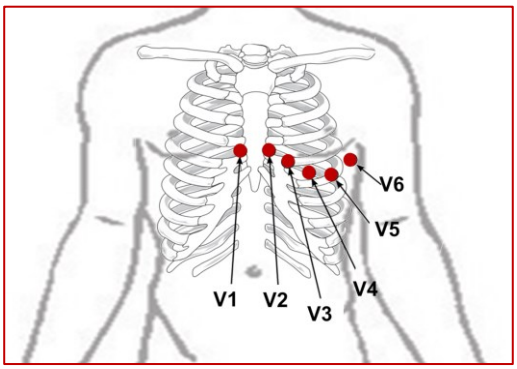

Figure 2.3.3. *The unipolar precordial chest leads.*

toward a positive electrode, the deflection in the ECG is negative; on the contrary if it is travelling away from a positive electrode, the deflection is positive.

Moreover, an instantaneous electric wave front (reflecting depolarization or repolarization) is travelling perpendicular to an electrode axis, no deflection occurs (*Klabunde, 2011*).

At each time instant the voltage detected by the electrodes corresponds to the summation of the electrical activity of all the regions of the heart that are depolarizing or repolarizing. For example, when the sinoatrial node is firing, several depolarization waves spread from the sinoatrial node to all possible directions within the atria. Each one of these waves (spreading in different directions) can be modeled through an arrow reflecting the individual electrical vector [i] in that instant time. Obviously, at any time, many individual electrical vectors, reflecting action potentials spreading toward different directions, are generated. Thus, a resultant electrical vector can be derived by the integration of all these individual electrical vectors and it assumes different orientation, instant by instant (*Klabunde, 2011*). In other words, since it is reasonable to model the electrical generator of the heart with an equivalent dipole, it is possible to consider it in vector form (*Man, 2015*). In general, the resultant vector represents the total strength and direction of the cardiac electrical dipole, instant after instant. The measured voltage amplitude in each ECG lead equals the projection of the resultant vector on the vector associated with each ECG lead. Distances of electrodes to the heart and inhomogeneous conductive properties in the body influence the direction and the sensitivity by which the lead detect the heart electrical activity (*Man, 2015*).

2.5 Arrhythmias Interpretation

The correct interpretation of the ECG morphology enables the clinician to evaluate normal and abnormal cardiac rhythms. In a normal ECG a stable timing correspondence exist between P wave and QRS complex, according to which each QRS complex follows P wave. This means that ventricular depolarization is triggered by atrial depolarization in normal conditions and the sinoatrial node controls the cardiac rhythm. The clinician evaluates this kind of ECG as a sinus rhythm. Sinus rhythm ranges from 60 bpm to 100 bpm [j]. Abnormal rhythms are all rhythms different from the normal sinus rhythms (**Fig. 2.5.1**). Sinus arrhythmias are determined by from disturbances in the action potential conduction, even if the sinoatrial node keeps its role in firing the action potential. Among sinus arrhythmias, there are the sinus bradycardia and the sinus tachycardia. These two kinds of arrhythmias are normal findings in some cases. A sinus rate less than 60 bpm is called sinus bradycardia. It can be considered as normal at rest: some people, particularly athletes, may have normal resting heart rates less than 60 bpm. In some other people, sinus bradycardia can mean a depressed function of the sinoatrial node. The resting sinus rhythm is extremely dependent on the influence of the vagal tone on the sinoatrial node; this dependence is particular evident in the sinus respirophasic arrhythmia, in which the sinus

i) Cardiac electrical vector: in Medicine, it represents what in Physics is known as the electric dipole moment; cardiac electrical vectors are associated with electrical dipoles.

j) bpm stands for "beat per minute"; strictly speaking, "beat" refers to the mechanical action of the heart, specifically to contraction, while the ECG gives information about the rate of electrical events, specifically, in this context, it refers to depolarization.

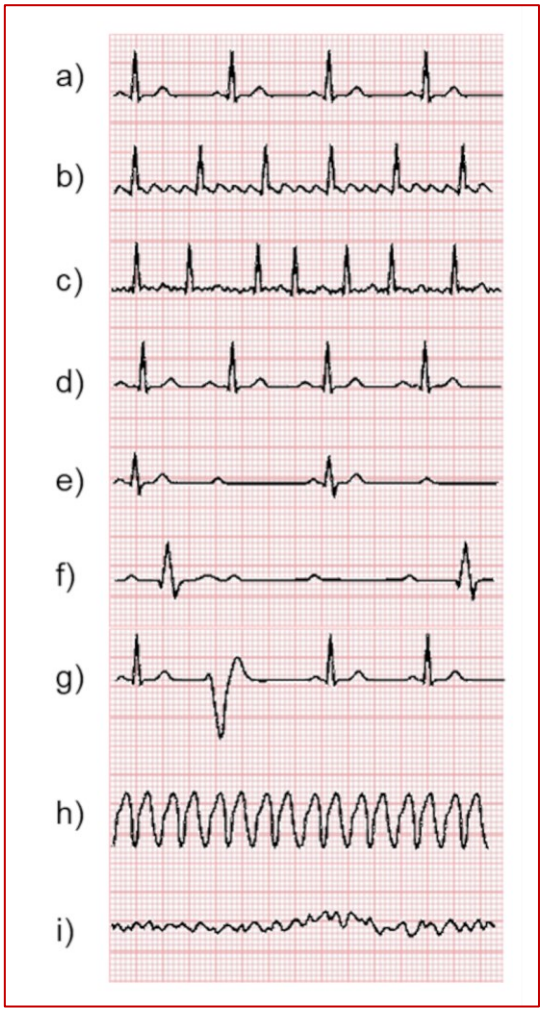

Figure 2.5.1. *Examples of: normal ECG (panel a); atrial flutter (panel b); atrial fibrillation (panel c); first-degree atrioventricular block (panel d); second-degree atrioventricular block (panel e); third-degree atrioventricular block (panel f); premature ventricular complex (panel g); ventricular tachycardia (panel h); ventricular fibrillation (panel i).*

rate is higher with inspiration and lower with expiration. A sinus rate between 100 bpm and 180 bpm is called sinus tachycardia. It can be considered as normal with exercise.

When the heartbeat period is temporarily too long, associated with the absence of P wave, a sinus node pause is occurred (*Klabunde, 2011*). In some other conditions, arrhythmias can be characterized by a frequency of P waves different than the frequency of QRS complexes. In atrial flutter, atrial rate is so high (250 bpm to 350 bpm) that not all the impulses are conducted in the atrioventricular node; as a consequence, the ventricular rate is lower. In atrial flutter, there is not isoelectric baseline between sequential flutter waves since in the atria there is a continuous electrical activity, due to a mechanism of reentrant circuit. In addition, ventricular rate can be regular or irregular, depending on the ability of the atrioventricular node to conduct only some or all the action potentials reaching it toward the ventricles. In atrial fibrillation, atrial depolarizations are not triggered by the sinoatrial node, but rather by many uncoordinated atrial sites; as a consequence, P waves are high-rate and low-voltage, so difficult to discriminate. Ventricular rate is irregular and high. Both in atrial flutter and in atrial fibrillation, atrioventricular node plays a fundamental role in limiting ventricular rate. In the atrioventricular block, the action potential conduction is depressed only due to a compromised ability of the atrioventricular node to conduct, since the sinoatrial node regularly generate it. The first-degree atrioventricular block represents the less severe form, in which the atrioventricular conduction is delayed but not suppressed, since the action potential still passes through the atrioventricular node and activates ventricles. For each P wave there is a QRS complex, but the PR interval is longer. The second-degree atrioventricular block there is no correspondence between the number of P waves and the number of QRS complexes: the atrioventricular node is not able to conduct all the action potentials and before having a QRS complex there can be two or three P waves. The third-degree atrioventricular block represents the most severe form, in which no action potentials from atria are conducted through the atrioventricular node toward the ventricles; so, QRS complexes are independent from P waves. Ventricular depolarization still occurs because of the activity of secondary pacemaker sites, usually

latent, like sites in the atrioventricular junction or ectopic foci in the ventricles. Ventricular bradycardia occurs, since the intrinsic firing rate of these ventricular pacemakers is lower than those of sinoatrial node. Pacemaker cells in the atrioventricular node and in the bundle of His have a rate of 50 bpm to 60 bpm, while pacemaker cells in the Purkinje system have a rate of 30 bpm to 40 bpm. Moreover, if the ectopic foci are within the ventricles, QRS-complex morphology changes because of the anomalous conduction pathways. In atrial flutter, atrial fibrillation and atrioventricular block, atrial rate is usually higher than ventricular one. On the contrary, in ventricular flutter and ventricular tachycardia atrial rate is lower than ventricular one. Ventricular tachycardia causes a heart rate of 100 bpm to 200 bpm, while ventricular flutter, which is the most severe form of ventricular tachycardia, can cause a heart rate higher than 200 bpm. At the origin of them, there is usually reentry circuits, due to abnormal action potential conduction in the ventricles, or ectopic foci in the ventricles. Being ventricular depolarizations not elicited by atria, the electrical activity of ventricles is not coordinated with that of atria. These conditions can become malignant if they degenerate into ventricular fibrillation. In case of ventricular fibrillation, the ECG morphology is completely compromised and abnormal, since it results in the repetition of rapid, low-voltage, uncoordinated depolarization waves. Premature depolarization is another type of arrhythmias in which ectopic pacemaker sites in the atria (premature atrial depolarization) or in the ventricles (premature ventricular depolarization) trigger the depolarization. On the ECG they appear as early P waves or QRS complexes. Since premature depolarization do not follow regular conduction pathways, the wave morphology results abnormal (*Klabunde, 2011*).

2.6 Interferences and Noises

As other types of biomedical signals, the ECG signals can be affected by non-stationarity, interference and noise susceptibility, and variability among subjects. In particular, in signal processing purposes, the most challenging task is to deal with susceptibility of these signals to several kinds of noises or interferences. The main sources of noise are:

- Changes in the body/electrode impedance, resulting from the physic-chemical processes occurring in correspondence of the electrode contact with the skin and on the possible subject movement. They are referred to as low-rate noises.
- Changes in the position and distance of the electrodes from the heart caused by the subject's movement due to breathing activity. They are referred to as low-rate interferences.
- Muscle interferences are caused by contraction of skeletal muscles due to movement of the subject or to the environment temperature. They are referred to as broad-spectrum interferences and can overlap the frequency band of the ECG.
- Noises of electromagnetic nature due to power line. They are referred to as high-rate power-induced electromagnetic noises.
- Electromagnetic noises of impulse character caused by high power devices.

The low-rate and muscle interferences are challenging to filter out without compromising important ECG diagnostic information. According to the modality of acquisition, the acquired ECG signal has a different amplitude and is corrupted by noises of different nature; this affects the

signal-to-noise ratio (SNR). Usually, the amplitudes of the ECG signals recorded by electrodes placed on the adult chest surface have amplitude of some millivolts (higher amplitudes are typical of ventricular electrical activity). Fetal signals have lower amplitudes, generally in the microvolts range; in this case SNR can be very low. Especially fetal ECG signals registered on the abdomen of the mother often have unfavorable SNR values. The acquired ECG signal comes from the combination of the fetus signal and mother signal; the first one has an amplitude of microvolts and is considered the signal of interest, while the second one has an amplitude of millivolts and is considered as interference (so, the amplitude of interferences is much higher the amplitude of the signal of interest).

Other features that are typical of the ECG imply variability among different subjects and in time. This is true in healthy population and in cardiac diseased population (*Gacek, 2011*). Therefore, automatic analysis methods should on one side have preprocessing steps able to manage different interferences or noises, on the other side show versatility to manage inter- and intra-subject variability.

3

ELECTRICAL CARDIAC ALTERNANS

Electrical cardiac alternans is an electrophysiological phenomenon manifesting in the ECG as the change in morphology (amplitude, polarity or shape) of one of its waves, which appears with regular rhythmicity on an every-other-beat basis (**Fig. 3.1**). Given its evidence on the ECG, it is often called ECG alternans (ECGA). ECGA can occur on various waves of the ECG (P wave, resulting in P-wave alternans; QRS complex, resulting in QRS-complex alternans, QRSA; T wave, resulting in T-wave alternans, TWA), but the most investigated form of ECGA was TWA. TWA was considered of particular interest because its evidence was found to be associated with electrical instability in the heart. It was firstly observed and reported by Hering in 1908. Then, in 1910, Thomas Lewis observed alternans in a man while having paroxysmal atrial tachycardia. From what he reported, ECG alternans is an evidence occurring in normal heart when its rate is very high or in intoxicated or impaired heart, also in case of normal rate; particularly, he reported: "alternation occurs either when the heart muscle is normal and the heart rate is very fast, or when there is serious cardiac disease and the rate is normal" (*Lewis, 1910*). In 1948, Kalter and Schwartz found 5 cases over 6,059 analyzed clinical ECG with macroscopically visible alternans on the T wave, but the incidence was very low and ECG alternans remained a curiosity of the ECG for many years (*Armoundas, 2002; Walker, 2003*).

In 1975, Schwartz and Malliani discovered its association with the long QT syndrome, so they hypothesized that TWA could be a precursor of ventricular arrhythmias, but this hypothesis remained so, since the lack of methods able to detect and quantify TWA from the ECG. In 1984, Adam et al. showed the possibility of TWA to occur at levels undetectable by visual inspection; they developed the first automatic method to detect microscopic level of TWA on the ECG and, thanks to it, TWA association with ventricular fibrillation was reaffirmed (*Armoundas, 2002; Walker, 2003*).

About 100 years later its first observation, prognostic implications of ECGA, especially TWA, start to be pointed out and thanks to many studies, it became a clinically useful risk marker of SCD (k). One

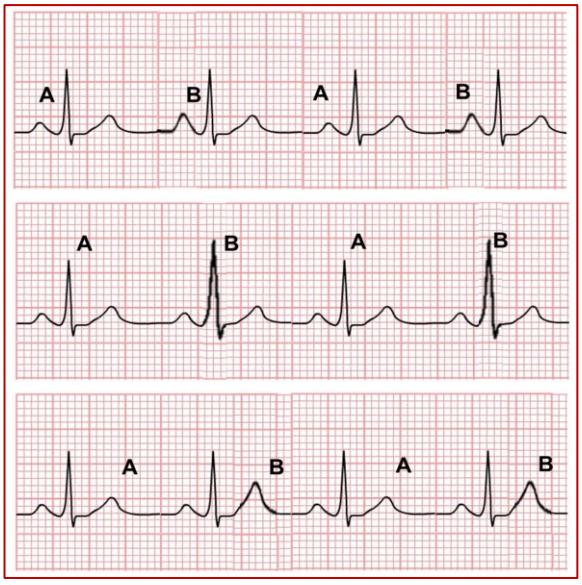

Figure 3.1. *Electrical cardiac alternans, visible in the ECG as PWA, QRSA and TWA, following an ABAB pattern.*

k) sudden cardiac death: unexpected natural death due to cardiac causes within a short period of time in a person without any prior condition that would seem fatal.

of the recognized advantages of TWA was its ability to predict arrhythmia-free survival as well as electrophysiologic testing. Indeed, moderate exercise to rise heart rate was enough to highlight TWA; instead, electrophysiologic testing requires pacing electrode implantation to induct arrhythmia. TWA was observed in a variety of cardiac diseases: Prinzmetal's angina, acute myocardial infarction, coronary vasospasm, antiarrhythmic therapy, and long-QT syndrome. The wide variety of cardiac disease to which TWA was observed and recognized as a precursor of arrhythmias suggests common mechanisms expressing as various forms of ECG alternans (*Armoundas, 2002; Walker, 2003*).

The relationship between TWA and heart rate is very clear. TWA is highlighted by pacing or by exercise increasing heart rate. Moreover, the heart rate corresponding to TWA manifestation roughly indicates the risk level: normal subjects show TWA at heart rate higher than 120 bpm, while patients at risk for SCD can show TWA at heart rate lower than 110 bpm (*Walker, 2003*).

3.1 Pathophysiological Genesis: Action Potential Dynamics and Cellular Mechanisms

TWA is highly correlated with an increased vulnerability to ventricular tachyarrhythmias. This leads to question whether TWA acts only as the risk marker or also as arrhythmogenic factor. This intriguing question is still open.

Many hypotheses have been made trying to explain the physiological factors at the origin of TWA. Its strong dependence on heart rate suggests that TWA appears when heart rate is too high to allow certain ionic channels to recover from activation or inactivation. For example, if they do not have sufficient time to recover from inactivation on the previous heartbeat, they cannot totally contribute to the next heartbeat: this results in a shortened action potential duration (APD). The following diastolic interval (DI) will be lengthened, since ionic channels fully recover. Then, a lengthened APD follows eliciting a shortened DI and the alternant mechanism feeds itself cyclically (*Walker, 2003*). It is not clear which ion channels are actually involved in the TWA eliciting and if they are the cause or the manifestation of TWA. The TWA/heart rate relationship is often described in terms of "restitution hypothesis" that is based on the evaluation of APD restitution (*Walker, 2003; Tse, 2005*). APD restitution relies on the dependence of APD from its prematurity degree, i.e. from the DI preceding it. Indeed, if DI becomes shorter, gates of inward ions can fail to fully reactivate (or gates of outward ions can fail to fully deactivate); this, in turn, causes a shortened APD. Short DI results in short APD, which in turn leads to long DI resulting in a long APD in the next heartbeat. This dynamic is represented in the restitution curve (**Fig. 3.1.1**). In the APD restitution curve, when the slope is steep, the entity of the change in the DI of one heartbeat is matched by the entity of the change in the APD of the next heartbeat; so, the sum of APD and DI in the same heartbeat (basic cycle length) is

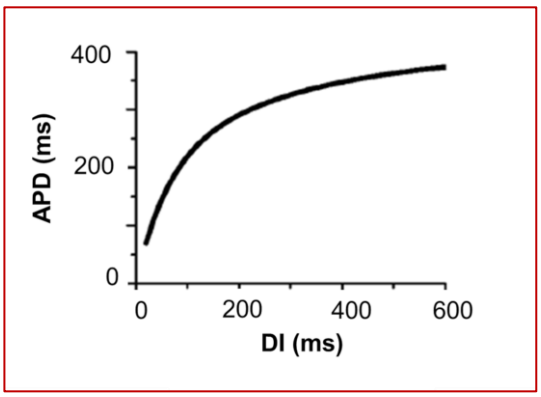

Figure 3.1.1. *Restitution curve: APD vs previous DI (Qu, 2010).*

constant and this results in a stable alternans phenomenon. Instead, when the slope is slight, high changes in the DI of one heartbeat is not matched by a comparable change in the APD of the heartbeat; this results in a non-alternans state. Experiments showed the slope of restitution curve can be reduced by changing kinetics of one or more ions across the cellular membrane (*Walker, 2003*). Anyway, interpretation of the restitution curve has to be careful and attentive, since the cellular mechanisms regulating the phenomenon can differ according to species and cell type (*Walker, 2003*). This information should be known to correctly interpret the curve in alternans vision.

In order to study "restitution hypothesis", a particular protocol was designed based on the direct control of DI. Experiments based on this protocol showed APD alternation can occur also in case of constant DI, suggesting that in some situations DI do not have to change to cause ADP alternation (*Tse, 2005*). Consequently, other factors may influence and may be at the pathogenesis of TWA.

The phenomenon referred to as cardiac memory is another important aspect to keep in consideration. Cardiac memory derives from the slow recovery of ion channels and from the gradual ion accumulation on one of the sides of the cell membrane. As a consequence, APD can depend not only from the just preceding DI, but also on the series of DI before (*Qu, 2010; Tse, 2005*). In this perspective, TWA/heart rate relationship is also described in terms of "rate-dependent alternans memory" (also called "hysteresis" (*Tse, 2005*)), born on the observation that microscopic TWA, after being induced by high atrial pacing, can continue also when reducing pacing rate below the values at which alternans was elicited (*Tse, 2005; Walker, 2003*). Thus, it seems that TWA can appear also at low heart rate, while it is decelerating relative to accelerating. Not only high heart rates, but also the dynamics of heart rates become important factors related to alternans. "Rate-dependent alternans memory" is reported both at level of the whole heart and at level of the single cardiac cell. Indeed, cardiac electrical alternans likely arises from alternans at cellular level (*Walker, 2003*). Experimental evidence about the role of Ca^{++} handling in ADP restitution dynamics are referred by many studies and agree that altered Ca^{++} handling dynamics may also cause alternans. Impairment in the kinetics of a component of cellular Ca^{++} cycling can cause a situation where Ca^{++} is not able to fully recover in each heartbeat, as it happens in normal homeostasis, but only in alternating heartbeat, i.e. in a condition of stable alternans. Thus, Ca^{++} cycling has surely a role in the mechanism of alternans, but the reciprocal role of alternans and intracellular Ca^{++} cycling represents an unresolved chicken and egg problem: impairment of Ca cycling can precede alternans, or, vice versa, alternans can precede impairment of Ca^{++} cycling. Nowadays, the first hypothesis is the most accredited one, but in any case, the role played by Ca^{++} handling in alternans phenomenon is clinically very interesting, because many cardiac pathologies have association with altered intracellular Ca^{++} handling (*Walker, 2003*). Other ions, like Na^{+} and K^{+}, seem to control the initial and final part of the APD restitution curve.

Many hypotheses were grown, and many are growing on the possible pathophysiological mechanism leading to alternans. The pathophysiological bases at the genesis of alternans phenomenon represent an open and not completely resolved debate.

3.2 Spatially Concordant and Discordant Alternans

APD alternans can be spatially concordant or discordant (*Qu, 2010*). In spatially concordant alternans, alternation occurs in phase throughout the cardiac tissue, i.e. APD is long throughout the whole cardiac tissue during one heartbeat, and it is short throughout the whole cardiac tissue during the following heartbeat. In discordant alternans, alternation occurs out of phase in neighboring regions of the cardiac tissue, i.e. APD is long in one region of the cardiac tissue during one heartbeat, and it is short in the adjacent region during the same heartbeat, and it changes phase in the following heartbeat. Discordant alternans occurs especially in case of short heartbeats and has been linked to life-threatening arrhythmias (*Qu, 2010; Mironov, 2008*). Moreover, spatially discordant alternans in the cardiac tissue can be triggered via a dynamical mechanism that does not require tissue heterogeneity (*Armoundas, 2002; Hayashi, 2007; Mironov, 2008*). About this hypothesis, it has been speculated that in case APD alternans occurs in a DI in which conduction velocity is stable, alternans is spatially concordant; on the contrary, in case APD alternans occurs in a DI in which conduction velocity is also changing, alternans can be spatially discordant (*Qu, 2010*).

QT interval and T wave are associated with APD and its spatial distribution pattern. Spatially discordant alternans implies a variation in conduction velocity and this manifests in the affection of the width and amplitude of QRS in the ECG. Thus, both TWA and QRSA can result. Indeed, experimental studies showed spatially concordant alternans results in only TWA in the ECG, whereas spatially discordant alternans results in both QRSA and TWA in the ECG (*Qu, 2010*).

3.3 Autonomic Nervous System Influence

Alternans can be induced in experiments where the heart is isolated with respect the autonomic nervous system, but it is known that the autonomic nervous system plays a fundamental role in physiologic conditions.

Although it is true that parasympathetic innervation of ventricles is limited, it seems that it plays a role in regulating ventricular electrophysiological characteristics. Indeed, preclinical studies found out that vagus nerve stimulation inhibit atrial and ventricular arrhythmias. Ventricular nerve stimulation seems to be able to decrease the maximum slope of restitution curve and electrical alternans (*Kulkarni, 2019*).

The result of sympathetic nervous system stimulation on the heart is complex and driven by the myocardium state. While in the normal ventricle sympathetic stimulation shows the capability to reduce arrhythmogenic tendency, in pathologic states sympathetic stimulation seems to become a stimulus for arrhythmias generation. In the literature, there are conflicting observations on the effect of sympathetic nervous system favoring or inhibiting alternans, especially if we consider experiments on isolated myocytes or experiments in vivo (*Walker, 2003*). Several experiments studied the effects of sympathomimetic drugs [l], e.g. β-adrenergic,

l) sympathomimetic drug: drug that mimics the effects of stimulation of the transmitting substances of the sympathetic nervous system, e.g. catecholamine, epinephrine (adrenaline), noradrenaline, dopamine, on various tissues; a sympathomimetic drug is also called an adrenergic drug.

and β-blockers [m]. β-Adrenergic stimulation seems to enhance the activity of Ca^{++} cycling proteins, maintaining Ca^{++} homeostasis under conditions that normally promote alternans (*Hüser, 2000*). On the other hand, β-blockers reduced TWA in case of coronary artery disease or left ventricular dysfunction (*Rashba, 2000a*). These conflicting findings may suggest the importance of considering levels of sympathetic tone at baseline in experiments in vivo. Also, more insights on β-blockers role in reducing mortality and prevent SCD in several cardiac diseases are needed.

Preclinical studies led to many clinical trials testing the vagus-nerve-stimulation efficacy in the treatment of cardiovascular diseases in patients, but they showed mixed results (*Kulkarni, 2019*). Many groups are trying to discover the mechanisms underlying the cardiovascular effects of vagus nerve stimulation. Thus, it keeps being an active area of preclinical and clinical researches, opening the possibility of non-pharmacological treatment for cardiac arrhythmias and cardiovascular pathologies like heart failure, hypertension, and myocardial infarction.

Defining autonomic nervous system influence on alternans may mean relevant clinical and therapeutic implications (*Walker, 2003*).

3.4 Clinical Utility

Clinical utility of TWA was the most tested in the literature among ECGA forms. TWA is recognized as a marker of long-term heart electrical instability, stratifying patients for implanted cardiac defibrillator therapy.

Recent studies have recognized its role as a predictor of short-term arrhythmia susceptibility. Heightened levels of TWA were observed within minutes before spontaneous ventricular tachyarrhythmia events in patients who previously experienced cardiac arrest or hospitalized for acute heart failure (*Kulkarni, 2019*). TWA changes measured from body surface ECG may predict acute arrhythmia vulnerability. Intracardiac electrogram obviously can provide more reliable assessment of the association between TWA and short-term arrhythmia vulnerability, being based on higher TWA magnitude. Nevertheless, a correlation between the two kinds of measurement exists. TWA magnitude measured on implanted cardiac defibrillator patients rises before spontaneous ventricular tachyarrhythmia events (*Kulkarni, 2019*). Detection of higher levels of TWA may be an important short-term predictor of impending ventricular tachyarrhythmia events and open to the possibility that prompt therapy may prevent them.

TWA can be able to drive therapy preventing the development of proarrhythmic substrate. Attempts to drive therapy depend on the ability to reliably detect TWA despite the region where it originates in the heart. Kulkarni et al. developed a new intracardiac electrode configuration able to detect TWA despite spatiotemporal heterogeneity. The ability to detect higher levels of TWA from implantable devices opens the door to adaptive pacing protocols, which may be incorporated into the implantable device: if an elevated level of TWA was measured, the adaptive pacing protocol would be triggered to restore the substrate in order to prevent ventricular tachyarrhythmia events (*Kulkarni, 2019*).

Most of the mechanisms pertaining to cardiac alternans nowadays comes from experimental and theoretical analysis of ventricular myocytes. More recently, there is evidence

m) β-Blocker: drugs with blocking action of β-adrenergic receptors.

enforcing the role of alternans in favoring arrhythmogenic substrates also in atria, suggesting that atrial alternans can be an index of vulnerability to severe atrial arrhythmias, e.g. atrial fibrillation. P-wave alternans have also been observed before and during atrial flutter preceding atrial fibrillation (*Siniorakis, 2017; Narayan, 2002*). Differences in physiology and action potential morphologies exist between atria and ventricles, but mechanisms of alternans origin seem to be common. Nevertheless, strategies to treat and control atrial and ventricular alternans may be different, given the evident differences that were found out (*Kanaporis, 2017*). Kanaporis and Blatter observed higher pacing rate threshold for triggering alternans in atria with respect to ventricles. Triggering and spreading of atrial arrhythmias may occur differently than ventricular arrhythmias (*Kulkarni, 2019*).

4

AUTOMATED DETECTION OF MICROSCOPIC ELECTROCARDIOGRAPHIC ALTERNANS

ECGA can appear in macroscopic and microscopic manifestations. Macroscopic ECGA is visible at naked eye by visually inspecting the ECG; it is related to malignant cardiac events and is the rarest form. Microscopic ECGA is not detectable by visual inspection, but it needs to be detected by digital signal-processing techniques. Microscopic ECGA is more frequent than macroscopic one, but it was demonstrated its clinical utility as a risk marker. Its importance can be justified considering that microvolt-level ECGA is detected on the ECG acquired on the body surface, but its genesis is at cellular level, where its magnitude is several orders greater than the corresponding magnitude at surface-ECG level (*Walker, 2003*). Many automated methods were reported to detect ECGA. Particularly, all the methods present in the literature were thought and implemented to detect only TWA; indeed, historically, it is the most investigated and studied ECGA form. Only very few of them have been adapted to detect alternans affecting the other waves (*Suszko, 2020*). Most methods from the literature are based on the short-time Fourier Transform of the heartbeat series. Some of the most used by literature are the fast-Fourier-transform spectral method, the complex-demodulation method, the modified-moving-average method, the Laplacian-likelihood method, the correlation method (CM) and the heart-rate adaptive match filter method (AMFM). The fast-Fourier-transform spectral method and the modified-moving-average method are available in commercial ECG machines, so they were widely used (*Burattini, 2009a*).

The fast-Fourier-transform spectral method employs a spectral method to measure alternans (*Smith, 1988*). All the ECG heartbeats are time aligned, and the power spectrum is computed for each sequence containing corresponding T-wave samples along the considered ECG. The power spectrum is defined as the squared magnitude of the fast Fourier transform. All the obtained spectra are then summed to have a cumulative spectrum related to all the T waves. In this spectrum a peak is identified at 0.5 cycle per beat (cpb): it is defined the alternans peak. Alternans measurement is performed through the alternans peak magnitude; alternans is detected only if this amplitude peak is greater than a threshold, based on predefined spectral noise. Indeed, two measures are the outputs of the method: the alternans magnitude and the alternans ratio, to be interpreted as the alternans statistical significance with respect the noise variability. The fast-Fourier-transform spectral method considers alternans uniformly distributed along the T-wave duration and gives one only value of alternans, valid for all the T waves of the considered ECG (*Armoundas, 2002; Burattini, 2009a*).

The complex-demodulation method models alternans through a sinusoid having frequency equal to 0.5 cpb, with varying amplitude and phase (*Nearing, 1991*). All the ECG

heartbeats are aligned, and T waves are divided in portions of 10 ms. Then, time series areas are defined, where each series is composed by areas of individual 10-ms portions from all the heartbeats. Each area of the series is high pass filtered and modelled as sinusoid multiplied by two times a complex exponential at the alternans frequency. The obtained signal is low pass filtered with a cutoff frequency of one fortieth of heart rate. Average amplitude over all the portions is defined as the alternans amplitude of each T wave.

The modified-moving-average method is based on the average of alternating heartbeats (*Nearing, 2002*). Heartbeats are divided into even and odd ones. Each heartbeat sample is computed and corrected to maintain track of its specific morphology and reduce the effect of noise. Alternans amplitude is given by the maximum absolute difference between even and odd heartbeats, considering only T waves. One alternans amplitude value for each couple even/odd heartbeat was obtained.

The Laplacian- likelihood method is based on the consideration of consecutive 32-beat ECG windows centered around the analyzed heartbeat (*Martinez, 2006*). The difference between each T wave and the previous one is computed. The obtained signal is modelled as alternans waveform plus noise with zero-mean Laplacian distribution. A generalized likelihood ratio test verifies the validity of alternans estimation.

CM is a time-domain technique based on a cross correlation procedure.

AMFM is based on a very narrow-band filtering of the ECG around the typical spectral alternans component. The filtered ECG results a pseudo-sinusoid: only if its zero-derivative points fall in correspondence of the T wave, alternans was considered present and its amplitude was based on the pseudo-sinusoid amplitude, otherwise the case is classified as non-alternans.

PWA and QRSA have been less investigated and most studies in the literature are case reports (*Brembilla-Perrot, 1997; Maury, 2002; McCarron, 2019; Pulignano, 1990 Rinkenberger, 1978; Siniorakis, 2017; Tsiaousis, 2016*). Nevertheless, PWA has been referred as a rare phenomenon predictor of atrial fibrillation (*Siniorakis, 2017*). P wave reflects atrial depolarization and its association with atrial electrical instabilities is possible. Analogously, representing QRS complex ventricular depolarization, QRSA association with supraventricular and ventricular tachycardias was observed (*Maury, 2002; Pulignano, 1990*). Thus, ECGA can be clinically introduced as a risk index of cardiac arrhythmia, specifically manifesting as severe ventricular arrhythmias, atrial fibrillations, and SCD in the worst cases. Moreover, recently, it was recognized that investigation of ECGA would deserve a wider perspective vision on the electrical activity of all cardiac cells (both atrial and ventricular ones) and on all phases of the heart cycle (both diastolic and systolic ones) (*Marcantoni, 2019a*). The fundamental requirement to make feasible studies on ECGA is the availability of reliable automated methods to identify and measure ECGA in all its possible forms, i.e. PWA, QRSA or TWA.

As far as it is known, algorithms especially thought and implemented to do this are not reported in the literature so far. The updated version of CM and the updated version of AMFM can be considered the first attempts to detect concurrently all possible forms of ECGA. CM results, by its nature, particularly affected by any artefacts, noises or interferences that may survive the preprocessing phase, while the AMFM is robust against noises and interferences, but, in its updated version, the alternans amplitude results overestimated when more than one only ECG wave is alternating (*Marcantoni, 2019a*).

The enhanced AMFM (EAMFM) is the first method specifically implemented to reliably identify and measure ECGA: PWA, QRSA and TWA are reliably and concurrently analyzed. It introduces as an output a new ECGA feature used the very first time in one of the applications of the updated version of AMFM: ECGA area. Moreover, on the contrary of many methods present in the literature, it provides alternans features heartbeat by heartbeat, not giving only a mean value representative of the whole ECG. Eventually, EAMFM overcomes the limitations of updated version of AMFM in the measurement of ECGA and results more robust against noises and interferences than CM. The only limitation of EAMFM is its applicability only on ECG that are longer than the clinically standard 10-s ECG (where, instead, CM and its updated version are still applicable).

A wider evaluation of the electrical cardiac alternans phenomenon in all its possible forms needs attention, in order to discover new cardiac risk indexes (e.g. PWA, QRSA, or ECGA in general) or to boost up the existent ones (e.g. TWA) in an integrated evaluation. Optimized digital signal-processing techniques are fundamental to pursue the goal.

4.1 Correlation Method: Original vs. Updated Version

4.1.1 Original Version

CM is a time-domain algorithm relying on a non-conventional correlation index (*Burattini, 1999*). It can deal with any length of the ECG and any sampling frequency equal or higher than 200 Hz. CM procedure basically consists of two steps:

- preprocessing step;
- alternans identification and measurement step.

The preprocessing usually consists of a low-pass filtering with a cutoff frequency of 45 Hz to reduce the high-frequency noise. Then, heart-rate stability is tested, evaluating RR standard deviation that can be considered as a heart-rate-variability assessment. If RR standard deviation is greater than 10% mean RR interval, the ECG cannot be analyzed and is rejected. Moreover, each QRS-complex morphology is tested, evaluating its correlation with the QRS-complex template. QRS-complex template is the median QRS complex over the ones present in the ECG. If the evaluated correlation is equal or less than a correlation threshold (0.8), the heartbeat is not considered a sinus heartbeat, but ectopic (i.e. resulting from an arrhythmic event) or affected by interference, noise, or artefact; so, in case, it is replaced by the QRS-complex template. If the amount of the replaced heartbeats is less than 10% the total amount of heartbeats (and the RR variability is equal or less than 10% mean RR), the ECG is considered suitable for the analysis. For suitable ECG, subtraction of baseline follows. Baseline is estimated through a third order spline interpolation of PR-interval fiducial points (located 80-100 ms before the R-peak positions in adult applications).

A procedure of sectioning is performed around the ECG wave of which alternans is analyzed. The sectioning can be performed either using annotations of fiducial points at the end of the waves or estimating them. Sectioned ECG-wave alignment is accomplished by means of a cross-correlation technique: the ECG-wave width is kept constant, but its position is let moving ±30 ms from the original one with predefined increments. Increments definition can be set as the reciprocal of the sampling frequency of the signal (e.g. if the sampling frequency is

1000 Hz the increment is 1 ms; if the sampling frequency is 200 Hz the increment is 5 ms; and accordingly for possible other sampling frequencies). For each position of the ECG wave, the cross-correlation coefficient between the ECG wave and the ECG-wave template, defined as the median ECG wave over all the heartbeats present in the ECG, is computed. Optimal alignment is the one corresponding to the highest correlation. After ECG-wave alignment, alternans is measured through an alternans correlation index (ACI), defined as in (3):

$$ACI_i = \frac{\sum_{j=1}^{N} wave_i(j) \cdot wave_{mdn}(j)}{\sum_{j=1}^{N} wave_{mdn}^2(j)}, \quad (3)$$

where $wave_i$ is the generic ECG wave, $wave_{mdn}$ in the median ECG wave, N is the number of samples encompassed in the ECG wave.

ACI is a dimensionless quantity, defined as the highest cross-correlation between the generic ECG wave and the ECG-wave template over the autocorrelation of the ECG-wave template. Considering all the heartbeats present in the ECG, ACI is a function of the number of heartbeats. ACI function can alternate around 1: if it is more than 1, ECG wave overcomes the template, while if it is less than 1, the opposite occurs. If ACI function is negative, ECG wave and the ECG-wave template have opposite polarity. Thus, if ACI function alternates around 1, alternans is monophasic, while if ACI function alternates around 0, alternans is biphasic. Particularly, alternans is detected if the number of alternating heartbeats overcomes a threshold of alternating heartbeats.

In the assumption ACI is more than 1:

$$ACI_i - 1 = \\ = \frac{\sum_{j=1}^{N} wave_{mdn}(j) \cdot wave_i(j) - wave_{mdn}(j)}{\sum_{j=1}^{N} wave_{mdn}^2(j)} \quad (4)$$

Moreover, assuming that all samples of the ECG wave alternates of the same quantity:

$$(wave_i(j) - wave_{mdn}(j)) \cdot 2 = A_{CM}(j) \quad (5)$$

where A_{CM} is the local alternans amplitude by CM, depending on the heartbeat, but not on the sample.

Eventually, alternans amplitude is estimated as:

$$A_{CM}(i) = 2 \cdot \left[|ACI_i - 1| \cdot \left(\frac{\sum_{j=1}^{N} wave_{mdn}^2(j)}{\sum_{j=1}^{N} wave_{mdn}(j)} \right) \right] \quad (6)$$

where the absolute value is justified by the fact that ECG wave can have positive or negative amplitudes.

A_{CM} is computed only for alternating heartbeats, otherwise it is set to zero. As a consequence, alternans amplitude is greater than zero if alternans is detected, or equal to zero if alternans is not detected.

4.1.2 Updated Version

The theory by which CM was conceived makes it easily adaptable to study either PWA, QRSA, or TWA, even if it was mostly used for TWA detection purpose; so, it is the same as the original version of the method but the ECG wave of interest. The method was modified and adapted to be sensitive to short alternans events; this was made possible dealing with two possible thresholds of consecutive alternating heartbeats necessary to detect alternans event: 7 heartbeats, as in its original implementation, or 5 in its updated implementation (*Marcantoni, 2019b*).

The method results, by its nature, particularly affected by any artefacts, noises or interferences (like that of respiration, which can affect especially QRSA analysis) that may survive the preprocessing phase. Nevertheless, it remains a reliable method to analyze ECGA in clinically standard 10-s ECG, where the subject is in a completely

resting condition, without even breathing. Indeed, this set up of acquisition would guarantee a clean ECG. In cases the acquisition set up cannot be in controlled conditions, the preprocessing of the signal is fundamental.

The output of the method is the alternans amplitude (AAm, μV), computed as the mean A_{CM} over the available heartbeats. If the ECG is particularly long consecutive or overlapping ECG windows (of 10 s or longer) can be extracted to have a trend in time of alternans and then also a mean/median AAm can be then computed to have also a representative value of the whole ECG tracing.

4.2 Adaptive Match Filter Method: Original vs. Updated Version

4.2.1 Original Version

The original version of AMFM is implemented to only analyze TWA (*Burattini, 2008*). The analysis procedure of the AMFM basically consists of two steps (analogously to CM):

- preprocessing step (the same of CM);
- alternans identification and measurement step.

AMFM is based on the assumption that alternans is characterized by a narrow frequency band (centered around half heart rate), instead of a single frequency (equal to half heart rate, by definition). This assumption makes the method able to account for limited variability of heart rate that is physiological. Under this assumption, AMFM is a 6^{th}-order bidirectional Butterworth passband filter. Its passing band is 0.12 Hz-wide and centered around the alternans frequency (half heart rate). If alternans occurs, the output of the filter is a pseudo-sinusoidal signal, amplitude modulated. If zero-derivative points of the pseudo-sinusoid fall in correspondence of T waves, TWA is detected and locally measured in amplitude (A_{AMFM}), as twice zero-derivative amplitude, and in position, as zero-derivative location with respect T-wave peak, in correspondence of each heartbeat. If zero-derivative points of the pseudo-sinusoid do not fall in correspondence of T waves, alternans is not detected. Thus, cases not classifiable as TWA are considered non-alternans cases. Eventually, if alternans does not occur, the output of the filter is a constant signal, of which amplitude is null. In case of TWA occurrence, the outputs of AMFM are the overall ECG alternans amplitude (AAm, μV) and the position (APos, ms) of alternans, computed as averaged local amplitudes and positions over all heartbeats, respectively; while in the other cases, AAm is set to zero and APos cannot be defined (*Burattini, 2008*).

4.2.2 Updated Version

As in the original version, in the updated AMFM, the ECG needs to be tested in its suitability for the analysis, before being fed to the algorithm: reduced heart rate variability (less than 10% of the mean RR interval) and few ectopic/noisy beats (less than 10% of the total number of heartbeats (NHB), which should be at least 32). Differently from the original version, in the updated version of AMFM, those cases in which zero-derivative points fall outside the T wave, are not considered as non-alternans cases, but, on the contrary, discriminated between PWA and QRSA. Thus, the updated version of the method can measure PWA, QRSA and TWA, but the outputs of the updated AMFM are AAm and APos of the prevalent alternans, defined on the barycenter of alternans. AAm is computed basing on the pseudo-sinusoid amplitude in correspondence of the wave that

is mostly alternating (as the original AMFM). APos is computed based on the barycenter of alternans and it is defined with respect to the relative R peak (positive values indicate positions following the R peak and vice versa) (*Marcantoni, 2019a*). Moreover, the updated version of the method was implemented so that it can be set for fetal and preterm applications, keeping in consideration that the fetal and preterm subjects have a lower ECG amplitude and more affected by interferences, due to modality of ECG acquisition, different from adult ones (e.g. the threshold for evaluating a fetal/preterm heartbeat as ectopic or too noisy is 0.7 (*Marcantoni, 2017*)) and also a different heart rate (due to the smaller heart dimensions than adults ones).

If the ECG is particularly long consecutive or overlapping ECG windows (of 32 heartbeats or longer) can be extracted to have a trend in time of alternans and then a mean/median AAm and APos can be then computed to have also representative values of the whole ECG tracing.

4.3 Enhanced Adaptive Matched Filter Method

EAMFM is thought to detect all forms of ECGA (i.e. PWA; QRSA; TWA). It represents the enhanced version of the AMFM (*Burattini, 2008*). EAMFM is designed to deal with ECG tracings including at least NHB equal to 32. In case of ECG tracings longer than 32 heartbeats, processing is still feasible because sliding and overlapping ECG windows including NHB (≥32) heartbeats are iteratively extracted until the end of the ECG is reached. Iteration is accomplished every certain number of seconds (NS) that has to be equal or greater than 1 s, **Fig. 4.3.1** (*Burattini, 2010; Burattini, 2016*). No limitations exist in the sampling frequency of the ECG to be processed, but it should be ≥ 200 Hz.

The EAMFM-based procedure basically consists of two steps:

- preprocessing step:
  - filtering;
  - ECG suitability assessment;
  - signal enhancement;
- alternans identification and measurement step:
  - signal filtering;
  - extraction of alternans features.

Being likely ECGA a lead-dependent phenomenon (like TWA (*Burattini, 2012b*)), the procedure has to be accomplished (in the same way) on each available lead.

The block diagram of EAMFM for automated identification and measurement of ECGA is shown in **Fig. 4.3.2**.

Preprocessing consists of high-frequency noise removal, R-peak identification, heartbeat segmentation and baseline removal. Thus, first, the ECG tracing is low pass filtered

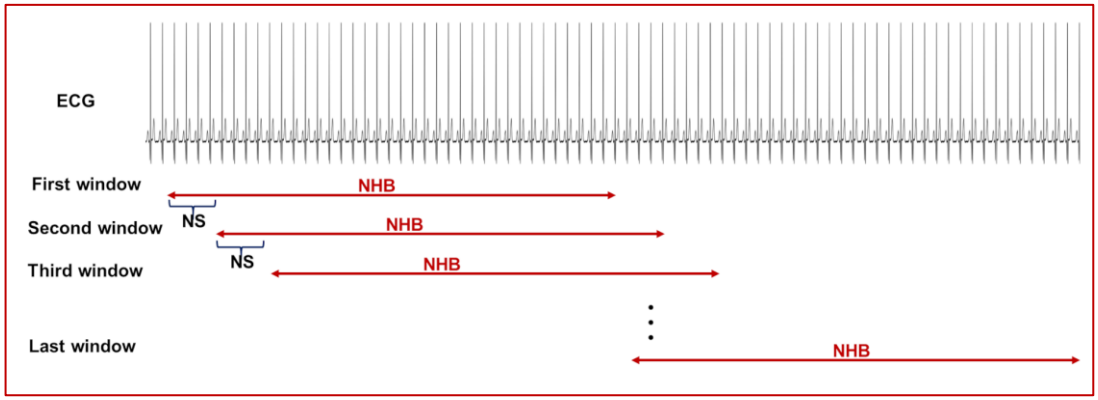

Figure 4.3.1. *ECG windowing procedure.*

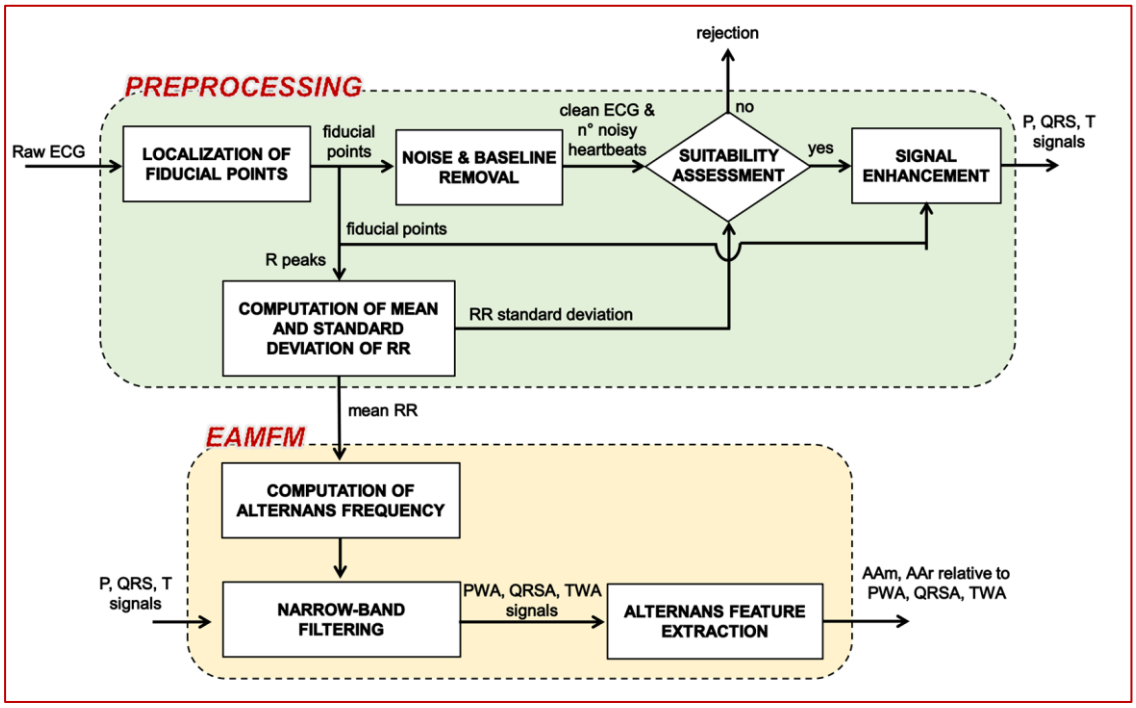

Figure 4.3.2. *Block diagram of the whole procedure for ECGA identification and measurement through EAMFM. P signal, QRS signal and T signal, which are the outputs of the preprocessing phase, are the inputs of the EAMFM (same name of the arrows in the block diagram).*

with a cutoff frequency of 35 Hz, through a 6th-order bidirectional Butterworth filter to attenuate high-frequency noise or interference. Then, R-peak detection has to be performed in case QRS complexes are not previously annotated and annotations made available in the database under analysis. Any R-peak-detection algorithm can be used for the purpose, such as the Pan Tompkins' algorithm, one of the most known and used (freely available). In heartbeat segmentation, each heartbeat is segmented between two fiducial points, P-wave onset and T-wave offset. Three adjoining sections are identified inside each heartbeat: one including P wave, another including QRS complex, and the last including T wave. More specifically, the first section is defined between P-wave onset (Pon) and Q-wave onset (Qon) and it is called P-wave section (P section); the second is defined between Qon and J point (J) and it is called QRS-complex section (QRS section); the third is defined between J and T-wave end (Tend) and it is called T-wave section (T section). If section landmarks are available in form of annotations (e.g. by cardiologists), they can be used as ECG-section landmarks, otherwise they have to be retrospectively estimated. A procedure of landmark identification based on experimental formulas (eventually adapted to the peculiar case under examination) or by visual inspection can be considered suitable. In general, in case of sinus rhythm, P section fills the 25-30% the heartbeat from Pon to Tend, QRS section fills the 20-25% the heartbeat from Pon to Tend, and T section fills the 45-55% the heartbeat from Pon to Tend (**Fig. 4.3.3**). The baseline wandering has to be reduced, if present; in this case, it can be computed through a cubic spline interpolation of fiducial points located in the PR interval (located 80-100 ms before the R-peak positions in adult applications) and linearly subtracted from the ECG tracing. Then, a procedure of replacement of artifacts and ectopic heartbeats follows, where noisy or non-sinus heartbeats are detected through a correlation-based technique. The correlation-

based technique implies that each heartbeat was previously sectioned into adjoint sections: P section, QRS section and T section, **Fig. 4.3.3**. Correlations between each ECG waveform included in the QRS and T sections and the corresponding ECG waveforms of the template heartbeat are estimated, where the template heartbeat is defined as the median one computed over all heartbeats. If correlations afferent to QRS and T waves are both higher than 0.85, the examined heartbeat is considered as a sinus heartbeat; otherwise, it is replaced by the template heartbeat. Number of replaced heartbeats (NRHB) is computed. Basing on R-peak positions, mean RR interval (s) and RR standard deviation (s) are estimated. The number of replaced heartbeats together with RR standard deviation are used in the suitability-assessment phase: if NRHB is lower than 10% NHB and RR standard deviation is lower than 10% mean RR, the ECG is assumed suitable for the analysis; on the contrary, the ECG is rejected from the analysis procedure. Specifically, the rejection of the ECG from the analysis stands for an a-priori evaluation of ECGA related to the ECG as possibly unreliable. The theoretic approach of the method would permit to detect alternans of ECG characterized by any heart rate and even by ectopic beats, but the suitability assessment prevents cases where ECGA is driven by variability of heart rate or influenced by occurrence of ectopic beats.

ECG considered as suitable go on with the analysis undergoing the signal-enhancement phase. The signal enhancement is performed by setting to baseline all ECG sections except the one of which alternans has to be evaluated. Consequently, from the single ECG three resultant enhanced signals are obtained (**Fig. 4.3.4**): the P signal (with all sections set to baseline except for P section); the QRS signal (with all sections set to baseline except for QRS section); and the T signal (with all sections set to baseline except for T section). In EAMFM, ECGA is studied on each wave in parallel. Indeed, the input of the following narrow-band filtering is different according to the ECG wave of which alternans is being detected (because of the signal enhancement).

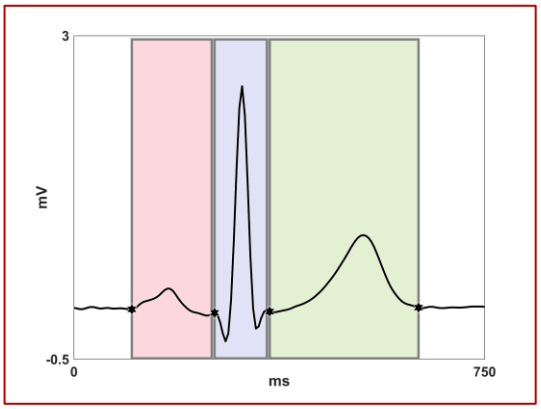

Figure 4.3.3. *The three adjoining sections inside a heartbeat: P section, highlighted in pink, from the P-wave onset, to the Q-wave onset; QRS section, highlighted in light blue, from Qon, to the J point; T section, highlighted in green, from J to the T-wave end. Stars localize section landmarks.*

In the non-physiological condition of stationary heart rate (i.e. without any heart-rate variability), alternans would be characterized by one specific frequency, defined as half heart rate. In the physiological condition of stable heart rate, having some limited variability, ECGA is characterized by a narrow frequency band centered around half mean heart rate.

The band-pass filtering phase of EAMFM extracts the alternans signal. Computing of the alternans frequency (1/(2·mean RR); Hz) is crucial for the implementation of the filter. Indeed, the band-pass filter is implemented as a 6th-order bidirectional (not to introduce any phase delay) Butterworth filter with cutoff frequencies of F_L and F_H, equal to 0.06 Hz higher and lower than alternans frequency,

respectively [18]. In Eq. (7) the filter transfer function:

$$|H(f)|^2 = |H_L(f)|^2 \cdot |H_H(f)|^2 = \\ = \frac{1}{1+\left(\frac{f}{F_L}\right)^6} \cdot \frac{\left(\frac{f}{F_H}\right)^6}{1+\left(\frac{f}{F_H}\right)^6} \qquad (7)$$

Thus, each of the three obtained signals (P signal, QRS signal and T signal) is filtered. The effect of the filter is the cancelation of any frequency component but the narrow band pertaining to ECGA and it gives in output a pseudo-sinusoidal signal. The pseudo-sinusoidal signal is different according to the input: if the input is the P signal, the pseudo-sinusoid signal is called PWA signal; if the input is the QRS signal, the pseudo-sinusoid signal is called QRSA signal; if the input is the T signal, the pseudo-sinusoid signal is called TWA signal. P signal, QRS signal and T signal have a different modulated amplitude. From each of them, two local features are extracted: heartbeat alternans amplitude (μV) and heartbeat alternans area (μV·ms). The first is defined as twice the alternans-signal amplitude (*Burattini, 2008*), while the other is defined as the product of the first and the time width of the analyzed wave (P-wave time width, QRS-complex time width, or T-wave time width). Both features are defined for each heartbeat included in the ECG window and then averaged over the heartbeats, obtaining AAm and overall ECG alternans area (AAr).

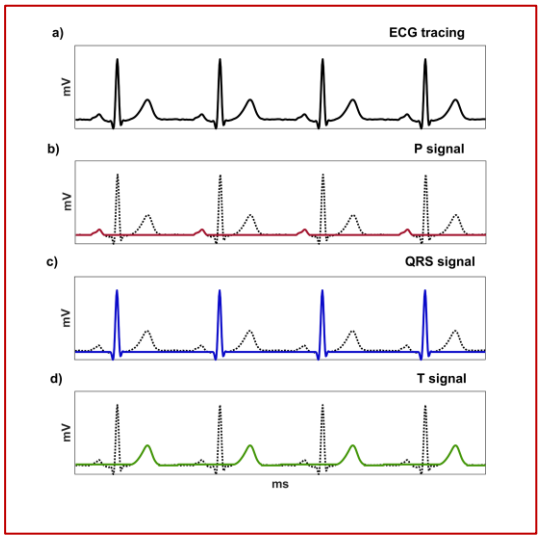

Figure 4.3.4. *Signal enhancement: from each ECG tracing (panel a), three signals are generated by setting to baseline all ECG segments except for the one of which occurrence of alternans has to be evaluated: P signal (panel b), QRS signal (panel c); T signal (panel d).*

Then, as in the updated AMFM, if ECG windows are iteratively extracted, a median/mean AAm and AAr over all the extracted windows can be computed.

Remarks

EAMFM is the first automated method able to identify and measure ECGA in all its possible single or multiple evidences and forms (i.e. PWA, QRSA or TWA). In order to do this, EAMFM performs an ECG sectioning discriminating the three ECG waves. Being cardiac alternans physiologically related to electrical activity of cardiac cells, the sectioning is accomplished only between P-wave onset and T-wave offset (ECG baseline reflects no electrical activity). Each ECG section has to completely include the wave, but the exact localization of ECG section landmarks is not crucial for EAMFM aim.

EAMFM has a more general applicability than most of the existing alternans detecting methods because it can deal with ECG signals acquired in many clinical conditions. Indeed, being basically implemented as a band-pass filter, it can tolerate physiological heart-rate-variability levels; moreover, being the filter characterized by a very narrow passing band, it results robust against interferences and noises in most frequency bands. The filtering procedure does not change the phase of the ECGA frequency component because it is applied in bidirectional mode.

The application-customized setting of the number of beats to be included in the analyzed ECG window, as well as of the period of ECG-window extraction widens applicability range of the method. Indeed, also ECG recording performed with high level of heart-rate variability can be analyzed, since extraction of short ECG windows allows to adapt to the local heart rate, respecting in the meantime the fundamental criterion of stable heart rate for alternans detection inside each ECG window. Moreover, ECG recording performed even in presence of some ectopic beats or local artefacts can be analyzed, since reduced period of ECG window extraction allows to reliably detect alternans in the ECG sections that are adjacent to ectopic heartbeat/artefact, avoiding that it can bias alternans interpretation and in the meantime that several clean sinus heartbeats are excluded from the analysis (relevant aspect in case of short ECG recordings).

The technical methodological improvement of the method with respect is original implementation consists in the enhancement phase of the procedure, besides the extraction of a new feature that is the alternans area, in the feature-extraction phase. The enhancement phase represents the core of this new method and is crucial in the reliable alternans identification in case of multiple wave alternans, but also in case of single wave alternans. The application of the band-pass filter is common between the original AMFM and EAMFM, but the enhancement phase completely changes its effect. In general, the output of the band-pass filter is a pseudo-sinusoidal signal of which amplitude modulation integrates all the possible alternans present in the input signal. As a consequence, if the input signal includes the P section, the QRS section and the T section (as in the approach of original AMFM implementation), the pseudo-sinusoidal signal is amplitude modulated by the alternans possibly affecting all the ECG sections and the AAm quantification referring to P section or QRS section or T section will be affected by the reciprocal influence of alternans on the different ECG sections. On the contrary, if the input signal includes only P section/QRS section/T section, the pseudo-sinusoidal signal is amplitude modulated only by the alternans possibly affecting singularly one of the ECG sections and AAm quantification referring to P section or QRS section or T section is reciprocally independent and so, more reliable. Practically, in the original version of the AMFM, alternans, i.e. TWA, was assessed as present checking that zero-derivative points occur in correspondence of T waves. Nevertheless, it should be considered that they actually occur in correspondence of the center of mass of all ECG fluctuations (e.g. if PWA and TWA are concurrently occurring, the alternans center of mass will fall between the two fluctuating waves and the phenomenon will be erroneously interpreted as QRSA). The signal enhancement phase overcomes this issue because it makes the alternans analysis reciprocally independent among ECG sections, by maintaining only the section of interest in the ECG tracing that will be the input of the narrow-band filter, while deleting the others. Obviously, the new approach of EAMFM implies that the band-pass filter to be applied three times, on all the three signals coming from the enhancement phase.

The band-pass filtering procedure assumes, by its nature, that alternans is uniformly distributed along the wave of interest and this implies that the same alternans amplitude relative to ECG waves of different time durations may likely involve a different cardiac tissue extension, so a different quantity of cardiac cells of which the action potential is alternating. AAr computation overcomes this issue keeping in consideration the time duration of the wave, and so indirectly the cumulative effect of the cells involved in its alternation. AAr is preliminarily defined as an area under a rectangle, assuming that all the wave is affected uniformly by the alternans

phenomenon. This seems realistic in case of spatially concordant alternans. Moreover, this assumption of uniform profile for alternans along the affected wave is common to other methods, as the fast-Fourier-transform spectral method, the complex-demodulation method, the Laplacian- likelihood method and the original AMFM (*Burattini, 2009a*). Nevertheless, a different AAr evaluation can be thought in order to generalize its applicability.

From a clinical point of view, a reliable quantification of alternans would permit a correct evaluation and interpretation of entity of the possible electrophysiological anomaly, without overestimation, underestimation and consequent misinterpretations. Besides this aspect, a physical localization of the cardiac tissue (atrial or ventricular) together with a correct identification of the amount of cells actually involved in the electrophysiological anomaly (possible with future optimizations of the method, possibly including an intra-wave ECG sectioning) can become a crucial starting point, in a more practical clinical perspective, to allow an investigation of the triggering causes of alternans and an intervention to recover a normal electrophysiological function.

5

SIMULATED STUDY FOR TESTING THE UPDATED ADAPTIVE MATCH FILTER METHOD

The testing of the updated AMFM was accomplished through its application in controlled conditions, i.e. through a simulated study (*Marcantoni, 2019a*).

Simulated Data

The testing of the updated version of AMFM was performed on a small cohort of synthetic ECG data. Synthetic ECG tracings were achieved by 128-fold joining the same single clean heartbeat, previously extracted from a real ECG acquisition (*Burattini, 2012a*). Each single heartbeat was 750 ms long and sampled at 200 Hz. For each ECG wave the onset and offset were identified: P-wave onset and offset were set at 195 ms and 95 ms before the R peak, respectively; QRS-complex onset and offset were set at 40 ms before and 40 ms after the R peak, respectively; T-wave onset and offset were set at 100 ms and 300 ms after the R peak. ECGA was applied to the synthetic ECG tracings, considering a uniform rectangular profile, in which alternans was equally distributed all along the fluctuating wave. Three alternans ECGA sets were synthesized, considering different simulated alternans amplitude (10 μV, 100 μV and 200 μV). Particularly, each set included three ECG tracings simulating single wave alternans (i.e. only PWA, only QRSA and only TWA) and four ECG tracings simulating multiple wave alternans in all possible combinations. One ECG tracing not influenced by any alternans was also synthetized.

Statistics

Performance on AAm estimation by updated AMFM was assessed computing the error (ε, %), defined as the percentage difference between the estimated AAm by updated AMFM and the simulated alternans amplitude. Alternans underestimations are identified by negative values of the error, and analogously alternans overestimations are identified by positive error.

Results

Simulation results are reported in **Table 5.1**. ECGA absence was correctly identified and measured (ε: 0%), while APos could not be assessed. AAm in cases of single wave alternans was also correctly identified and measured: ε is at most 1% in case of 200 μV-amplitude PWA (mean ε: 0%). APos in these cases was identified around middle part of the alternating wave. AAm in cases of multiple wave alternans was estimated with higher ε. AAm was always overestimated (mean ε: 42%); particularly, when TWA occurred combined to PWA or QRSA, TWA was identified as the prevalent alternans with an AAm overestimation (mean ε: 23%); when PWA and QRSA occur together, PWA was

Table 5.1. *Results of the simulated study in terms of simulated alternans amplitude and estimated AAm and APos by updated AMFM for all combinations of PWA, QRSA and TWA (Marcantoni, 2019a).*

Simulated alternans amplitude (μV)	Alternating wave	PWA		QRSA		TWA	
		AAm (μV)	APos (ms)	AAm (μV)	APos (ms)	AAm (μV)	APos (ms)
0	-	0	-	0	-	0	-
10	T	-	-	-	-	10	+200
	QRS	-	-	10	-1	-	-
	QRS-T	-	-	-	-	13	+149
	P	10	-146	-	-	-	-
	P-T	-	-	-	-	12	+100
	P-QRS	17	-95	-	-	-	-
	P-QRS-T	-	-	-	-	15	+100
100	T	-	-	-	-	100	+200
	QRS	-	-	100	0	-	-
	QRS-T	-	-	-	-	128	+149
	P	100	-145	-	-	-	-
	P-T	-	-	-	-	116	+100
	P-QRS	172	-95	-	-	-	-
	P-QRS-T	-	-	-	-	151	+100
200	T	-	-	-	-	200	+200
	QRS	-	-	200	0	-	-
	QRS-T	-	-	-	-	257	+149
	P	201	-145	-	-	-	-
	P-T	-	-	-	-	232	+100
	P-QRS	343	-95	-	-	-	-
	P-QRS-T	-	-	-	-	301	+100

identified as the prevalent alternans, with an AAm overestimation (mean ε: 71%). Furthermore, in these cases, APos was not identified in the middle part of the wave classified as affected by prevalent alternans, but it resulted moved towards one of the two wave sides. Thus, in cases of multiple alternans, prevalent alternans was usually defined as TWA and located in the first middle part of the T wave.

Remarks

In the approach of the updated AMFM, the procedure estimates AAm and APos related to the ECG wave that is identified as the mostly alternating. The updated AMFM is specific, being able to identify absence of alternans. Furthermore, it is able to correctly identify TWA in all cases it is present. The method filters the ECG tracing in a very small band, so the output is a pseudo-sinusoid with maxima and minima (i.e. local zero-derivative points) located where the center of alternans distribution falls in each heartbeat, i.e. where its barycenter falls. Single wave alternans are correctly identified: the method can identify them according to the barycenter position, and then, it can measure them without errors. The updated AMFM identifies TWA as the prevalent alternans in all cases T wave is fluctuating together with the other waves. Indeed, the barycenter

position is affected by the duration of the alternating waves, if alternans has the same morphology and amplitude along the wave and T wave is the longest among the three considered ECG waves. For the same reason, in case TWA does not occur, between PWA and QRSA, PWA was usually identified as the prevalent alternans, since P wave is longer than QRS complex. AAm is always overestimated in case of multiple wave alternans because the wave identified as the mostly alternating is influenced by the oscillation of the other/s wave/s. This is confirmed by APos, no more identified exactly on the center of the alternating wave. The reliable identification of the wave mostly fluctuating is useful to localize a possible electrophysiological cardiac anomaly, between atrial and ventricular. Moreover, the method can reveal alternans absence and can reliably quantify alternans amplitude in the assumption that the anomaly affects only one ECG wave. Nevertheless, in the occurrence of alternans on more than one wave, the existence of the anomaly, as well as its entity, reflecting in a high or low alternans amplitude, remain unreliable, since quantification is unreliable. Even if in clinical applications, overestimation of the entity of an anomaly is preferable then underestimation. In general, this makes not very reliable the quantification of the alternans through the updated version of AMFM in any case because in real applications it is not possible a-priori assessing single or multiple alternans. Pointing out these limitations was fundamental to design EAMFM. In a perspective oriented to the optimization of available resources, knowledge and testing of existing methods is essential to be aware both of the signal-processing approaches to keep and of the limits to overcome in designing of new optimized analysis methods.

6

SIMULATED AND EXPERIMENTAL STUDIES FOR TESTING THE ENHANCED ADAPTIVE MATCHED FILTER METHOD

The testing of the EAMFM was performed applying it in controlled conditions, i.e. through a simulated study to evaluate its performance, and also in 266 heart failure patients with implanted cardiac defibrillator, i.e. through an experimental study, to evaluate its applicability in a real scenario.

6.1 Simulated Study

Simulated Data

The primary ECG for the simulation derives from the 64-fold repetition of a clean heartbeat extracted by a real ECG acquisition on a healthy subject. The heartbeat consists of an PQRST complex, sampled at 200 Hz, 750 ms long and not affected by any noise or interference (*Burattini, 2012a*). The most evident ECG waves (i.e. P wave, R wave and T wave) are monophasic, with a positive polarity; their amplitudes were: 0.24 mV, 2.76 mV and 0.77 mV, respectively. In each heartbeat, ECG sections necessary for alternans measurement by EAMFM are located so that the P section (150 ms long) is included between 200 ms and 50 ms before the R peak, the QRS section (100 ms long) is defined between 50 ms before and 50 ms after the R peak, the T section (270 ms long) is defined between 50 ms and 320 ms after R peak.

The synthetic ECG was corrupted by stationary alternans; particularly, an alternating rectangular waveform was added to the different considered ECG waves (*Burattini, 2009a*). Both low-amplitude and high-amplitude microscopic ECGA were considered, through the following simulated alternans amplitudes: 10 μV and 100 μV. Consequently, if simulated alternans amplitude was 10 μV, relative simulated alternans area values for PWA, QRSA and TWA were 1000 μV·ms, 800 μV·ms and 2000 μV·ms, respectively; if simulated alternans amplitude was 100 μV, relative simulated alternans area values for PWA, QRSA and TWA were 10000 μV·ms, 8000 μV·ms and 20000 μV·ms, respectively. All combinations of alternans forms were considered, **Fig. 6.1.1**. Overall, 27 simulations (indicated as S1 to S27), reflecting combinations of alternans forms (i.e. PWA and/or QRSA and/or TWA) with low-amplitude and high-amplitude microscopic ECGA were used to test the EAMFM, **Table 6.1.1**. If each beat is 750 ms long, the heart rate is constantly equal to 80 bpm and alternans frequency is 0.67 Hz.

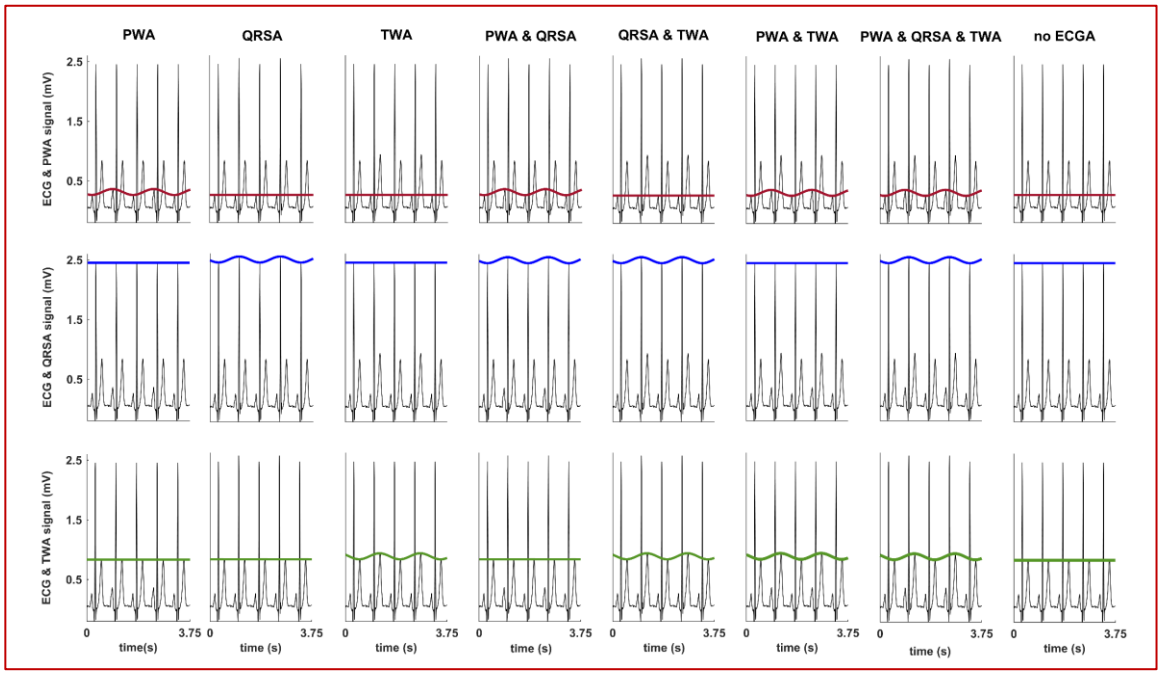

Figure 6.1.1. *Examples of ECG affected by possible combinations of PWA, QRSA and TWA, together with the three corresponding alternans signals (PWA signal in red, QRSA signal in blue and TWA signal in green lines). Case of no ECGA is also depicted.*

Statistics

EAMFM performances were estimated computing ε (%), defined as the percentage difference between the estimated AAm (or AAr) and the simulated alternans amplitude (or alternans area). The definition of ε, computed using AAm is the same as using AAr, since AAr is AAm by wave time width. Alternans underestimations are identified by negative values of the error, and analogously alternans overestimations are identified by positive error.

Results

Simulation results are reported in **Table 6.1.1**, where simulated alternans amplitude and area and estimated AAm and AAr are shown, and **Table 6.1.2.**, where values of ε are shown. Overall, EAMFM was able to accurately measure AAm and AAr. Alternans absence was correctly identified (ε=0%), both when affecting only one wave (S4 to S6, S11 to S13, S15 to S20), two waves (S1 to S3, S8 to S10) and all waves (S27). Low-amplitude microscopic alternans (S1 to S7 and S15 to S26) was exactly estimated (ε=0%), regardless of which are the alternating waves or how many alternating waves there are. High-amplitude microscopic alternans (S8 to S26) was underestimated, but negligibly (-2%≤ε≤-1%). PWA was less underestimated than QRSA and TWA.

Remarks

The simulated study demonstrates EAMFM ability to reliably identify all possible single or multiple evidences and forms of ECGA, regardless of amplitude and avoiding false-positive detections (e.g. due to reciprocal influence in case of multiple evidence). Signal-enhancement phase was resolutive to reach such results. This is confirmed by preliminary results obtained by the application of the updated AMFM, in which the signal enhancement was not present (*Marcantoni, 2019a*). Alternans of single waves is reliably measured, while if involving more than

one wave, AMFM overestimated it. As an example, in case of PWA and QRSA were occurring simultaneously, only PWA would be identified (P wave is longer than QRS complex) with significant errors for PWA measurement: practically, QRSA would not be identified, but its actual occurrence would provoke an overestimation in PWA measurement. For multiple wave alternans with the same amplitude that include also T wave, always only TWA would be identified and highly overestimated in amplitude, since it is the longest among the three waves. For multiple wave alternans with different amplitudes, only the wave in correspondence of which the center of mass fell would be identified as alternating and highly overestimated in amplitude (its value would depend on the different alternans entities).

EAMFM keeps the signal-processing approach of AMFM, based on exploiting the frequency band pertaining alternans because it guarantees robustness against noises and interferences in most of frequency bands. At the same time, considering that PWA, QRSA and TWA frequency bands are completely overlapped, it hampers the discrimination of different forms of ECGA and reliability of ECGA quantification. This is a big limitation in ECGA analysis of updated AMFM, as of all frequency-domain methods adopting similar approach. EAMFM successfully overcomes these issues because filtering is not performed on the same signal but on three different signals, each maintaining only the ECG wave of interest. Moreover, entity of ECGA depends on the duration of the wave, in turn influenced by the number of cardiac cells involved in the electrophysiological process, and this is the reason why EAMFM introduces quantification of AAr.

Table 6.1.1. *Results of the simulated study in terms of simulated alternans amplitude and area and estimated AAm and AAr by EAMFM for all combinations of PWA, QRSA and TWA, characterized by low amplitude (10 μV) and high amplitude (100 μV).*

Simulated Signal	Simulated alternans amplitude;area (μV;μV·ms)			AAm;AAr (μV;μV·ms)		
	PWA	QRSA	TWA	PWA	QRSA	TWA
S1	10;1000	0;0	0;0	10;1000	0;0	0;0
S2	0;0	10;800	0;0	0;0	10;800	0;0
S3	0;0	0;0	10;2000	0;0	0;0	10;2000
S4	10;1000	10;800	0;0	10;1000	10;800	0;0
S5	0;0	10;800	10;2000	0;0	10;800	10;2000
S6	10;1000	0;0	10;2000	10;1000	0;0	10;2000
S7	10;1000	10;800	10;2000	10;1000	10;800	10;2000
S8	100;10000	0;0	0;0	99;9900	0;0	0;0
S9	0;0	100;8000	0;0	0;0	98;7840	0;0
S10	0;0	0;0	100;20000	0;0	0;0	98;19600
S11	100;10000	100;8000	0;0	99;9900	98;7840	0;0
S12	0;0	100;8000	100;20000	0;0	98;7840	98;19600
S13	100;10000	0;0	100;20000	99;9900	0;0	98;19600
S14	100;10000	100;8000	100;20000	99;9900	98;7840	98;19600
S15	10;1000	100;8000	0;0	10;1000	98;7840	0;0
S16	100;10000	10;800	0;0	99;9900	10;1000	0;0
S17	10;1000	0;0	100;20000	10;1000	0;0	98;19600
S18	100;10000	0;0	10;2000	99;9900	0;0	10;2000
S19	0;0	10;800	100;20000	0;0	10;1000	98;19600
S20	0;0	100;8000	10;2000	0;0	98;7840	10;2000
S21	10;1000	10;800	100;20000	10;1000	10;800	98;19600
S22	10;1000	100;8000	10;2000	10;1000	98;7840	10;2000
S23	100;10000	10;800	10;2000	99;9900	10;800	10;2000
S24	100;10000	100;8000	10;2000	99;9900	98;7840	10;2000
S25	100;10000	10;800	100;20000	99;9900	10;800	98;19600
S26	10;1000	100;8000	100;20000	10;1000	98;7840	98;19600
S27	0;0	0;0	0;0	0;0	0;0	0;0

Table 6.1.2. *Results of the simulated study in terms of errors in alternans estimation (ε) for all combinations of PWA, QRSA and TWA, characterized by low amplitude (10 μV) and high amplitude (100 μV).*

Simulated Signal	PWA ε (%)	QRSA ε (%)	TWA ε (%)
S1	0	0	0
S2	0	0	0
S3	0	0	0
S4	0	0	0
S5	0	0	0
S6	0	0	0
S7	0	0	0
S8	-1	0	0
S9	0	-2	0
S10	0	0	-2
S11	-1	-2	0
S12	0	-2	-2
S13	-1	0	-2
S14	-1	-2	-2
S15	0	-2	0
S16	-1	0	0
S17	0	0	-2
S18	-1	0	0
S19	0	0	-2
S20	0	-2	0
S21	0	0	-2
S22	0	-2	0
S23	-1	0	0
S24	-1	-2	0
S25	-1	0	-2
S26	0	-2	-2
S27	0	0	0

6.2 Experimental Study [n]

Clinical Data

Experimental data consisted of 12-lead ECG recordings, acquired from 266 heart failure patients with an implanted cardioverter defibrillator for primary prevention. During the acquisitions, the patients underwent a bicycle exercise test that lasted 10 min. ECG were recorded by a CASE 8000 stress test recorder (GE Healthcare, Freiburg, Germany), having a sampling frequency of 500 Hz and a resolution of 4.88 μV/LSB. Electrodes (3M Red Dot ECG Electrode Soft Cloth 2271) were applied following the Mason-Likar configuration.

The data belong to the Leiden University Medical Center ECG database (*Burattini, 2016*). According to "Guideline for Good Clinical Practice" (European Medicines Agency, CPMP/ICH/135/95) and the data privacy law in The Netherlands, no patients' informed consent was needed because their data were anonymized and were recorded during routine medical care, without experimental interventions.

ECGA study was accomplished through an iterative (NS=2 s) extraction of ECG windows (NHB=64). Suitability of each lead was assessed independently. An enrolment criterium was introduced for the patients: each patient had to have at least one ECG window with a stable heart rate (i.e. RR standard deviation < 10% mean RR) and 9 leads having a number of replaced beats not greater than 5 (i.e. lower than 10% NHB), to be enrolled in the study. For enrolled patients having more than one suitable ECG window, only the first one was considered.

Statistics

Each suitable lead was characterized by six measures, that were AAm and AAr values for PWA, QRSA and TWA, respectively. ECGA form with the highest AAr was identified as the prevalent alternans. AAm and AAr distributions over implanted-cardiac-defibrillator patients or over leads were expressed in terms of median value and interquartile range (iqr). Comparison between distributions were accomplished by the Wilcoxon signed rank test, where statistical significance level (p) was set at 0.05.

Results

Overall, 187 patients out of the 266 totally available in the considered database (70.3%) met the enrolment criterium of the study. Results are reported in **Table 6.2.1** and **Table 6.2.2**. **Table 6.2.1** reports the prevalence rate referring to PWA, QRSA and TWA, rate of alternans absence and rate of rejected windows (RW). Alternans absence rate was always low, ranging between 0% and 4%. RW was very high on lead I (65%) and aVL (40%), moderate on lead aVR (13%), and small (<10%) in the other leads. **Table 6.2.2** reports AAm and AAr values for PWA QRSA and TWA, where distributions are expressed as median (iqr). In case of alternans presence, AAm and AAr values vary among leads and in each lead AAr varies among ECGA forms, so prevalent alternans was always discriminated. For all leads, TWA was identified as the prevalent alternans, followed by QRSA and PWA. From a clinical point of view, AAm values are comparable among

n) Parameters used in the experimental study: RW: rate of rejected ECG windows.

ECGA forms of the same lead and lower than 10 μV, even if they were statistically different in some cases. Higher AAr values referring to TWA were only due to different duration of ECG waves (i.e. T wave is the longest).

Remarks

In a real scenario all ECGA forms may be simultaneously present and one form may be discriminated from the others as the prevalent. Heart failure patients with an implanted cardiac defibrillator are known to be at increased risk of cardiac complication usually related more to ventricles than to atria (*Man, 2011*) and indeed, in this experimental study, TWA is the prevalent ECGA form, followed by QRSA. The application to a real population put in evidence the need to consider both intensity and duration of alternans phenomenon to reliably compare among ECGA forms, practically it is necessary to combine AAm and wave duration. EAMFM uses AAr to integrate them in one parameter only. This observation was already suggested by the evaluation of alternans barycenter movement in the analysis performed through the updated version of the AMFM. Indeed, it might occur, as in this experimental study, that ECGA forms have comparable AAm, so comparison and discrimination among ECGA forms is possible through AAr.

Future evaluations will be performed to demonstrate the incremental clinical utility of ECGA as an index of cardiac risk, with respect to only TWA evaluation. To reach this aim, definition of reliable physiological reference values for PWA, QRSA and TWA is very important. Indeed, regarding TWA, it was observed the existence of physiological levels, i.e. low levels of AAm and a reduced duration of the phenomenon in healthy people (*Burattini, 2009b*). Under some particular conditions, due for example to cardiac pathologies, TWA reach higher levels, revealing a higher predisposition to develop malignant arrhythmias (*Burattini, 2009b*), playing its role as risk marker. Probably the mechanism underlying the physiological TWA is different with respect to that underlying pathological TWA. Nowadays, there are no fixed threshold levels, but they may reveal useful in clinical practice. As a consequence, assessment of ECGA in all its forms in a healthy population is fundamental to assess physiological levels and allow detecting anomalous cardiac conditions. Reference values for PWA and QRSA in healthy populations are not available, but also TWA reference values (available for example in studies analyzing healthy populations by original AMFM) should be revised, since it cannot be ruled out that they are affected by reciprocal influences for the concurrent occurrence of QRSA or PWA.

Table 6.2.1. *Results of experimental study in terms of rate of PWA, QRSA, TWA, ECGA absence and RW.*

Lead	PWA (%)	QRSA (%)	TWA (%)	No ECGA (%)	RW (%)
I	4	5	23	3	65
II	4	13	80	0	3
II	5	14	72	0	9
V1	3	17	69	2	9
V2	5	19	70	2	4
V3	3	14	75	2	6
V4	6	20	67	2	5
V5	4	19	65	1	11
V6	6	18	66	3	7
aVR	7	10	66	4	13
aVL	5	11	42	2	40
aVF	3	13	79	1	4

Table 6.2.2. *Results of experimental study in terms of estimated AAm and AAr values referred to PWA, QRSA and TWA.*

ECG lead	ECGA features	PWA Median (iqr)	QRSA Median (iqr)	TWA Median (iqr)
I	**AAm (μV)**	4 (6)	6 (7)	5 (5)
	AAr (μV·ms)	426 (602)*	500 (548)*	902 (933)
II	**AAm (μV)**	8 (8)	11 (11)*	9 (7)
	AAr (μV·ms)	760 (763)*	890 (904)*	1725 (1390)
III	**AAm (μV)**	7 (7)	11 (12)*	9 (6)
	AAr (μV·ms)	728 (787)*	890 (1006)*	1706 (1367)
V1	**AAm (μV)**	4 (5)	9 (8)*	6 (6)
	AAr (μV·ms)	352 (498)*	693 (642)*	1124 (1199)
V2	**AAm (μV)**	4 (7)	10 (13)*	7 (8)
	AAr (μV·ms)	449 (624)*	828 (1086)*	1454 (1606)
V3	**AAm (μV)**	6 (7)	12 (13)*	8 (9)
	AAr (μV·ms)	575 (732)*	955 (1062)*	1629 (1814)
V4	**AAm (μV)**	5 (7)	10 (10)*	7 (6)
	AAr (μV·ms)	534 (679)*	826 (851)*	1496 (1320)
V5	**AAm (μV)**	5 (7)	11 (13)*	8 (8)
	AAr (μV·ms)	547 (651)*	891 (1042)*	1533 (1725)
V6	**AAm (μV)**	5 (6)	9 (9)*	6 (6)
	AAr (μV·ms)	501 (676)*	750 (791)*	1267 (1313)
aVR	**AAm (μV)**	5 (6)	7 (7)*	6 (5)
	AAr (μV·ms)	506 (602)*	547 (584)*	1136 (997)
aVL	**AAm (μV)**	5 (5)	8 (7)	5 (4)
	AAr (μV·ms)	500 (458)*	623 (566)*	1059 (930)
aVF	**AAm (μV)**	7 (7)	9 (12)*	8 (7)
	AAr (μV·ms)	665 (708)*	750 (980)*	1549 (1256)
Total	**AAm (μV)**	**5 (7)**	**9 (10)**	**7 (6)**
	AAr (μV·ms)	**545 (648)**	**762 (839)**	**1382 (1321)**

7

T-WAVE ALTERNANS IN CONDITIONS OTHER THAN CARDIAC PATHOLOGY

TWA analysis is more recent with respect to other risk markers, like the QT interval or the reduced ventricular ejection fraction. So, it still misses to be deeply analyzed in certain conditions, like in association with drug assumption, in case of pathologies not directly afferent to the heart, e.g. epilepsy, in the fetal period, or in case of prematurity, here considered (*Marcantoni, 2017; Marcantoni, 2018a; Marcantoni, 2018b; Marcantoni, 2019b; Marcantoni, 2020c*). Below, four clinical studies are reported in conditions that are other than cardiac pathology (†).

7.1 Association with Dofetilide Assumption: A Clinical Study

Hundreds of studies that have enrolled more than ten thousand patients have validated the predictivity of TWA in highlighting the susceptibility to cardiac mortality and SCD. The main purpose has been to use TWA as decision-making factor for cardioverter-defibrillator implantation. The vision that TWA may be used to guide clinical pharmacologic intervention has a great potential, but it is not so much investigated still. Particularly, TWA can be used as a therapeutic marker of antiarrhythmic or proarrhythmic effects (*Verrier, 2010*).

Nowadays, prescription of antiarrhythmic drugs raises, and its use is bound to increase due to the aging of population. Longer life expectation implies a higher incidence of arrhythmias (e.g. atrial fibrillation and atrial flutter) and it is important to recover a normal rhythm, if it is compromised (*Jaiswal, 2014*). Antiarrhythmic drugs help maintaining the sinus rhythm in case pathophysiological conditions do not allow the heart to keep a regular electrical function independently. Nevertheless, agents constituting the antiarrhythmic drugs do not have always a benign effect and they can even become proarrhythmic (*Jaiswal, 2014*). Dofetilide is one of the antiarrhythmic drugs, used in case of atrial fibrillation, the most common arrhythmia requiring drug treatment. Dofetilide was approved by the Food and Drug Administration in 1999 to reverse atrial fibrillation and atrial flutter and maintain sinus rhythm in symptomatic patients. Dofetilide selectively acts on a single K^+ channel, the delayed rectifier K^+ current, inhibiting one of its components. Its effect is prolonging the action potential and the refractory period. It was observed that the effect of prolonging the refractory period is of greater extent in atria than in ventricles and this may explain its greater efficacy in the treatment of atrial arrhythmias. Delayed rectifier K^+ currents attend in the accomplishment of ventricular repolarization (**Table 1.2**). Thus, if they are reduced because of the blocking action of an antiarrhythmic, as dofetilide,

† For clarity, the parameters used in the clinical studies will be defined in each paragraph. Common parameters are reported with the same name, even if referring to different populations under analysis.

repolarization is prolonged. This results in a longer QT interval (*Jaiswal, 2014; Wolbrette, 2019*). Pharmacological agents prolonging QT interval bring the risk of inducing ventricular arrhythmias. Dofetilide can provoke severe ventricular arrhythmias, first of all Torsade de Pointes [o]. Torsade de Pointes can degenerate into ventricular fibrillation that is a dangerous condition for the heart, possibly leading to SCD. Torsade de Pointes and other ventricular arrhythmias can occur in the first 48 h to 72 h after initiation of the drug therapy. Thus, adjustment of the dose while monitoring renal and cardiac function is crucial (*Wolbrette, 2019; Torp-Pedersen, 1999*). Increasing of predisposition to develop Torsade de Pointes or in general ventricular arrhythmias should be deeply defined. Gender, age, preexisting heart diseases, electrolyte disorders, hepatic or renal disfunction, bradycardia or cardiac rhythm characterized by long pauses, use of other antiarrhythmic drugs and genetic predisposition are considered among the most important risk factors for dofetilide-induced Torsade de Pointes and ventricular arrhythmias (*Jaiswal, 2014*).

After administration, dofetilide is almost totally absorbed and has a bioavailability more than 90%; maximum plasma concentration is reached in about 2 h, regardless of the dose (*Jaiswal, 2014; Wolbrette, 2019*). Its plasma half-life, i.e. reduction of drug concentration in the plasma of one-half, is 8 h to 10 h in patients without renal function problems (*Jaiswal, 2014; Lande, 1998; Roukoz, 2007; Wolbrette, 2019*).

TWA is a risk marker able to highlight predisposition to develop Torsade de Pointes and other ventricular life-threatening arrhythmias and has all the potential to be successfully used to guide dofetilide therapy and the adjustment of the dose.

Clinical Study [p]

Data

The ECG data of this study are part of the "ECG Effects of Ranolazine, Dofetilide, Verapamil, and Quinidine in Healthy Subjects" database (*Johannesen, 2014*), available on Physionet (*Goldberger, 2000*). ECG data were acquired on a healthy population of 22 healthy volunteers. Half subjects were male and the remaining female. At the time of acquisition, they were 18 years old to 35 years old, weighed at least 50 kg, with a body mass index of 18 kg/m² to 27 kg/m². All have no history of heart disease or unexplained syncope or a family history of long QT syndrome. They underwent a screening involving a continuous ECG recording lasting 3 h; during it, they experienced no more than 10 ectopic beats. During the experiment, in the morning, subjects were given a single 500 µg dose of dofetilide, without food. During and after dofetilide administration, a continuous standard 10-s 12-lead ECG acquisition was accomplished. Specifically, three replicate ECG recordings were recorded at 16 instants

o) Torsade de Pointes: polymorphic ventricular tachycardia that can lead to sudden cardiac death.

p) Parameters: BTWA: baseline TWA (mMTWA value at 0.5 hours before dofetilide administration); GTWA: TWA gain (= PTWA / BTWA); mMTWA: mean MTWA over available ECG recordings in each time instant of acquisition; mRR: mean RR interval; MTWA: maximum value of TWA AAm over leads; PTWA: peak of TWA (highest value over all time instants of acquisition); sdRR: RR standard deviation; TP: time of occurrence of peak of TWA; ΔTWA: maximum TWA increment (= PTWA − BTWA).

in time, with no regular periodicity: one at 0.5 h before administration, the others at 0.5, 1, 1.5, 2, 2.5, 3, 3.5, 4, 5, 6, 7, 8, 12, 14 and 24 h after administration. The ECG recorder was settled at 500 Hz, with an amplitude resolution of 2.5 μV. Subjects were resting in a supine position for 10 min. Eventually, 48 ECG tracings (3 ECG tracings by 16 instants in time) per subject were acquired (1056 in total). All data coming from Physionet can be employed without further approval of independent ethics committee. All subjects were able to read and understand the informed consent before giving it.

Automated T-wave Alternans Detection

ECG data underwent a preprocessing procedure before being analyzed for TWA identification and measurement. Each ECG was band-pass filtered between 0.05 Hz and 40 Hz, through a bidirectional Butterworth 6^{th}-order filter. After R-peak detection, mean RR interval (mRR, ms) and RR standard deviation (sdRR, ms) were computed. Suitability assessment based only on heart rate of all ECG followed. Moreover, heart-rate dependent formulae were employed to identify T-wave sections to feed the updated CM. Indeed, ECG meeting suitability assessment underwent the automated TWA detection through the application of the updated version of the CM for TWA analysis (*Marcantoni, 2019b*). TWA AAm is the output obtained from the CM for each suitable lead. Thus, 12 TWA AAm values were obtained for each ECG (one per lead). Among them, the higher one (maximum of TWA AAm, MTWA, μV) was saved and considered as reference for the ECG. Thus, 3 MTWA values were obtained for each instant in time. The mean of them was computed (mean MTWA, mMTWA, μV) in order to manage a single measurement per instant in time for each subject. Peak of TWA (PTWA) was defined as the highest value among the 16 mMTWA obtained for each subject; time of PTWA occurrence (TP) was its timing of occurrence (among the 16 instants in time). Baseline TWA was defined as mMTWA value at 0.5 hours before dofetilide administration (BTWA) and used to compute both maximum TWA increment (ΔTWA), as the difference between PTWA and BTWA, and TWA gain (GTWA), as the ratio between PTWA and BTWA.

All features distributions were expressed in terms of $50^{th}[25^{th};75^{th}]$ percentiles over subjects.

Statistical differences between pre-administration vs post administration mMTWA values were evaluated by applying the non-parametric Wilcoxon rank-sum test for independent samples, where statistical significance level (p) was set at 0.05.

Results

The suitability assessment for heart rate was always met. Results of the analysis are reported in **Table 7.1.1**. All subjects but one experienced an increasing mMTWA until PTWA, after which mMTWA tended to BTWA. TP varied among subjects: TP=1 hour in 4 subjects; TP=2 hours in 2 subjects; TP=3 hours in 1 subject; TP=4 hours in 3 subjects; TP=5 hours in 1 subject; TP=7 hours in 2 subjects; TP=8 hours in 4 subjects; TP=12 hours in 2 subjects; and TP=14 hours in 2 subjects. For 20 subjects, PTWA was higher than 10 μV; for 17 subjects, higher than 20 μV; for 6 subjects, higher than 50 μV. ΔTWA went from -9 μV to 116 μV, overcoming 50 μV in 6 subjects. GTWA went from 0.7 to 22.2, overcoming 5 in 13 subjects.

Trend of mMTWA in time is shown in **Fig. 7.1.1**. Increments of mMTWA with respect to BTWA were registered at 6 h (p=0.02), 7 h (p=0.03) and 8 h (p=0.01).

Table 7.1.1. *Alternans features over population, besides heart-rate features and personal data. Total values (50th[25th;75th] percentiles over subjects) related to the entire population in bold (Marcantoni, 2019b).*

S	Gender	Age (year)	mRR (ms)	sdRR (ms)	BTWA (μV)	PTWA (μV)	TP (h)	ΔTWA (μV)	GTWA
1	F	25	908	44	6	18	7	12	3.0
2	F	20	861	32	9	67	4	58	7.4
3	F	30	1145	97	8	25	1	17	3.1
4	F	32	868	28	5	14	4	9	2.8
5	F	23	981	51	4	89	1	85	22.3
6	F	22	966	88	8	45	4	37	5.6
7	F	27	832	38	8	48	2	40	6.0
8	F	33	899	22	5	26	8	21	5.2
9	F	29	837	24	15	38	8	23	2.5
10	F	21	978	73	3	18	3	15	6.0
11	F	31	903	39	3	15	2	12	5.0
12	M	21	961	30	6	122	12	116	20.3
13	M	32	910	31	10	92	1	82	9.2
14	M	35	954	12	6	43	5	37	7.2
15	M	19	1016	34	4	17	14	13	4.3
16	M	25	1039	41	5	28	12	23	5.6
17	M	21	1183	27	5	91	14	86	18.2
18	M	30	1165	62	5	66	7	61	13.2
19	M	26	1177	28	4	24	8	20	6.0
20	M	20	985	47	9	29	1	20	3.2
21	M	35	1076	24	27	18	2.5	-9	0.7
22	M	35	1095	25	11	34	8	23	3.1
T	**n.a.**	**27 [21;32]**	**972 [903;1076]**	**33 [27;47]**	**6 [5;9]**	**32 [18;66]**	**5 [2;8]**	**23 [15;58]**	**6 [3;7]**

F: female; M: male; n.a.: not applicable; S: subject; T: total

Remarks

Among the methods present in literature, CM is the only one allowing an analysis on very short-time ECG, like the standard 10-s ECG constituting the "ECG Effects of Ranolazine, Dofetilide, Verapamil, and Quinidine in Healthy Subjects" database. CM could provide the measurement of all the ECGA forms in its updated version; here, the study focuses on TWA because it could have a more reliable prognostic role given dofetilide electrophysiological effects, but further studies

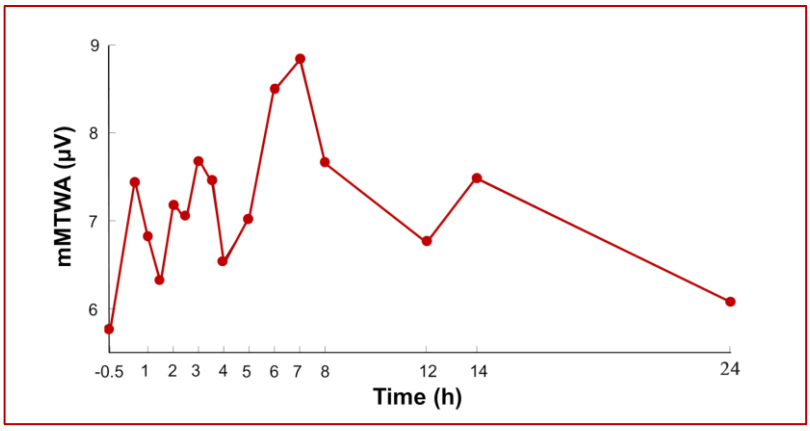

Figure 7.1.1. *Population trend of mMTWA (median over subjects) (Marcantoni, 2019b).*

measuring also PWA and QRSA might confirm this assumption. Given the short ECG duration and low heart rate, the updated CM was chosen, which detected alternans phenomenon when there were 5 heartbeats consecutively alternating. Since TWA is a lead-dependent phenomenon (*Burattini, 2012b*), higher value over leads was chosen in order to consider alternans measure on the more affected one. Dofetilide induced an increment of TWA in the hours following its administration, in the healthy population under examination in this study. TWA was three (less evident cases) to over twenty (more evident cases) times higher than before drug administration. After dofetilide administration, in some subjects, values were very high suggesting a possible predisposition to dofetilide-induced Torsade de Pointes and ventricular arrhythmias, like the literature suggested. In the case where the PTWA did not overcome BTWA, it is not excluded the possibility of a higher peak value in a different instant than those considered from the acquisition protocol. Being the recording not continuous over the 24 h following the drug administration, some time periods remained undetected. Future studies on dofetilide-induced ECGA should set up a different protocol of acquisition using Holter 24-h continuous ECG recordings after drug administration. Gender is among the risk factors for dofetilide-induced ventricular arrhythmias (*Jaiswal, 2014*). Females usually show a higher (14-22%) plasma concentration of dofetilide than males, even keeping in consideration necessary adjustments for physic and physiologic differences due to gender. Also, TWA seems to be a gender-related phenomenon, affecting more females than males (*Burattini, 2010*). Here there were no differences related to gender, but any kind of stratification was impossible with this population, due the reduced size. The study performed here has to be considered a preliminary pilot study. Further investigations considering optimized protocol of acquisition and wider datasets, enrolling both healthy and pathological subjects, are fundamental to possibly confirm these preliminary results. Moreover, other drug agents as well as other ECGA forms will be put in relationship in order to determine the role of ECGA as risk marker in the guide of therapy monitoring to optimize clinical intervention. From a clinical perspective, ECGA analysis in relation to the intake of a pharmacological agent (such as dofetilide) in a therapy can be very useful for noninvasively following the reaction of cardiac electrical activity. Therefore, the ECGA can be used as a marker of possible antiarrhythmic or proarrhythmic effects following the body absorption of the pharmacological agent, targeting the appropriate therapy for each patient.

7.2 Trend in Proximity of Epileptic Seizures: A Clinical Study

Epilepsy is a disorder affecting the central nervous system that occurs when brain activity becomes abnormal. Among the anomalous neurologic conditions, it is recognized as one of the most common and disabling. Epilepsy is, by definition, the pathologic status of sudden and recurrent episodes of sensory disturbance, associated with loss of consciousness, or seizures. Seizures are not always provoked by epilepsy and sometimes they are a transitory condition rather than a chronic state; so, it would be more proper to talk about epileptic seizures when they are elicited by abnormal neuronal firing. In turn, epilepsy syndrome exists if some specific clinical features occur consistently (e.g. type of epileptic seizure, onset age, or genetics) (*Stafstrom, 2015*). Epilepsy can affect individuals of any age, but 75% of epilepsy starts in the childhood, evidence that reflects the high susceptibility to epileptic seizures of the developing brain. Epileptic seizures represent the principal hallmark of this disorder, and their most severe complications are damages and deaths.

A common cause of demise from epileptic seizures is the sudden unexpected death in epilepsy (SUDEP). SUDEP is more frequently experienced by patient suffering from the most severe form of epilepsy and generally occurs in concomitance with ictal events. Many conditions can favor SUDEP, e.g. age, disease duration, polytherapy, as well as, on the contrary, absence of treatment. Moreover, factors as cardiorespiratory dysregulation, anomalous circulation, hormonal or metabolic changes can trigger this irreversible occurrence (*Stafstrom, 2015; Strzelczyk, 2011*).

Epilepsy and epileptic seizures may highly affect the cardiac function. Furthermore, some silent arrhythmic conditions happening in concomitance with ictal events may be employed by automatic techniques as biomarkers able to forecast and detect epileptic seizure occurrence. Indeed, SUDEP phenomenon is strictly related to heart function changes due to ictal event (*Jansen, 2010*). Therefore, anticipation of SUDEP through the use of reliable heart-function-based risk indexes may represent the key to prevent tragic events. Prevention is based on noninvasive and lasting monitoring of the biomarker. A possible index that can be used with this aim is TWA. Until now, in the literature there are few studies that analyzed TWA evidence in the peri-ictal period, but the present ones point out a relationship between TWA and epileptic seizures. Strzelczyk et al. found out that in patients suffering from chronic uncontrolled epilepsy imbalance of autonomic control and TWA increase after generalized tonic-clonic epileptic seizures (*Strzelczyk, 2011*). Sheng et al. found out that epileptic seizures, particularly tonic-clonic and absence ones, rise occurrence of TWA, concluding TWA monitoring can provide a useful guidance for prevention of SUDEP (*Sheng, 2017*). Schomer et al. found out abnormal TWA levels in patients with drug-resistant focal epilepsy before vagus nerve stimulation; using TWA as a therapeutic target, a reduction of cardiac electrical instability was registered after vagus nerve stimulation, probably determining an improvement in the sympathetic/parasympathetic balance (*Schomer, 2014*). This was confirmed by Verrier et al., who performed a similar analysis (*Verrier, 2016*). Pang et al. observed significantly higher TWA in chronic epileptic patients than in newly diagnosed ones (*Pang, 2019*). Very recently, Verrier introduced the concept of "epileptic heart" (*Verrier, 2020*) as a heart compromised by chronic epilepsy showing electrical and mechanical dysfunction. Therefore, the literature encourages further studies to detect cardiac electrical instability linked to epilepsy, to identify the abnormal TWA incidence in SUDEP and better define the TWA role as cardiac risk biomarker and therapeutic target (*Schomer, 2014;*

Verrier, 2016). Moreover, analysis of ECGA trend in association to epileptic seizures is especially important to prevent SCD due to epileptic seizures.

Clinical Study [s]

Data

The ECG data of this study are part of the "Post-Ictal Heart Rate Oscillations in Partial Epilepsy" database (*Al-Aweel, 1999*), available on Physionet (*Goldberger, 2000*). ECG data consists of continuous 1-lead ECG recordings. Acquisitions were performed on 5 female patients suffering from partial epilepsy, from 31 years old to 48 years old. ECG acquisitions were performed concurrently with electroencephalographic acquisition. During the recordings, they experienced partial epileptic seizures with or without secondary generalization from frontal or temporal foci. They did not show clinical evidence of any cardiac disease. More than one only recording was performed on some patients and for three recordings two epileptic seizures happened for a total of ten partial epileptic seizures (for record durations, onset and offset timing, *Marcantoni, 2018a*). An experienced electroencephalographer visually identified all epileptic seizures to the nearest 0.1 s. Sampling rate of ECG recordings was 200 Hz. All data coming from Physionet can be employed without further approval of independent ethics committee. Recordings were made under a protocol approved by Beth Israel Deaconess Medical Center's Committee on Clinical Investigations.

Automated T-wave Alternans Detection

All ECG from the database were studied. From each ECG, 32-beat windows were iteratively extracted every 1 s. All ECG windows were preprocessed: they were band-pass filtered between 0.5 Hz and 40 Hz by a 6th-order bidirectional Butterworth filter. R-peak-position detection was performed using the Pan-Tompkins' algorithm. Baseline was removed, where baseline was computed through a 3rd-order spline interpolation of PR fiducial points. R-peak positions were then used to identify fiducial points relative to ECG T wave. After suitability assessment, automated TWA detection follows through the application of the AMFM to ECG tracings that met both the conditions of the suitability assessment.

ECG portions starting 10 min before and ending 10 min after each epileptic seizure were selected (*Marcantoni, 2018a*). Then, heart rate and TWA occurring 10-to-9 min before epileptic seizure onset, 9-to-10 min after epileptic seizure offset and during epileptic seizure were considered. In these ECG portions, the number of suitable ECG windows (NW) was computed. An epileptic seizure enrolling criterion was considered: each one of the three ECG tracing segments around the same epileptic seizure (before, during, or after it) had to have at least one suitable ECG window, otherwise the epileptic seizure was rejected from the analysis. The value of median heart rate (mHR), median TWA AAm over extracted ECG windows (mTWA) and maximum of TWA AAm over extracted ECG windows (MTWA) were computed over each ECG portion, for all

s) Parameters: mHR: median heart rate; mTWA: median TWA AAm over extracted ECG windows; MTWA: maximum of TWA AAm over extracted ECG windows; NW: rate of suitable ECG windows.

suitable ECG windows. Trends of analyzed features were expressed in terms of $50^{th}[25^{th};75^{th}]$ percentiles. Wilcoxon rank-sum test was used for statistical comparisons among distributions of these features in the three epileptic seizure-related time periods and against the literature, where statistical significance level (p) was set at 0.05.

Results

Table 7.2.1, **Table 7.2.2** and **Table 7.2.3** reported NW (%), mTWA (μV), MTWA (μV) and mHR (bpm) related to the time periods before, during and after epileptic seizures, respectively. Overall, TWA was analyzed in proximity of 9 epileptic seizures. Indeed, in compliance with the enrolling criterion, the last epileptic seizure was not enrolled in the analysis because no suitable ECG windows were present within the epileptic seizure. Thus, the last ECG recording, which included only this epileptic seizure, was completely excluded from the study. Epileptic seizure durations ranged from 25 s to 110 s; mHR values were significantly different (generally higher) during epileptic seizures ($p<0.05$). Despite epileptic seizures were few, mTWA values were compared with values of TWA measured on a healthy female population using AMFM (*Burattini, 2010*). TWA was significantly ($p<0.02$) higher in the epileptic population considered here than in the healthy population, both in epileptic seizure and near- epileptic seizure conditions. Values of mTWA and MTWA changed during epileptic seizure (returning to previous values after epileptic seizure), even if not reaching statistical significance. This was more evident computing mTWA absolute differences before vs during epileptic seizure (17[4;23] μV) and during vs after epileptic seizure (16[4;21] μV): they resulted statistically different from 0 μV ($p<10^{-4}$), but not between them. Analogously, MTWA absolute differences before vs during epileptic seizure (47[26;65] μV) and during vs after epileptic seizure (56[17;72] μV): they resulted statistically different from 0 μV ($p<10^{-4}$), but not between them.

Table 7.2.1. *Trend of TWA features extracted from ECG tracing portions before epileptic seizure (Marcantoni, 2018a). Results related to the all epileptic seizures in bold.*

ES	NW (%)	mTWA (μV)	MTWA (μV)	mHR (bpm)
1	100	11	16	72
2	10	63	83	67
3	100	26	46	61
4	100	31	48	65
5	100	40	54	70
6	100	25	40	60
7	100	25	84	91
8	100	62	84	72
9	100	98	158	70
T	**100 [100;100]**	**31 [25;62]**	**54 [45;84]**	**70 [64;72]**

ES: epileptic seizure; T: total

Table 7.2.2. *Trend of TWA features extracted from ECG tracing portions during epileptic seizure (Marcantoni, 2018a). Results related to the all epileptic seizures in bold.*

ES	NW (%)	mTWA (μV)	MTWA (μV)	mHR (bpm)
1	64	10	45	114
2	100	46	105	86
3	100	47	70	84
4	72	54	145	96
5	66	34	102	119
6	9	27	194	98
7	26	20	30	125
8	79	85	110	68
9	100	74	111	69
T	**72 [55;100]**	**46 [25;59]**	**105 [64;120]**	**96 [81;115]**

ES: epileptic seizure; T: total

Table 7.2.3. *Trend of TWA features extracted from ECG tracing portions after epileptic seizure (Marcantoni, 2018a). Results related to the all epileptic seizures in bold.*

ES	NW (%)	mTWA (μV)	MTWA (μV)	mHR (bpm)
1	100	14	33	103
2	100	30	66	59
3	94	45	89	61
4	100	29	42	70
5	100	27	41	69
6	100	23	35	71
7	100	62	90	85
8	100	66	113	69
9	100	90	167	70
T	**100 [100;100]**	**30 [26;63]**	**66 [40;96]**	**70 [67;75]**

ES: epileptic seizure; T: total

Remarks

In case of epileptic ECG, the most critical period to analyze is during epileptic seizures, in which cardiac conduction disorders are known (*Jansen, 2010; Nei, 2000*). This explains why the majority of not suitable ECG windows were present within epileptic seizures. Changes of mHR within epileptic seizures confirmed findings of several studies in the literature. Indeed, they reflect the state of the autonomic nervous system and epileptic patients seem to show an altered autonomic cardiac control (*Eggleston, 2014; Jansen, 2010; Jansen, 2013; Pavei, 2017; Opherk, 2002; Suorsa, 2011; Tomson, 1998*).

Results obtained here are comparable with the few studies in the literature considering risk index, like QT dispersion or TWA, if measurement conditions are similar (*Strzelczyk, 2011; Schomer, 2014; Verrier, 2016*). Being the population under examination here completely female, results were compared with those obtained in the female population treated in *Burattini, 2010*. In the present study, TWA was high in proximity of epileptic seizures and during epileptic seizures; furthermore, it changed during the attack. Therefore, SCD risk, possibly related to SUDEP, may be higher for these epileptic patients than healthy population. Findings of this study are preliminary, considering the small size of the epileptic population, the general epilepsy classification, and ECGA measurements reflecting only in TWA measurement. Further studies involving larger population and longer ECG acquisition (involving the actual basal state, far from epileptic seizures) are needed to define ECGA role (and not only TWA) as cardiac risk biomarker and therapeutic target. Indeed, clinically, ECGA may have the potentialities to be used as a marker to monitor the status of cardiac electrical activity in order to verify if it can be compromised consequently to the epilepsy, especially in case of chronic forms (according to the very recent concept of "epileptic heart"). Additionally, ECGA may be tested as marker of risk in the prevention of ES.

7.3 Behavior in Fetal Condition: A Clinical Study

Infant mortality often provides a reliable measure of the health status and well-being of a nation. Indeed, circumstances leading infant mortality have afferences on the health of the whole population (*Parks, 2017*). Thus, clinically, a society is fully developed when has all the possible means that can prevent the causes of infant mortality.

Clinical prevention requires monitoring the risk factors before and during their usual period of manifestation, to take action in time against their evolution. Infant death is often related to genetics, e.g. genetic abnormalities in the ion channel functionality can compromise the cardiac electrical activity (*Marcantoni, 2017*). In this perspective, having a risk marker that is able to reveal possible dangerous or even malignant anomalies of the heart is fundamental. One of the most reliable cardiac risk markers is TWA. It is mostly investigated in adult population, but its role in the fetus population has not been defined yet. Knowledge on the TWA etiology before birth is very reduced (*Marcantoni, 2017; Yu, 2013*), but fundamental, considering that in lifetime, the highest probability of death is registered during the 40 weeks preceding birth. A deeper evaluation of electrophysiology of heart electrical activity in utero can allow diagnosis and management of fetuses at risk of arrhythmic events even leading to suboptimal outcome, infant death, or in utero death. The causes of death in fetuses remain still mostly undiscovered, but it seems that many of fetuses demising in utero have an abnormal electrophysiologic substrate, such as repolarization anomalies, or conduction system disorder that instead is better known in newborn and infant. Probably the causes can be common, and fetuses can die to the same arrhythmias occurring after birth (*Cuneo, 2008; Cuneo, 2013*). The woman hormonal state in pregnancy can influence the electrophysiologic substrate of both mother and fetus, but in opposite way: high estrogen level can balance ion channels of maternal adult heart, but not those of the fetal immature heart (*Cuneo, 2008*).

Studies on fetal magnetocardiography observed TWA in fetuses (*Cuneo, 2013; Yu, 2013; Zhao, 2006*) and underlined the possible utility of fetal TWA assessment, considering the high incidence of TWA in fetuses showing cardiac arrhythmias (*Zhao, 2006*). Furthermore, in fetuses TWA is often observed in association with long QT (known association in adults); thus, an accurate diagnosis linked to TWA detection might permit an efficient treatment of fetuses before birth (*Zhao, 2006; Cuneo, 2013*). TWA assessment may permit an effective in-utero pharmacological treatment to establish a regular cardiac activity. This, in turn, may prevent premature delivery and allow well-timed care after birth (*Marcantoni, 2017*).

Clinical Study [q]

Data

The ECG data of this study are part of the "Abdominal and Direct Fetal Electrocardiogram Database" (*Jezewski, 2012*), available on Physionet (*Goldberger, 2000*). ECG data consist in direct and indirect fetal ECG recordings. ECG recordings last 5 min and were performed on 5 different women in labor, from 38th to 41st gestation week. The acquisition was accomplished in the Department of Obstetrics at the Medical University of Silesia. The configuration of the abdominal electrodes for indirect acquisition was made by four electrodes applied around the navel, a reference electrode applied above the pubic symphysis and a common mode reference electrode applied on the left leg. Skin conductance was improved abrading areas under the electrodes prior to their application. The acquisition of direct fetal ECG was accomplished through a spiral electrode, placed in correspondence of the fetus scalp. Indirect and direct fetal ECG were recorded concurrently. Sampling rate of ECG recordings was 1000 Hz.

All data coming from Physionet can be employed without further approval of independent ethics committee.

Automated T-wave Alternans Detection

All ECG from the database were studied. Before the analysis, indirect fetal ECG underwent a specific a preliminary elaboration. Indeed, they were deprived of maternal ECG interference: maternal R peaks were detected on indirect fetal ECG, by the use of Pan-Tompkins' algorithm and then segmented beat modulation method (*Agostinelli, 2014; Agostinelli, 2016*) was applied to estimate maternal ECG to be subtracted from indirect fetal ECG. Eventually, the obtained denoised indirect fetal ECG underwent an amplification by a scale factor (4.8). The following analysis procedure was the same for both direct fetal ECG and denoised indirect fetal ECG (in the following, simply referred to as indirect fetal ECG).

From each fetal ECG, 32-beat windows were iteratively extracted every 1 s. All ECG windows were preprocessed: they were low pass filtered at 35 Hz by a 6th-order bidirectional Butterworth filter. R-peak-position detection was performed using the improved Pan-Tompkins' algorithm for fetal applications (*Agostinelli, 2017*). Baseline was removed, where baseline was computed through a 3rd-order spline interpolation of PR fiducial points. R-peak positions were then used to identify fiducial points relative to ECG T section, using heart rate-dependent formulae (*Burattini, 1999*). After suitability assessment, automated TWA detection follows, through the application of the updated version of AMFM with settings adapted for fetal applications to ECG tracings that met both the conditions of the suitability assessment (*Marcantoni, 2017*). For each fetal ECG, rate of suitable ECG windows (NW) was computed.

Quality of fetal ECG was assessed in terms of fetal SNR (f_SNR), expressed in decibel and computed as the signal amplitude (median

q) Parameters: F_SNR: fetal signal to noise ratio; mHR: mean heart rate; mTWA: mean TWA AAm over extracted ECG windows; MTWA: maximum of TWA AAm over extracted ECG windows; NW: rate of suitable ECG windows; sdRR: standard deviation of RR; sdTWA: standard deviation of TWA AAm over extracted ECG windows.

peak-to-peak difference over heartbeats) over the noise amplitude (four times standard deviation of fetal noise) (*Marcantoni, 2018b*). From suitable ECG windows mean heart rate (mHR) and standard deviation of RR interval (sdRR) were computed, while extracted TWA features were mean TWA AAm over extracted ECG windows (mTWA), maximum of TWA AAm over extracted ECG windows (MTWA) and standard deviation of TWA AAm over extracted ECG windows (sdTWA).

Comparison between direct fetal ECG and one of the concurrently acquired indirect fetal ECG was performed, where the indirect fetal ECG was chosen as the one having the highest MTWA and the highest NW (>15%, in any case) among the indirect fetal ECG of the same acquisition. Wilcoxon rank-sum test was used for statistical comparison between MTWA and mHR, in direct fetal ECG and selected indirect fetal ECG, where statistical significance level (p) was set at 0.05.

Results

All computed features are reported in **Table 7.3.1** (*Marcantoni, 2017; Marcantoni, 2018b*). All direct fetal ECG were suitable, while 9 out of 20 indirect fetal ECG were rejected. NW (69 ± 29%) and f_SNR (−1 ± 8 dB) of direct fetal ECG were higher than NW (17 ± 18%) and f_SNR (−4 ± 5 dB) of indirect fetal ECG; mHR (129 ± 3 bpm for direct fetal ECG; 130 ± 5 bpm for indirect fetal ECG) was homogenous among all considered fetal ECG. Distributions of TWA features extracted from direct and indirect fetal ECG were of the same order of magnitude (mTWA = 9 ± 2 μV for direct fetal ECG and 11 ± 5 μV for indirect fetal ECG; MTWA = 30 ± 11 μV for direct fetal ECG and 21 ± 12 μV for indirect fetal ECG; sdTWA = 6 ± 2 μV for direct fetal ECG and 7 ± 3 μV for indirect fetal ECG). Furthermore, sdTWA had the same order of magnitude as mTWA, in both direct and indirect fetal ECG.

In compliance with the enrolling criterion, the selected indirect fetal ECG are the fourth of fetus 1, the fourth of fetus 4, and the first of fetus 5. Pearson's correlation coefficients between MTWA and mHR were moderate for direct fetal ECG (0.64; p = 0.24) and very high for indirect fetal ECG (0.99; p = 0.02).

Remarks

ECGA in the form of TWA at this first (as far as I know) attempt of identification on fetal ECG was possible on both direct and indirect ones. Comparable results were found on direct fetal ECG and indirect fetal ECG, even if it is necessary the consideration of an amplitude-correction factor.

From a morphological point of view, fetuses and adults have quite similar ECG signals containing the same fundamental waves. ECG differences mainly rely on amplitude: fetal QRS amplitude depends on lead, gestational age and fetus position and typically is two to several times lower than an adult QRS. Interferences and noises affect fetal ECG, especially in indirect acquisition modality. The indirect fetal ECG is obtained placing electrodes on the maternal abdomen, following specific configurations. The definition of the optimal configuration is not possible because the position of the fetus is not predictable. Some of the procedures imply few electrodes (four to eight) to simplify application (as in the database here considered); others, on the opposite, imply many electrodes to improve acquisition quality (*Agostinelli, 2015*). The direct fetal ECG is obtained by placing a spiral wire electrode on the fetal scalp. Due to acquisition modality, indirect fetal ECG is noninvasive, but signal quality is low; on the other hand, direct

Table 7.3.1. *Values of f_SNR, heart-rate features and TWA features extracted from direct and indirect fetal ECG tracing (Marcantoni, 2018b). Results related to direct fetal ECG are reported in bold, while those related to the selected indirect fetal ECG are reported in bold on gray background.*

Fetus_Lead	f_SNR (dB)	NW (%)	mHR (bpm)	sdRR (ms)	mTWA (μV)	MTWA (μV)	sdTWA (μV)
F1_D	**5**	**91.7**	**129**	**14**	**6**	**20**	**4**
F1_I1	-1	0.8	128	0	6	7	3
F1_I2	-3	0	-	-	-	-	-
F1_I3	1	16.7	127	5	6	10	4
F1_I4	**3**	**26.9**	**127**	**6**	**6**	**24**	**5**
F2_D	**-3**	**65.5**	**129**	**23**	**8**	**29**	**6**
F2_I1	-15	0	-	-	-	-	-
F2_I2	-8	0	-	-	-	-	-
F2_I3	-9	0	-	-	-	-	-
F2_I4	-7	0	-	-	-	-	-
F3_D	**-4**	**19.7**	**124**	**11**	**8**	**19**	**5**
F3_I1	-16	0	-	-	-	-	-
F3_I2	-7	0	-	-	-	-	-
F3_I3	-8	0	-	-	-	-	-
F3_I4	-6	3.8	126	1	23	34	10
F4_D	**9**	**89.4**	**131**	**15**	**9**	**34**	**8**
F4_I1	-2	0.8	128	1	5	6	4
F4_I2	-5	0.4	144	0	14	14	9
F4_I3	1	17.0	132	17	8	19	5
F4_I4	**4**	**40.5**	**130**	**16**	**12**	**33**	**10**
F5_D	**-12**	**76.5**	**130**	**23**	**12**	**47**	**8**
F5_I1	**1**	**52.3**	**133**	**21**	**12**	**41**	**9**
F5_I2	-3	28.0	131	14	11	32	7
F5_I3	-4	0	-	-	-	-	-
F5_I4	-1	1.1	127	1	14	15	8

D: direct fetal electrocardiogram; F: fetus; I: indirect fetal electrocardiogram.
On visual inspection, f_SNR of F5_D (<F5_I) is possibly due to displacement of scalp electrode.

fetal ECG is invasive, but signal quality is higher. As a consequence, the direct fetal ECG is cleaner and so more suitable for TWA detection than indirect fetal ECG. The indirect fetal ECG has a reduced amplitude, is more affected by interferences (especially due to the mother), but it is more feasible in clinical practice because noninvasive and eventually, it can be acquired in a less stressful status (not necessarily during delivery) for the fetus allowing TWA not to be driven by it. AMFM is robust against noises and interferences and this characteristic is fundamental in case of indirect fetal electrocardiography. Indeed, in this study, indirect fetal ECG were cleaned from the mother ECG interference by applying the segmented beat modulation method, but they are still noisy due to the presence of noises and interferences of different nature. This can make difficult T-wave identification and ECG segmentation around it. The exact identification of T wave ends is not crucial for TWA analysis, the important thing is to completely include T wave in the ECG section that is segmented. Electrical cardiac function in fetuses does not deviate

from that in adults, except for the timing due to the different heart dimensions (specifically, heart rate is higher in fetuses). Thus, the identification of ends of T wave was performed adopting the same heart rate-dependent formulae as in *Burattini, 1999*, since they can easily be adapted to different heart rates. The complexity of analyzing indirect fetal ECG with respect direct fetal ECG is worsen considering the amplitude of the first ones, lower than the latter. To overcome this issue and allow a comparison of results between the direct fetal ECG and indirect fetal ECG (preferable in clinical application), amplitude of indirect fetal ECG was amplified by a scale factor, so to make its amplitude comparable with direct fetal ECG.

The main finding from this study is that fetuses show TWA, even if they are healthy, while adult TWA manifestation is usually related to a pathological condition. Furthermore, fetal ECG has a very reduced amplitude with respect adult ECG, and this can affect measurement of TWA. Thus, a value evaluated as physiologic in healthy adult heart can have a different meaning in healthy immature heart. At the same time, in this fetus population, TWA levels considered high if referred to ECG amplitude may be influenced by high fetal heart rate and by the stressful condition during delivery. Nevertheless, reference values are not defined yet, both in case of adults and in case of fetuses (also because TWA measurements depend on the detecting method). Moreover, the clinically useful remark of this study is that the analysis performed on indirect fetal ECG gave comparable results to those obtained analyzing direct fetal ECG, also in case of high rate of not suitable ECG windows. Nevertheless, even if noninvasive fetal electrocardiography has the advantage of noninvasiveness, in routine clinical practice, noninvasive fetal ECG monitoring is not usually performed. The possible reasons can be a lot. One of them surely relies on the reading of the ECG tracing: from one side, a unified interpretation cannot be possible, since there is not a standardization of electrode location, mainly due to the unpredictability of fetus position, from the other side, quality of the signal is often compromised because of the acquisition modality. Nevertheless, it is uniformly recognized that ECG plays a fundamental role in monitoring electrical function of the adult heart and in detecting possible anomalies of the cardiac rhythm through risk indexes, where heart-rate monitoring (usually performed on fetuses) is not enough. From fetal ECG, many fetal parameters and risk indexes, such as fetal ECGA, may be deduced and they may become important if reliably identified. Fetal ECG signal processing is challenging but knowing the role of ECG risk indexes in adult case should represent a good reason to keep studying them in fetal case in the perspective of efficient treatment of fetuses before and after birth in the evidence of possible anomalies or disfunctions. Thus, future studies are needed to analyze ECGA in all its possible forms in fetal condition. Both a wider healthy fetal population and pathologic fetal populations should be analyzed using EAMFM, which can be easily adapted for fetal applications. The final aim is defining its possible role in the prevention of fetal cardiac complications that could mine fetus survival, through a timely clinical intervention.

7.4 Behavior in Prematurity: A Clinical Study

In compliance with the World Health Organization (www.who.int) definition, an infant is preterm when he was born alive before the end of 37th week of pregnancy. Prematurity is not a rare occurrence.

It is estimated that, every year, 15 million infants are born too early, i.e. more than 1 in 10 infants. About 1 million children die each year because of complications due to preterm birth (*Liu, 2016*). All over the world, preterm birth is the leading cause of death in children under 5 years old. Moreover, in quite all countries with reliable data, prematurity rate is increasing. Prematurity has not been so much studied still and knowledge about developmental biology and disease phenomena is still limited (Engle, 2007). Prematurity involves physiological immaturity and limited compensatory responses to the extrauterine condition. Thus, morbidity and mortality risks are higher in preterm infants (*Engle, 2007*). Particularly, preterm infants have a higher risk to develop sudden infant death syndrome (SIDS) than term infants (*Rohana, 2018; Thompson, 2006*).

SIDS recently found a formal definition (about 50 years ago): it is the sudden death of a seemingly healthy infant under 1 year that remains unexplainable despite investigations, like knowledge of the infant's clinical history, death scene examination, and autopsy (*Haas, 2018; Randall, 2019; Rohana, 2018*). SIDS is counted among the leading causes of infant death (*Kojima, 2018*). In spite of this, the mechanism underlying SIDS is still unknown, and its etiology is possibly multifactorial (*Idriss,* 2002; Rohana, 2018*; Schwartz, 1998*). Not considering risk factors due to infant living habits and parental practices, anamnestic data (e.g. low gestational age or weight at birth) and physiological dysfunctions (e.g. dysfunctions affecting the central nervous system, the respiratory system, the cardiovascular system, or more of them) have been accounted as the main triggering factors for the onset of this syndrome (*Idriss, 2002; Rohana, 2018*). Cardiac causes of SIDS have been found in a higher arrhythmia vulnerability (*Idriss, 2002*). At birth, cardiac electrophysiology is immature (*Idriss, 2002*); this reflects on QT variability that may act as an index of the evolution of the cardiac autonomic nervous system and cardiac depolarization (*Kojima, 2018*), and QT dispersion that may act as a prognostic factor for neonatal mortality (*Pishva, 2003*). Few experimental studies performed on animals have suggested that cardiac repolarization alterations at birth may also reflect in TWA (*Idriss, 2008; Idriss, 2002*). TWA is widely studied in adult ECG, but much less in children. Infant TWA interpretation is still far from being established (*Idriss, 2008; Idriss, 2002; Makarov, 2010a; Makarov, 2010b*). As far as I know, only a couple of studies are present in the literature about human infant TWA (*Makarov, 2010a; Makarov, 2010b*), but none on preterm infant TWA. In 2010, Makarov et al. detected TWA in twenty apparently healthy newborns during the first, second, and fourth day of life, finding out a peak level of TWA in the second life day, likely reflecting a restructuring of cardiac activity in the immature heart. According to Madias, TWA changes in newborn ECG examined by Makarov et al. may be associated to changes in the amplitude of T wave, rather than necessarily meaning a vulnerability to arrhythmias (*Madias, 2010*).

A more insights on TWA role in prematurity condition is needed and further studies can solve this still open issue on the possibility of considering TWA in nonpathological preterm infants (and more in general in newborns) as a cardiac immaturity marker, rather than an arrhythmias-risk index.

Clinical Study [r]

Data

The ECG data of this study are part of the "Preterm infant cardio-respiratory signals database" (*Gee, 2017*), available on Physionet (*Goldberger, 2000*). ECG data were recorded and collected in the neonatal intensive care unit at the University of Massachusetts Memorial Health care. Preterm infants' gestational age (GA) ranged from 29·(3/7) weeks to 34·(2/7) weeks (mean: 31·(1/7) ± 1·(3/7) weeks), preterm infants' birth weight (BW) ranged from 0.84 kg to 2.10 kg (mean: 1.47 ± 0.41 kg), preterm infants' GA/BW (days/kg) ranged from 108 days/kg to 251 days/kg (mean: 159 ± 44 days/kg), **Table 7.4.1** (*Marcantoni, 2020c*). Preterm infants' GA/BW ratio, reflecting the correct infant development with respect to gestational age, ranged from 108 days/kg to 251 days/kg. All infants were able to breath independently and showed no congenital or perinatal infection of the central nervous system, no intraventricular hemorrhage of grade II or higher, and no hypoxic–ischemic encephalopathy. Their hospitalization was made necessary by prematurity, since nursing daily monitoring was fundamental until their weight could guarantee a complete physical and physiological maturity, essential for a risk-free growth. A single channel of a 3-lead ECG signal was acquired when available from bedside infant patient monitors (Intellivue MP70, Philips Medical Systems). The choice of the available ECG depended on nursing preference. Acquisitions lasted from 20.3 h to 70.3 h per infant. According to what explicitly said in the description of the database, acquisitions were not affected by equipment interferences having a frequency content close to a multiple of ECGA frequency (e.g. breathing or feeding pump). Sampling rate of ECG recordings was 500 Hz and band-pass cutoff frequencies: 0.5–55.0 Hz.

Acquisition was approved by the University of Massachusetts School Institutional Review Board of human subjects. All data coming from Physionet can be employed without further approval of independent ethics committee.

Table 7.4.1. *Clinical features at birth related to each preterm infant (Marcantoni, 2020c).*

PI	GA (weeks)	BW (kg)	GA/BW (days/kg)
1	$29 \cdot {}^{3}/_{7}$	1.20	172
2	$30 \cdot {}^{5}/_{7}$	1.76	122
3	$30 \cdot {}^{5}/_{7}$	1.71	126
4	$30 \cdot {}^{1}/_{7}$	0.84	251
5	$32 \cdot {}^{2}/_{7}$	1.67	135
6	$30 \cdot {}^{1}/_{7}$	1.14	185
7	$30 \cdot {}^{1}/_{7}$	1.11	190
8	$32 \cdot {}^{3}/_{7}$	2.10	108
9	$30 \cdot {}^{4}/_{7}$	1.23	174
10	$34 \cdot {}^{2}/_{7}$	1.90	126

PI: preterm infant

Automated T-wave Alternans Detection

The first minute of the recorded preterm ECG were analyzed. From each 1-min ECG, 64-beat windows were iteratively extracted every 1 s. All ECG windows were preprocessed: they were band-pass filtered between 0.8 Hz and

r) Parameters: BW: birth weight; GA: gestational age; mHR: median heart rate; mQT: median QT interval; mQTc: median corrected QT interval; mRR: median RR; mTWA: median TWA AAm over extracted ECG windows; NW: rate of suitable ECG windows; QRSD: median QRS-complex duration; sdRR: standard deviation of RR; TA: median T-wave amplitude.

35 Hz by a 6th-order bidirectional Butterworth filter. R-peak-position detection follows. Then, baseline was removed, where baseline was computed through a 3rd-order spline interpolation of PR fiducial points. R-peak positions were then used to identify fiducial points relative to T section using heart rate-dependent formulae (*Burattini, 1999*). After suitability assessment, automated TWA detection follows through the application of the updated version of AMFM with the same settings of fetal applications to ECG tracings that met both the conditions of the suitability assessment (*Marcantoni, 2020c*). For each preterm ECG, rate of suitable ECG windows (NW) was computed. Then the value of median TWA AAm over the NW ECG windows considered as suitable (mTWA, μV) was computed. If NW < 80% of total windows, analysis was considered unreliable. Thus, in this case, the procedure was iterated for the next following minute in the ECG tracing.

Additional common ECG features, which in adults were found or supposed to correlate with TWA (*Burattini., 2012c; Hanna, 2013; Madias, 2007; Rashba, 2002; Zareba, 1994*) were evaluated: median RR interval (mRR); median heart rate (mHR); RR standard deviation (sdRR); median T-wave amplitude (TA, μV); median QRS-complex duration (QRSD, ms); median QT interval (mQT, ms); median corrected QT interval (mQTc, ms) following Bazett's formula (*Bazett, 1920*). Distributions of features were expressed in terms of mean±standard deviation. Possible associations between TWA and the features were evaluated through the Spearman rank correlation coefficient, where statistical significance level (p) was set at 0.05.

Results

All the computed features are reported in **Table 7.4.2**. Out of 10 preterm infants, 6 had 100% of suitable windows, 2 had 93% of suitable windows, and 2 had 80% of suitable windows. Rejection of ECG windows was due to the occurrence of ectopic beats, rather than high sdRR. TWA varies among preterm infants. Evaluated correlations are reported in **Table 7.4.3**. mTWA correlates with BW, with GA/BW and with sdRR: correlations are strong and statistically significant.

Table 7.4.2. *T-wave alternans and additional electrocardiographic features (Marcantoni, 2020c).*

PI	NW (%)	mTWA (μV)	mHR (bpm)	mRR (ms)	sdRR (ms)	QRSD (ms)	TA (μV)	mQT (ms)	mQTc (ms)
1	100	16	163	369	8	85	258	285	469
2	100	10	117	514	11	120	57	340	474
3	93	18	114	525	43	95	168	360	497
4	100	40	163	369	4	105	170	265	436
5	93	26	171	350	20	95	504	295	499
6	100	38	135	445	8	90	176	300	450
7	100	39	182	329	8	100	328	265	462
8	100	29	160	376	10	105	372	270	440
9	80	32	138	436	7	90	132	325	492
10	80	12	150	400	23	105	95	285	451
T	**95±8**	**26±11**	**149±23**	**411±67**	**14±12**	**99±10**	**226±139**	**299±33**	**467±23**

PI: preterm infant; T: total

Remarks

Table 7.4.3. *Correlations of TWA with all considered features (Marcantoni, 2020c).*

GA	-0.46 (p=0.19)
BW	-0.72* (p=0.02)
GA/BW	0.76* (p=0.02)
mHR	0.41 (p=0.24)
mRR	-0.41 (p=0.24)
sdRR	-0.71* (p=0.02)
QRSD	-0.17 (p=0.65)
TA	0.42 (p=0.23)
mQT	-0.52 (p=0.12)
mQTc	-0.44 (p=0.20)

*p<0.05

The limited number of considered preterm infants finds its reason in the deliberate selection of preterm infants free of any comorbidity and they are statistically very difficult to have in clinical practice. Although ECG recordings were very long, only one minute of ECG was analyzed to develop a procedure applicable also in case of analysis of short ECG recordings. The first evidence of this study is that preterm infants show TWA, even without having any evident cardiac diseases.

In the preterm population under examination, TWA was evaluated in relationship with clinical features at birth and with additional ECG features that were found to be linked to TWA in adults (*Burattini, 2012c; Hanna, 2013; Madias, 2007; Rashba, 2002; Zareba, 1994*).

TWA inversely correlated with sdRR, which is a sign of health and maturity (particularly, reduced heart-rate variability is symptom of a late development of the autonomic cardiac control) (*Kojima, 2018*). Moreover, TWA decreased with BW and increased with GA/BW, thus indicating that TWA was higher in very small infants, mostly if considering weight in relation to gestational age at birth. These observations suggest that TWA in non-pathological preterm infants may still act as a cardiac risk, likely related to the uncomplete development status of the infant, indicated by low BW and low heart rate variability and thus, an indirect index of heart immaturity.

This conclusion is strengthened by the comparison performed between TWA levels in this preterm population and term healthy fetuses. In general, comparison of ECGA levels among different studies is always difficult, since ECGA measurements is strictly dependent on the analysis method used (*Burattini, 2009a*). In a previous TWA analysis on healthy term fetuses (*Marcantoni, 2017; Marcantoni, 2018b*), the measurement was performed at birth by using the same method used for this preterm population. The age at birth of those fetuses ranged between 38 and 41 gestational weeks. Thus, according to age of gestation, they were actually older than the preterm infants taken in consideration in this study. TWA measured in term healthy fetuses was around 10 μV (**Table 7.3.1**), so, smaller than that measured in preterm infants. Therefore, TWA was found to decrease with age at birth. This finding would confirm the hypothesis that TWA in preterm infants should likely be considered as an ECG evidence of heart-maturity level, rather than severe heart pathology predisposing to arrhythmias. The small size of population involved in the study makes this conclusion preliminary and further analysis involving wider populations of both term and preterm infants is necessary. Differently from adults, in this non-pathological preterm population TWA does not correlate to heart rate neither to QT interval: this different behavior would suggest a possible different mechanism and significance of the electrophysiological phenomenon. This preliminary hypothesis encourages further studies to be possibly confirmed. Indeed, it cannot be excluded that low correlation with heart rate may be due to the low variability of heart rate values among preterm infants. Furthermore, TWA occurs

as a spontaneous phenomenon in this case, thus not highlighted by rising heart rate through pacemaker or exercise (*Nearing, 2002; Rosenbaum, 1996*).

This study provided some insights on the TWA interpretation in non-pathological preterm infants and opened an issue on ECGA role as a heart-maturity marker in this condition, rather than an arrhythmia-risk marker, which requires further studies to be solved. Prematurity is a not so rare tricky condition in which monitoring of the newborn plays an essential role in his/her good growth since the newborn is forced to prematurely face life outside the womb. The research in this particular non-pathological but tricky condition deserve to be reinforced through further studies that can focus on the most important and useful markers to be monitored in order to guarantee a well-timed care if needed. Thus, availability of reliable growth/risk markers, such as ECGA, may reveal fundamental.

8

ELECTROCARDIOGRAPHIC ALTERNANS IN CARDIAC AND NON-CARDIAC PATHOLOGIES

Only few studies on ECGA analysis exist in the literature. So, it still misses to be deeply analyzed both in cardiac and non-cardiac pathologies, like in case of kidney disease requiring hemodialysis treatment and in case of myocardial bridging anomaly, here considered (*Marcantoni, 2020b; Marcantoni, 2020a*). Below, two case reports are reported about ECGA measurement through the updated AMFM, in a myocardial bridging case and in a hemodialysis case (†).

8.1 Study on Hemodialysis: A Case Report

Hemodialysis is a therapeutic procedure mainly practiced in the treatment of patients with chronic kidney disease, defined as the progressive loss of kidney function. Practically, the state of kidney disease does not allow kidneys to work normally and hemodialysis replaces their function, through a process of purifying the blood from toxic substances by the use of a machine. Cardiovascular disease has an incidence more than 50% on patients undergoing hemodialysis and the relative death risk becomes 20 times higher than in the general population; for example, the incidence of left ventricular hypertrophy can reach 75% at hemodialysis initiation (*Cozzolino, 2018*). For the general population, there have been relevant improvements in the treatment of cardiovascular disease, but interventions that are valid for the general population sometimes have no the same positive effects on hemodialysis patients. Some cardiovascular complications increase the risk for hemodialysis patients to undergo arrhythmias and even SCD. Moreover, fluctuations of levels of Na^+, K^+ and Ca^{++} and magnesium in plasma occurring during hemodialysis treatment may create the conditions triggering life-threatening cardiac arrhythmias (*Cozzolino, 2018*).

The first study investigating TWA on hemodialysis patients is recent: it was performed in 2007 on a small population of 9 patients and among them 7 out 9 showed TWA, before or after the hemodialysis treatment (*Friedman, 2007*). In 2009 another study analyzed TWA in a hemodialysis population of 59 patients: they found out that 13 patients were positive to TWA and that physical exercise training did not seem to reduce it (*Kouidi, 2009*). A following study, in 2011, pointed out that incidence of TWA defined as abnormal was higher in end-stage renal disease patients than

† For clarity, the parameters used in the clinical studies will be defined in each paragraph. Common parameters are reported with the same name, even if referring to different populations under analysis.

in ventricle hypertrophy patients (57.7% vs 26.7%) (*Patel, 2011*). These studies neglected the intra-hemodialysis treatment period. Starting from 2011, researchers began to consider it. A study analyzed 72-h Holter ECG recordings in hemodialysis patients, and results were compared among the three 24-h periods, with the second one including hemodialysis session. Findings of this study showed abnormal TWA values in 96% of patients without significative difference among periods (*Secemsky, 2011*). Quite different findings were observed in a study considering a 48-h period, including hemodialysis session: the distribution of TWA peaks was constant before, during and after hemodialysis session, but mean TWA increased during hemodialysis and returned to baseline two hours after hemodialysis (*Green, 2012*).

Given the fluctuations of ion plasma concentrations due to hemodialysis treatment, ECGA analysis may represent the best means to monitor their trend in order to notice in time possible abnormal oscillations visible on the ECG and possibly leading to severe or malignant arrhythmias. Being involved most of the ions acting to determine action potential, it is reasonable the analysis of ECGA in all its possible forms.

Case Report [s]

Data

The patient of this study is an 82-years-old male subject with chronic kidney failure, treated by hemodialysis procedure. A 12-lead-ECG recording was acquired from the patient. The ECG recording was continuously acquired for 24 h in a hemodialysis-session day: the acquisition started at 11:00 am (hour zero) of a hemodialysis treatment day and ended at 11:00 am of the next day, with hemodialysis starting at 4:00 pm and lasting 4 h. The ECG acquisition was performed by a wearable 12-lead M12 Holter ECG recorder by Global Instrumentation®, having a sampling rate of 1000 Hz (www.globalinstrumentation.com;). During the acquisition, the subject accomplished normal daily activities (walking, eating and sleeping). Specifically, during the hemodialysis session, he rested lying on his back (*Leoni, 2019*).

The ECG acquisition procedure was accomplished in accordance with the ethical principles of Helsinki Declaration and approved by the institutional expert committee. The patient gave informed consent prior to the acquisition.

Automated Electrocardiographic Alternans Detection

All the concurrently recorded 12 ECG leads of the entire acquisition were studied. From each ECG lead, 128-beat windows were iteratively extracted every 1 s. All ECG windows were preprocessed: they were resampled from 1000 Hz to 200 Hz and band-pass filtered between 0.3 Hz and 35 Hz by a 6^{th}-order bidirectional Butterworth filter. R-peak-position detection was performed always on one lead only (they were effectual for all the others). R-peak positions were then used to identify fiducial points relative to ECG sections. After suitability assessment, automated ECGA detection follows through the application of the updated AMFM to ECG leads that met both the conditions of the suitability

s) Parameters: mHR: median heart rate; NW: rate of suitable ECG windows.

assessment (*Marcantoni, 2019a; Marcantoni, 2020b*).

The ECG recording was discriminated into four hemodialysis-related time periods: from 11:00 am to 4:00 pm, before hemodialysis session; from 4:00 pm to 8:00 pm, during the hemodialysis session; from 8:00 pm to 1:00 am, immediately after hemodialysis session; from 1:00 am to 6:00 am, during the night after hemodialysis session. Analysis proceeded considering in parallel hemodialysis-related time periods and all leads.

Mean percentage of PWA, QRSA and TWA rates (%) were computed. This allows the definition of the form of ECGA considered as the prevalent alternans. Then, only AAm values of the prevalent alternans were computed, as well as median heart rate (mHR). Lilliefors test was used to evaluate the normality of distributions for heart rate and prevalent alternans amplitudes. Non-normal distributions were reported in terms of 50^{th} [25^{th};75^{th}] percentiles. Rate of suitable ECG windows (NW) was also evaluated. Median value of prevalent alternans amplitude was evaluated over all leads. Wilcoxon rank-sum test was used for statistical comparisons among distributions of prevalent alternans amplitudes in the four hemodialysis-related time periods, where statistical significance level (p) was set at 0.05.

Results

Mean rates of PWA, QRSA and TWA are reported in **Table 8.1.1**, **Table 8.1.2**, **Table 8.1.3** and **Table 8.1.4**. For all hemodialysis-related time periods and all leads, TWA was the prevalent alternans since TWA rate was always the highest (81% across all leads and time periods) with respect to PWA (11%) and QRSA (8%). In **Table 8.1.5**, TWA AAm distributions and NW are reported. All values but one (corresponding to lead I in the night after hemodialysis) are higher if compared with TWA values that were obtained analyzing a healthy male population using the original version of AMFM (*Burattini, 2010*). TWA AAm resulted high before hemodialysis (62 μV, lead V5), and even higher during hemodialysis (66 μV, lead V6). Then, it progressively decreased in the subsequent time periods, after hemodialysis (43 μV, lead

Table 8.1.1. *PWA, QRSA, TWA rates before hemodialysis session (Marcantoni, 2020b).*

ECG Lead	I	II	III	V1	V2	V3	V4	V5	V6	aVR	aVL	aVF	T
PWA (%)	10	10	11	10	11	10	10	12	11	11	10	10	**10**
QRSA (%)	7	7	6	7	7	7	7	8	8	7	7	6	**7**
TWA (%)	83	83	83	83	82	83	83	80	81	82	83	84	**83**

T: total

Table 8.1.2. *PWA, QRSA, TWA rates during hemodialysis session (Marcantoni, 2020b).*

Lead	I	II	III	V1	V2	V3	V4	V5	V6	aVR	aVL	aVF	T
PWA (%)	19	13	12	11	12	12	12	17	10	13	11	9	**13**
QRSA (%)	9	8	7	7	10	7	10	10	8	8	8	6	**8**
TWA (%)	72	79	81	82	78	81	78	73	82	79	81	85	**79**

T: total

Table 8.1.3. *PWA, QRSA, TWA rates after hemodialysis session (Marcantoni, 2020b).*

Lead	I	II	III	V1	V2	V3	V4	V5	V6	aVR	aVL	aVF	T
PWA (%)	11	10	9	9	10	9	10	11	20	12	11	12	**11**
QRSA (%)	8	6	5	6	6	6	8	8	16	8	6	7	**8**
TWA (%)	81	84	86	85	84	85	82	81	64	80	83	81	**81**

T: total

Table 8.1.4. *PWA, QRSA, TWA rates in the night after hemodialysis session (Marcantoni, 2020b).*

Lead	I	II	III	V1	V2	V3	V4	V5	V6	aVR	aVL	aVF	T
PWA (%)	11	8	7	9	8	8	11	12	12	10	9	9	**10**
QRSA (%)	9	5	5	6	6	5	7	8	9	6	6	7	**7**
TWA (%)	80	87	88	85	86	87	82	80	79	84	85	84	**83**

T: total

Table 8.1.5. *Distribution of TWA AAm in the hemodialysis-related time periods (Marcantoni, 2020b).*

ECG lead	PRE-HD (µV)	IN-HD (µV)	POST-HD (µV)	NT-HD (µV)	NW (%)
I	33 [27;41]	31 [27;46]	19 [15;29]	13 [10;17]	31
II	54 [35;75]	57 [46;76]	34 [25;47]	38 [27;57]	61
III	51 [32;84]	54 [41;80]	43 [29;76]	38 [28;56]	47
V1	32 [24;45]	37 [32;41]	24 [17;34]	24 [17;37]	44
V2	43 [30;57]	40 [35;44]	28 [18;45]	22 [17;31]	30
V3	57 [36;82]	52 [42;72]	40 [27;59]	37 [27;52]	59
V4	55 [31;74]	55 [41;73]	21 [16;37]	17 [13;25]	66
V5	62 [38;92]	59 [42;77]	28 [19;42]	18 [14;23]	70
V6	42 [30;63]	66 [47;112]	37 [32;47]	24 [14;40]	29
aVR	58 [40;82]	52 [33;79]	37 [28;53]	21 [15;33]	62
aVL	50 [35;66]	46 [34;70]	25 [17;35]	19 [14;28]	59
aVF	38 [29;53]	56 [45;68]	19 [14;29]	20 [14;31]	47
T	**51 [32;70]**	**53 [41;73]**	**28 [19;44]***	**22 [15;32]***	**53**

IN-HD: time period during hemodialysis; PRE-HD: time period before hemodialysis; POST-HD: time period after hemodialysis; NT-HD: time period during the night after hemodialysis; Total: total

III) and in the night after hemodialysis (38 µV, leads II and III). If interquartile range had been evaluated, it would have assumed the same trend from the time period before hemodialysis to the night after hemodialysis. NW was lower or equal to 70% for all leads, with ECG windows being rejected especially before and during hemodialysis. The patient's

mHR ranged between 59 bpm, before hemodialysis and in the night after hemodialysis, to 66 bpm, after hemodialysis. Statistical differences of the time period before hemodialysis against after hemodialysis ($p<10^{-3}$), and of the time period before hemodialysis against night after hemodialysis ($p<10^{-3}$), were revealed. Furthermore, differences of time period during hemodialysis against after hemodialysis ($p<10^{-3}$), and against night after hemodialysis ($p<10^{-3}$) were statistically significant. Instead, there was no statistical difference of time period before hemodialysis against during hemodialysis ($p=0.60$) and of time period after hemodialysis against night after hemodialysis ($p=0.12$). These results are visually perceived in the TWA trends represented in **Fig. 8.1.1**, where rejected windows were not represented, but occurrence-time information were maintained. In the graph, a peak can be noticed during hemodialysis, while values decreased two hours after the end hemodialysis session (<50 μV).

Remarks

This study was the first attempt to study ECGA in all its forms in a hemodialysis patient. PWA, QRSA and TWA rates showed that ECGA center of mass especially fell within section related to T wave along all the ECG recording, for all hemodialysis-related time periods and all leads. Here, TWA showed increased values and variability (assessable as interquartile range) before and during hemodialysis session, with a peak between the first and second hour of hemodialysis session. ECGA analysis pointed out that time periods before hemodialysis and during hemodialysis may be circumstances characterized by a higher risk of arrhythmias. Also, being TWA the prevalent form, the risk may be particularly linked to electrical anomalies of ventricular repolarization. TWA (quantified by AAm values) decreased two hours after the end of the treatment, assessing around values lower than 50 μV. Probably, TWA trend is driven by fluctuations of ionic plasma concentrations. The peak of TWA during hemodialysis may be explained by considering that before and during hemodialysis treatment, electrolyte concentrations shift (*Secemsky, 2011; Green, 2012*). Thus, consequent cardiac distress may lead to a high number of ectopic beats; this finds confirmation in the high rate of rejected ECG windows before and during hemodialysis. TWA behavior here observed endorsed results presented in *Green, 2012*, even if using different detecting methods. Moreover, all four hemodialysis-related time periods presented PWA and QRSA, even though in small percentages. Analogous behavior is observable on the 12 leads, except lead V6, which after hemodialysis was characterized by a higher PWA rate (20%) and QRSA rate (16%), while

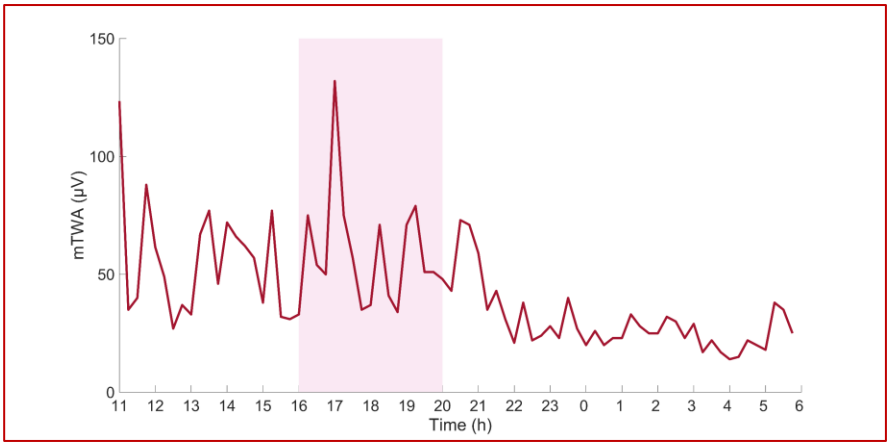

Figure 8.1.1. *TWA trend described through mTWA computed in intervals of 15 min over the whole ECG recording and all leads. Pink area corresponds to time period during hemodialysis session (Marcantoni, 2020b).*

TWA reached lower rate (64%) compared with all other leads and time periods. This observation may be justified by the lead dependency of TWA (*Burattini, 2012b*), behavior probably shared with PWA and QRSA. TWA AAm computed in this study may be overestimated, since the updated AMFM tends to overvaluation in case of multiple waves alternating (*Marcantoni, 2019a*). Also, the wave oscillation considered as prevalent is affected by oscillation of the other waves (*Madias, 2005; Marcantoni, 2019a*).

Nevertheless, results obtained in this case study, suggested a possible higher cardiac risk (mostly influencing ventricular repolarization) in hemodialysis patients with respect to healthy subjects and this risk showed to decrease after the end of hemodialysis session. Since only one subject was considered, this study should be considered preliminary but promising. It was based on the strictly link between the urinary system and the cardiovascular system. This is the reason why cardiovascular problems can occur if the function of the urinary system is compromised by a disease. Hemodialysis is an important treatment in case kidneys stop correctly performing their function and it can cause fluctuations in plasma concentration of ions. In turn, these ions are fundamental in the cardiac electrical function. This means that clinical monitoring of the cardiac function in relation to hemodialysis treatment is extremely important. In particular, monitoring of noninvasive ECG risk indexes, such as ECGA, may mean a prompt clinical intervention in case of complications, but at the same time it may highlight possible positive effects of the treatment on the cardiac electrical function. Actually, the positive or negative effect of hemodialysis treatment on the cardiac function and on the patient predisposition to develop arrhythmias deserve a deeper investigation. Thus, further analysis will be needed in the future, enrolling a wider hemodialysis population; this may also allow the analysis protocol proposed here to be validated for ECGA evaluation in hemodialysis.

8.2 Study on Myocardial Bridging: A Case Report

Myocardial bridging is a congenital heart anomaly affecting a coronary artery. Particularly, it consists of a portion of an epicardial coronary artery that has an intramuscular course, instead of running over the cardiac muscle. In this condition, myocardium results overlying the coronary artery portion, instead of being physiologically underneath it. As a consequence, the myocardium looks as a "bridge", while the coronary artery looks partially "tunneled".

The most common technique to diagnose the pathology is coronary angiography. Myocardial bridging frequently concerns the left anterior descending coronary, but it seems that angiography tends to undervalue the circumflex or the right coronaries. Data about the prevalence of myocardial bridging on general population differ on the mode of clinical assessment (*Lee, 2015*).

Interested blood vessels can result distorted or compressed and sometimes, electromechanical functionality of the heart is heavily compromised. The physical and functional abnormality is usually relieved through surgical intervention by resection of the muscle-fiber bridge or by-passing the coronary artery. Myocardial bridging influences the affected coronary artery, but it may also influence the growth and the function of the adjacent blood vessels, depending on its entity and depth. Indeed, sometimes this pathology remains latent for a long time or it is a benign finding, while in some subjects it can provoke severe cardiac complications, also malignant (*Ferreira, 1991; Lee, 2015*).

Mechanical stress in correspondence of myocardial bridged coronary portion can cause endothelial damage, atherosclerosis and vasospasm, conditions that can cause ischemia. Other cardiovascular complications of myocardial bridging include acute coronary syndromes, angina, dysfunction of the left ventricle, and arrhythmia (*Agirbasli, 1997; Ishikawa, 2011; Kastellanos, 2018; Lee, 2015; Yuan, 2016; Morales, 1980; Hostiuc, 2011*).

Pathophysiological studies have found an association between the anomalous coronary blood flow caused by myocardial bridging and SCD (*Yuan, 2016*). Myocardial bridging can be at the origin of myocardial fibrosis and edema, and both pathologies bring a higher susceptibility to electrical instability. This complication often occurs in case of hemodynamically significant myocardial bridging and its association with SCD can be met in an increased heterogeneity in cardiac electrical function (*Hostiuc, 2011*). Eventually, some studies reported an incidence of repolarization abnormalities that is significantly higher in myocardial bridging population than non-myocardial bridging population (*Aksan, 2015; Barutcu, 2004; Mandala, 2017; Nishikii-Tachibana, 2018*).

In order to monitor the effects of myocardial bridging on cardiac electrical functionality, reliable noninvasive risk markers, like ECGA, should be evaluated. ECGA can help to prevent severe cardiac events.

Case Report (t)

Data

The patient of this study is a 54-years-old male subject with myocardial bridging, who was hospitalized at "Ospedali Riuniti", in Ancona, before surgery. The coronary artery affected by myocardial bridging is the left coronary artery, specifically the interested portion is in the anterior descending branch.

A 12-lead-ECG recording was acquired from the patient. The ECG recording started during the afternoon, at 4:20 pm, and lasted 18 h. The ECG acquisition was performed by a wearable 12-lead M12 Holter ECG recorder by Global Instrumentation®, having a sampling rate of 1000 Hz (www.globalinstrumentation.com;). In the meantime, the patient carried out normal activities allowed by its hospitalization condition. During the ECG acquisition and particularly in the first hour, the patient remained in a resting condition, lying on the hospital bed. The ECG acquisition procedure was accomplished in accordance with the ethical principles of Helsinki Declaration and approved by the institutional expert committee. The patient gave informed consent prior to the acquisition.

Automated Electrocardiographic Alternans Detection

All the concurrently recorded 12 ECG leads of the first hour of acquisition were studied. From each 1-hour ECG lead, 64-beat windows were iteratively extracted every 1 s. All ECG windows were preprocessed: they were resampled from 1000 Hz to 200 Hz and band-pass filtered between 0.3 Hz and 35 Hz by a 6^{th}-order bidirectional Butterworth filter. R-peak-position detection was performed always on one lead only (they were effectual for all the others). R-peak positions were then used to identify fiducial points relative to ECG sections. After suitability assessment, automated ECGA detection follows through the application of the updated AMFM to ECG leads that met both the conditions of the suitability assessment (*Marcantoni, 2019a; Marcantoni, 2020a*). In this study, the updated AMFM was set to provide in output amplitudes of all ECGA forms, regardless the barycenter position. Mean (or median) values, over suitable ECG windows, of PWA AAm (mPWA), of QRSA AAm (mQRSA) and of TWA AAm (mTWA) were obtained for each lead. Then, mean (or median) values of ECGA AAr were computed as the product between mPWA and P-wave time width, mQRSA and QRS-complex time width and mTWA and T-wave time width (mPWA_ar, mQRSA_ar and mTWA_ar, respectively), expressed in μV·s. The form of ECGA showing the highest AAr was identified as the prevalent alternans. Furthermore, those leads having rate of rejected ECG windows (RW) inferior than 30% were considered reliable. For each lead, normality of PWA, QRSA and TWA distributions was tested by the Lilliefors test. Normal distributions were reported in terms of mean±standard deviation, while non-normal distributions were reported in terms of $50^{th}[25^{th};75^{th}]$ percentiles. Trend of prevalent alternans and mean heart rate

t) Parameters: mPWA: mean (or median) PWA AAm over suitable ECG windows; mPWA_ar: mean (or median) PWA AAr over suitable ECG windows; mQRSA: mean (or median) QRSA AAm over suitable ECG windows; mQRSA_ar: mean (or median) QRSA AAr over suitable ECG windows; mTWA: mean (or median) TWA AAm over suitable ECG windows; mTWA_ar: mean (or median) TWA AAr over suitable ECG windows; RW: rate of rejected ECG windows.

(mHR) were evaluated, by computing the relative mean AAr over reliable leads and mHR, every 5 min. The two trends were quantitively compared through Wilcoxon rank-sum test, where statistical significance level (p) was set at 0.05.

Results

For each lead, 3600 windows were preprocessed. In **Table 8.2.1**, distributions of mPWA_ar, mQRSA_ar and mTWA_ar are reported. The lead showing the highest values of AAr was lead II. For all leads, the prevalent alternans resulted TWA. Mean mPWA_ar, mQRSA_ar and mTWA_ar over leads were 4.7 μV·s, 4.3 μV·s and 6.3 μV·s, respectively.
In **Table 8.2.2**, results on prevalence rate are reported. RW went from 19% to 50%. Half of the available leads were considered as reliable (II, III, V1, V4, aVL, aVF); among them there was the one with the highest alternans. **Table 8.2.2** confirms TWA as the prevalent alternans, with a mean prevalence rate of 94%, followed by PWA (5%) and QRSA (1%). **Fig. 8.2.1** reported trend of mean±standard deviation of mTWA_ar over reliable leads and trend of mHR. Common trend was quantitively confirmed by their correlation, which was strong (0.72) and statistically significant ($p<10^{-2}$).

Remarks

This study analyzed ECGA of a myocardial bridging patient at rest. Even if only one patient was taken in consideration (rarity of the pathology makes difficult data availability), it could contribute to have more insight on the possibility that myocardial bridging can rise cardiac risk highlighted by ECGA. The prevalent form of ECGA is likely influenced by the coronary artery affected by myocardial bridging, since ECG waves reflect the function of a part of the heart in the cardiac cycle. The patient of this study has myocardial bridging

Table 8.2.1. *Distributions of ECGA AAr, reported as 50th[25th;75th] percentiles. The prevalent alternans in bold (Marcantoni, 2020a).*

ECG lead	mPWA_ar (μV·s)	mQRSA_ar (μV·s)	mTWA_ar (μV·s)
I	5.6 [4.1;7.7]	5.4 [4.2;7.3]	**7.2 [5.6;9.4]**
II	7.5 [5.6;9.5]	7.0 [5.3;9.0]	**10.0 [8.0;13.6]**
III	4.7 [3.7;5.7]	4.1 [3.2;5.1]	**6.6 [5.0;8.4]**
V1	6.4 [4.5;8.3]	5.9 [4.4;7.8]	**8.2 [6.6;10.4]**
V2	3.7 [2.8;4.6]	3.5 [2.8;4.5]	**5.2 [4.0;6.6]**
V3	4.8 [3.8;6.1]	4.2 [3.4;5.3]	**6.8 [5.4;8.6]**
V4	3.8 [2.4;5.2]	3.6 [2.6;5.0]	**5.0 [3.6;6.8]**
V5	2.8 [2.2;3.5]	2.5 [1.8;3.4]	**3.6 [2.6;4.8]**
V6	4.5 [3.3;5.8]	4.0 [3.1;5.3]	**5.8 [4.2;7.6]**
aVR	3.6 [2.6;4.9]	3.3 [2.4;4.6]	**5.4 [3.8;6.8]**
aVL	4.5 [3.5;6.4]	4.1 [3.0;5.6]	**6.0 [4.6;8.4]**
aVF	4.7 [3.3;7.0]	4.3 [3.1;6.5]	**6.2 [4.4;9.8]**

Table 8.2.2. *Prevalence rate of PWA, QRSA, TWA and RW. The reliable leads (RW<30%) are on gray background (Marcantoni, 2020a).*

ECG lead	PWA (%)	QRSA (%)	TWA (%)	RW (%)
I	6	1	**57**	36
II	4	1	**71**	24
III	1	0	**70**	29
V1	7	1	**65**	27
V2	1	0	**49**	50
V3	1	0	**50**	49
V4	6	1	**71**	22
V5	3	0	**47**	50
V6	3	1	**45**	51
aVR	2	0	**65**	33
aVL	3	0	**77**	20
aVF	2	0	**79**	19

on a coronary artery that supplies blood to ventricles. It seems foreseeable that the ventricular activity was the most affected and that the prevalent form is TWA. Mean mTWA_ar over leads is higher than 6 μV·s, having peaks over 10 μV·s, while mTWA_ar measured on a healthy male population by the original AMFM (which guarantees comparability of results) was estimated to be around 3 μV·s (*Burattini, 2010*). Thus, the expected mTWA_ar on a healthy subject is doubled by myocardial bridging patient of this study. Therefore, myocardial bridging seems to rise TWA with respect a healthy subject, and likely the cardiac risk associated to it. No values of PWA and QRSA in healthy subjects are available in the literature and this prevents comparison of results and further evaluations. Future studies will provide reference values also for PWA and QRSA. TWA had the typical behavior to be lead-dependent (wide pink shade in **Fig. 8.2.1**) (*Burattini, 2010*) and correlated with heart rate.

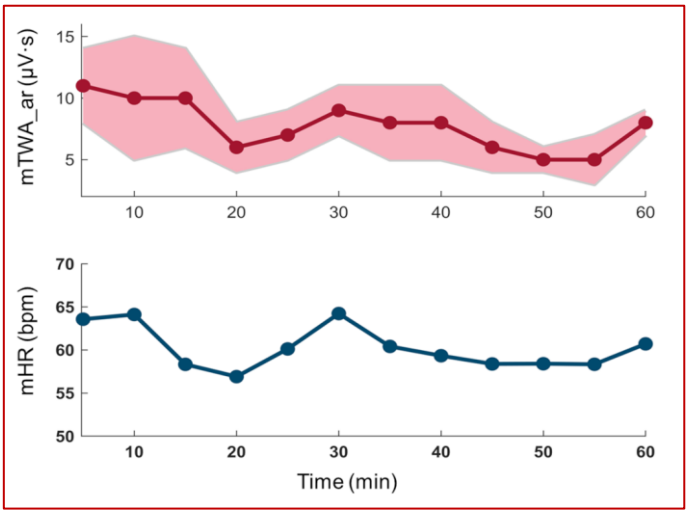

Figure 8.2.1. *Trend of mean±standard deviation mTWA_ar over reliable leads (upper panel, where mean and standard deviation of mTWA_ar are marked with full circles and through pink shade, respectively) and trend of mHR (lower panel) (Marcantoni, 2020a).*

An important final remark concerns the introduction of the computation of the amplitude area. This parameter is not an output of the updated AMFM, but it was introduced to take in consideration different durations of ECG waves. Area evaluation increases reliability of comparison, but measurement can be still affected by mutual ECGA influence. This issue is solved in the EAMFM.

In conclusion, the results obtained in this case study can point out that the cardiac risk to undergo arrhythmias is higher than healthy subjects and can grow up in case of physical activity involving higher heart rates. Further studies on wider populations may confirm this, which now remains a likely hypothesis. In the literature, there are some clinical cases of young athletes who experienced sudden death while practicing sport and who then were diagnosed with a myocardial bridging (*Agirbasli, 1997; Morales, 1980*). Consequently, it should be critically evaluated whether to include myocardial bridging among the causes of sport-related SCD in apparently healthy young athletes. One of the most powerful weapons against these kinds of severe cardiac events is prevention. Prevention can pass through the use of noninvasive risk markers that can be identified during standard clinical tests, of which one of the most common, especially in sport field, is the ECG. ECGA risk marker may be used. Further insights may confirm the possible usefulness of introducing this risk index in routine monitoring in the case of athletes.

CONCLUSIONS

The aim of this PhD thesis was to provide insights on ECGA, which is known, especially in its TWA form but not deeply investigated still. Its role and behavior were investigated in different scenarios, including also non-cardiac pathologies and non-pathological conditions, in order to test its generalization of applicability as risk index. These studies provided some observations opening evaluable research areas to be deeply analyzed in the future. Dofetilide seems to increase vulnerability to arrhythmias in a certain period following its assumption. In proximity of epileptic seizures, the risk to develop electrical instability rises. Fetuses show TWA even if they are healthy and the same happens in preterm infants, suggesting a different role of the parameter in these conditions, no more as risk index, but rather as heart maturity-level index. Risk of arrhythmias is high in a patient undergoing hemodialysis, but the treatment seems to decrease it, probably due to rebalancing of electrolytes. Myocardial bridging is a heart anomaly increasing vulnerability to arrhythmias, but the risk appears to even grow up while performing an activity implying high heart rates. All these observations deserve more studies to be possibly confirmed but, more in general, they have shown that the generalization of ECGA applicability as risk index may be possible. Fundamental is the availability of reliable instruments to assess cardiac risk, when associated to cardiac pathologies, but also non-cardiac pathologies, and even non-pathological conditions. Thus, a new method was introduced: EAMFM. It is the first method able to reliably identify and measure ECGA in all its possible forms. This new method of analysis, specially designed to strengthen the prognostic value of ECGA as an index of cardiac risk, may allow a more reliable risk assessment, a consequent more targeted clinical intervention to prevent SCD and a generalized assessment of cardiac risk in various scenarios.

There is not a threshold for ECGA evaluation, i.e. a value under which ECGA is physiological and over which ECGA is pathological. From a biomedical point of view, this is mainly due to a not uniform quantification of TWA among different identification methods and a lack of methods to identify also PWA and QRSA. The literature has shown that TWA is not an on/off phenomenon and that low values of TWA amplitude and duration can be physiological. Only if they reach high values it indicates a higher risk for arrhythmias, also malignant in some cases. Possibly, PWA and QRSA have the same behavior and an analogous mechanism of genesis. Nevertheless, a combined vision may be very useful. In clinical practice, reliable risk indexes are fundamental to highlight anomalies, especially in absence of evident signs. If their identification can become automatic and integrated in commonly spread and used machines, they would completely perform their function in prevention of SCD. Much remains to be discovered on the mechanisms governing SCD and on the most suitable methods to prevent it. New prevention paradigms have been introduced, e.g. the near-term prevention. Moreover, likely, the dynamic nature of SCD triggering factors together with complex disease substrates may suggest a possible helpful role played by mobile and wearable technology.

The prevention of SCD remains challenging, but not eludable. Future studies are intended to fill in the gap between these scientific research findings and routine clinical care, possibly validating ECGA prognostic role in the prevention of SCD.

This thesis is the attempt to give a contribution in this filed, starting from the study of the possibility to generalize TWA role as a risk index, not only in cardiac field, allowing a generalization of applicability. Then, the implementation of a reliable ECGA identification method was presented to quantify PWA and QRSA, contextually improving TWA detection and quantification. This may help to define physiological and pathological ECGA (studying wide healthy and pathological populations) and validate ECGA prognostic role (collaboration with physician and clinicians will be fundamental). Even if role of TWA and more in general ECGA in clinical settings is not focused yet, some of TWA detection techniques are already present in some ECG devices. So, the final aim will be possibly integrating EAMFM into the embedded systems or the interpretation software of new devices, passing from the research in electrophysiological studies to translational engineering.

REFERENCES

Agirbasli, M., Martin, G. S., Bunker Stout, J., Jennings, H. S., Lea, J. W., & Dixon, J. H. (1997). Myocardial bridge as a cause of thrombus formation and myocardial infarction in a young athlete. Clinical cardiology, 20(12), 1032-1036.

Agostinelli, A., Giuliani, C., & Burattini, L. (2014, September). Extracting a clean ECG from a noisy recording: a new method based on segmented-beat modulation. In Computing in Cardiology 2014 (pp. 49-52). IEEE.

Agostinelli, A., Grillo, M., Biagini, A., Giuliani, C., Burattini, L., Fioretti, S., ... & Burattini, L. (2015). Noninvasive fetal electrocardiography: an overview of the signal electrophysiological meaning, recording procedures, and processing techniques. Annals of Noninvasive Electrocardiology, 20(4), 303-313.

Agostinelli, A., Marcantoni, I., Moretti, E., Sbrollini, A., Fioretti, S., Di Nardo, F., & Burattini, L. (2017). Noninvasive fetal electrocardiography Part I: Pan-Tompkins' algorithm adaptation to fetal R-peak identification. The open biomedical engineering journal, 11, 17-24.

Agostinelli, A., Sbrollini, A., Giuliani, C., Fioretti, S., Di Nardo, F., & Burattini, L. (2016). Segmented beat modulation method for electrocardiogram estimation from noisy recordings. Medical Engineering & Physics, 38(6), 560-568.

Aksan, G., Nar, G., İnci, S., Yanık, A., Kılıçkesmez, K. O., Aksoy, O., & Soylu, K. (2015). Exercise-induced repolarization changes in patients with isolated myocardial bridging. Medical science monitor: international medical journal of experimental and clinical research, 21, 2116-2124.

Al-Aweel, I. C., Krishnamurthy, K. B., Hausdorff, J. M., Mietus, J. E., Ives, J. R., Blum, A. S., ... & Goldberger, A. L. (1999). Postictal heart rate oscillations in partial epilepsy. Neurology, 53(7), 1590-1592.

Armoundas, A. A., Tomaselli, G. F., & Esperer, H. D. (2002). Pathophysiological basis and clinical application of T-wave alternans. Journal of the American College of Cardiology, 40(2), 207-217.

Barutcu, I., Sezgin, A. T., Gullu, H., Topal, E., Acikgoz, N., & Ozdemir, R. (2004). Exercise-induced changes in QT interval duration and dispersion in patients with isolated myocardial bridging. International journal of cardiology, 94(2-3), 177-180.

Bazett, H. C. (1920). An analysis of the time relations of electrocardiograms. Heart 7, 353–370.

Brembilla-Perrot, B., Lucron, H., Schwalm, F., & Haouzi, A. (1997). Mechanism of QRS electrical alternans. Heart, 77(2), 180-182.

Burattini, L., Bini, S., & Burattini, R. (2009). Comparative analysis of methods for automatic detection and quantification of microvolt T-wave alternans. Medical engineering & physics, 31(10), 1290-1298.

Burattini, L., Bini, S., & Burattini, R. (2012). Repolarization alternans heterogeneity in healthy subjects and acute myocardial infarction patients. Medical engineering & physics, 34(3), 305-312.

Burattini, L., Man, S., Burattini, R., & Swenne, C. A. (2012). Comparison of standard versus orthogonal ECG leads for T-wave alternans identification. Annals of Noninvasive Electrocardiology, 17(2), 130-140.

Burattini, L., Man, S., Fioretti, S., Di Nardo, F., & Swenne, C. A. (2016). Heart rate–dependent hysteresis of T-wave alternans in primary prevention ICD patients. Annals of Noninvasive Electrocardiology, 21(5), 460-469.

Burattini, L., Zareba, W., & Burattini, R. (2008). Adaptive match filter based method for time vs. amplitude characterization of microvolt ECG T-wave alternans. Annals of Biomedical Engineering, 36(9), 1558-1564.

Burattini, L., Zareba, W., & Burattini, R. (2009). Assessment of physiological amplitude, duration, and magnitude of ECG T-wave alternans. Annals of Noninvasive Electrocardiology, 14(4), 366-374.

Burattini, L., Zareba, W., & Burattini, R. (2010). Identification of gender-related normality regions for T-wave alternans. Annals of Noninvasive Electrocardiology, 15(4), 328-336.

Burattini, L., Zareba, W., & Burattini, R. (2012). Is T-wave alternans T-wave amplitude dependent?. Biomedical Signal Processing and Control, 7(4), 358-364.

Burattini, L., Zareba, W., & Moss, A. J. (1999). Correlation method for detection of transient T-wave alternans in digital Holter ECG recordings. Annals of Noninvasive Electrocardiology, 4(4),416-424.

Castellucci, M., Cremona, O., De Luca, A., Giuliani Piccari, G., Lantini, M. S., Marchisio, P. C., Rodella, L. F. (2009). Anatomia Umana. Monduzzi.

Chugh, S. S. (2017). Sudden cardiac death in 2017: spotlight on prediction and prevention. International journal of cardiology, 237, 2-5.

Cozzolino, M., Mangano, M., Stucchi, A., Ciceri, P., Conte, F., & Galassi, A. (2018). Cardiovascular disease in dialysis patients. Nephrology Dialysis Transplantation, 33(suppl_3), iii28-iii34.

Cuneo, B. F., Strasburger, J. F., & Wakai, R. T. (2008). Magnetocardiography in the evaluation of fetuses at risk for sudden cardiac death before birth. Journal of electrocardiology, 41(2), 116-e1.

Cuneo, B. F., Strasburger, J. F., Yu, S., Horigome, H., Hosono, T., Kandori, A., & Wakai, R. T. (2013). In utero diagnosis of long QT syndrome by magnetocardiography. Circulation, 128(20), 2183-2191.

Eggleston, K. S., Olin, B. D., & Fisher, R. S. (2014). Ictal tachycardia: the head–heart connection. Seizure, 23(7), 496-505.

Engle, W. A., Tomashek, K. M., & Wallman, C. (2007). "Late-preterm" infants: a population at risk. Pediatrics, 120(6), 1390-1401.

Ferreira, A. G., Trotter, S. E., König, B., Decourt, L. V., Fox, K., & Olsen, E. G. (1991). Myocardial bridges: morphological and functional aspects. Heart, 66(5), 364-367.

Friedman, A. N., Groh, W. J., & Das, M. (2007). A pilot study in hemodialysis of an electrophysiological tool to measure sudden cardiac death risk. Clinical nephrology, 68(3), 159-164.

Gacek, A., & Pedrycz, W. (Eds.). (2011). ECG signal processing, classification and interpretation: a comprehensive framework of computational intelligence. Springer Science & Business Media.

Gimeno-Blanes, F. J., Blanco-Velasco, M., Barquero-Pérez, Ó., García-Alberola, A., & Rojo-Álvarez, J. L. (2016). Sudden cardiac risk stratification with electrocardiographic indices-a review on computational processing, technology transfer, and scientific evidence. Frontiers in physiology, 7, 82.

Goldberger, A. L., Amaral, L. A., Glass, L., Hausdorff, J. M., Ivanov, P. C., Mark, R. G., ... & Stanley, H. E. (2000). PhysioBank, PhysioToolkit, and PhysioNet: components of a new research resource for complex physiologic signals. circulation, 101(23), e215-e220.

Green, D., Batchvarov, V., Wijesekara, C., Kalra, P. A., & Camm, A. J. (2012). Dialysis-dependent changes in ventricular repolarization. Pacing and clinical electrophysiology, 35(6), 703-710.

Haas, E. A. (2018). Sudden unexplained death in childhood: An overview. SIDS sudden infant and early childhood death: the past, the present and the future, 51-72.

Hanna, E. B., & Ahmed, J. (2013). Prolonged QT interval with T-wave alternans: Electrocardiogram-based differential diagnosis. The American journal of the medical sciences, 346(2), 128.

Hayashi, H., Shiferaw, Y., Sato, D., Nihei, M., Lin, S. F., Chen, P. S., ... & Qu, Z. (2007). Dynamic origin of spatially discordant alternans in cardiac tissue. Biophysical journal, 92(2), 448-460.

Hostiuc, S., Curca, G. C., Dermengiu, D., Dermengiu, S., Hostiuc, M., & Rusu, M. C. (2011). Morphological changes associated with hemodynamically significant myocardial bridges in sudden cardiac death. The Thoracic and cardiovascular surgeon, 59(07), 393-398.

Hüser, J., Wang, Y. G., Sheehan, K. A., Cifuentes, F., Lipsius, S. L., & Blatter, L. A. (2000). Functional coupling between glycolysis and excitation—contraction coupling underlies alternans in cat heart cells. The Journal of physiology, 524(3), 795-806.

Iaizzo, P. A. (Ed.). (2009). Handbook of cardiac anatomy, physiology, and devices. Springer Science & Business Media.

Idriss, S. F., & Bell, J. A. (2008). Cardiac repolarization instability during normal postnatal development. Journal of electrocardiology, 41(6), 474-479.

Idriss, S. F., Van Hare, G. F., Fink, D., & Rosenbaum, D. S. (2002). Microvolt T wave alternans inducibility in normal newborn puppies: Effects of development. Journal of cardiovascular electrophysiology, 13(6), 593-598.

Ishikawa, Y., Kawawa, Y., Kohda, E., Shimada, K., & Ishii, T. (2011). Significance of the anatomical properties of a myocardial bridge in coronary heart disease. Circulation Journal, 75(7), 1559-1566.

Jaiswal, A., & Goldbarg, S. (2014). Dofetilide induced torsade de pointes: mechanism, risk factors and management strategies. Indian heart journal, 66(6), 640-648.

Jansen, K., & Lagae, L. (2010). Cardiac changes in epilepsy. Seizure, 19(8), 455-460.

Jansen, K., Varon, C., Van Huffel, S., & Lagae, L. (2013). Peri-ictal ECG changes in childhood epilepsy: implications for detection systems. Epilepsy & Behavior, 29(1), 72-76.

Jezewski, J., Matonia, A., Kupka, T., Roj, D., & Czabanski, R. (2012). Determination of fetal heart rate from abdominal signals: evaluation of beat-to-beat accuracy in relation to the direct fetal electrocardiogram. Biomedical Engineering/Biomedizinische Technik, 57(5), 383-394.

Johannesen, L., Vicente, J., Mason, J. W., Sanabria, C., Waite-Labott, K., Hong, M., ... & Florian, J. (2014). Differentiating drug-induced multichannel block on the electrocardiogram: randomized study of dofetilide, quinidine, ranolazine, and verapamil. Clinical Pharmacology & Therapeutics, 96(5), 549-558.

Kanaporis, G., & Blatter, L. A. (2017). Alternans in atria: Mechanisms and clinical relevance. Medicina, 53(3), 139-149.

Kastellanos, S., Aznaouridis, K., Vlachopoulos, C., Tsiamis, E., Oikonomou, E., & Tousoulis, D. (2018). Overview of coronary artery variants, aberrations and anomalies. World journal of cardiology, 10(10), 127-140.

Klabunde, R. (2011). Cardiovascular physiology concepts. Lippincott Williams & Wilkins.

Kojima, A., Hata, T., Sadanaga, T., Mizutani, Y., Uchida, H., Kawai, Y., ... & Miyata, M. (2018). Maturation of the QT variability index is impaired in preterm infants. Pediatric cardiology, 39(5), 902-905.

Kouidi, E. J., Grekas, D. M., & Deligiannis, A. P. (2009). Effects of exercise training on noninvasive cardiac measures in patients undergoing long-term hemodialysis: a randomized controlled trial. American Journal of Kidney Diseases, 54(3), 511-521.

Kulkarni, K., Merchant, F. M., Kassab, M. B., Sana, F., Moazzami, K., Sayadi, O., ... & Armoundas, A. A. (2019). Cardiac alternans: mechanisms and clinical utility in arrhythmia prevention. Journal of the American Heart Association, 8(21), e013750.

Lande, G., Maison-Blanche, P., Fayn, J., Ghadanfar, M., Coumel, P., & Funck-Brentano, C. (1998). Dynamic analysis of dofetilide-induced changes in ventricular repolarization. Clinical Pharmacology & Therapeutics, 64(3), 312-321.

Lee, M. S., & Chen, C. H. (2015). Myocardial bridging: an up-to-date review. The Journal of invasive cardiology, 27(11), 521-528.

Leoni, C., Marcantoni, I., Sbrollini, A., Morettini, M., & Burattini, L. (2019, June). TWA Identifier for cardiac risk self-monitoring during hemodialysis: A case report. In 2019 IEEE 23rd International Symposium on Consumer Technologies (ISCT) (pp. 143-146). IEEE.

Lewis, T. (1910). Notes upon alternation of the heart. Quart J Med, 4:141-144.

Liu, L., Oza, S., Hogan, D., Chu, Y., Perin, J., Zhu, J., ... & Black, R. E. (2016). Global, regional, and national causes of under-5 mortality in 2000–15: an updated systematic analysis with implications for the Sustainable Development Goals. The Lancet, 388(10063), 3027-3035.

Madias, J. E. (2005). Increases in P-wave duration and dispersion after hemodialysis are totally (or partially) due to the procedure-induced alleviation of the body fluid overload: A hypothesis with strong experimental support. Annals of noninvasive electrocardiology, 10(2), 129-133.

Madias, J. E. (2007). A proposal for a T-wave alternans index. Journal of electrocardiology, 40(6), 479–81.

Madias, J. E. (2010). T-wave alternans in 24-hour ambulatory electrocardiogram monitoring in healthy newborn of first to fourth day of life. Journal of electrocardiology, 3(43), 260.

Makarov, L., & Komoliatova, V. (2010). Microvolt T-wave alternans during Holter monitoring in children and adolescents. Annals of Noninvasive Electrocardiology, 15(2), 138-144.

Makarov, L., Komoliatova, V., Zevald, S., Schmidt, G., Muller, A., & Serebruany, V. (2010). QT dynamicity, microvolt T-wave alternans, and heart rate variability during 24-hour ambulatory electrocardiogram monitoring in the healthy newborn of first to fourth day of life. Journal of electrocardiology, 43(1), 8-14.

Man, S., De Winter, P. V., Maan, A. C., Thijssen, J., Borleffs, C. J. W., van Meerwijk, W. P., ... & Burattini, L. (2011). Predictive power of T-wave alternans and of ventricular gradient hysteresis for the occurrence of ventricular arrhythmias in primary prevention cardioverter-defibrillator patients. Journal of electrocardiology, 44(4), 453-459.

Man, S., Maan, A. C., Schalij, M. J., & Swenne, C. A. (2015). Vectorcardiographic diagnostic & prognostic information derived from the 12-lead electrocardiogram: Historical review and clinical perspective. Journal of electrocardiology, 48(4), 463-475.

Mandala, S., & Di, T. C. (2017). ECG parameters for malignant ventricular arrhythmias: a comprehensive review. Journal of medical and biological engineering, 37(4), 441-453.

Marcantoni, I., Calabrese, D., Chiriatti, G., Melchionda, R., Pambianco, B., Rafaiani, G., ... & Burattini, L. (2019, September). Electrocardiographic alternans: A new approach. In Mediterranean Conference on Medical and Biological Engineering and Computing (pp. 159-166). Springer, Cham.

Marcantoni, I., Cerquetti, V., Cotechini, V., Lattanzi, M., Sbrollini, A., Morettini, M., & Burattini, L. (2018, September). T-wave alternans in partial epileptic patients. In 2018 Computing in Cardiology Conference (CinC) (Vol. 45, pp. 1-4). IEEE.

Marcantoni, I., Di Menna, A., Rossini, F., Turco, F., Morettini, M., Sbrollini, A., Bianco, F., Pozzi, M., & Burattini, L. (2020, September). Electrocardiographic alternans in myocardial bridge: A case report. In 2020 Computing in Cardiology Conference (CinC) (Vol. 47, pp. 1-4).

Marcantoni, I., Di Monte, J., Leoni, C., Mansour, Z., Sbrollini, A., Morettini, M., & Burattini L. (2020, June). Electrocardiographic alternans in hemodialysis: A case report. In 2020 Congress of the National Group of Bioengineering (pp.1-4).

Marcantoni, I., Laratta, R., Mascia, G., Ricciardi, L., Sbrollini, A., Nasim, A., ... & Burattini, L. (2019, July). Dofetilide-induced microvolt T-wave alternans. In 2019 41st Annual International Conference of the IEEE Engineering in Medicine and Biology Society (EMBC) (pp. 95-98). IEEE.

Marcantoni, I., Sbrollini, A., Agostinelli, G., Surace, F. C., Colaneri, M., Morettini, M., ... & Burattini, L. (2020). T-wave alternans in nonpathological preterm infants. Annals of Noninvasive Electrocardiology, 25(4), e12745.

Marcantoni, I., Sbrollini, A., Burattini, L., Morettini, M., Fioretti, S., & Burattini, L. (2018, July). Automatic T-wave alternans identification in indirect and direct fetal electrocardiography. In 2018 40th Annual International Conference of the IEEE Engineering in Medicine and Biology Society (EMBC) (pp. 4852-4855). IEEE.

Marcantoni, I., Vagni, M., Agostinelli, A., Sbrollini, A., Morettini, M., Burattini, L., ... & Burattini, L. (2017, September). T-Wave alternans identification in direct fetal electrocardiography. In 2017 Computing in Cardiology (CinC) (pp. 1-4). IEEE.

Martinez, J. P., Olmos, S., Wagner, G., Laguna P. (2006). Characterization of repolarization alternans during ischemia: time-course and spatial analysis. IEEE Transaction on Biomedical Engineering, 53(4), 701-711.

Maury, P., & Metzger, J. (2002). Alternans in QRS amplitude during ventricular tachycardia. Pacing and clinical electrophysiology, 25(2), 142-150.

McCarron, É. P., Monaghan, M., & Sreenivasan, S. (2019). Images of the month 2: Electrocardiographic QRS alternans caused by gastric volvulus. Clinical Medicine, 19(6), 528-529.

Mironov, S., Jalife, J., Tolkacheva, E., G. (2008). Role of conduction velocity restitution and short-term memory in the development of action potential duration alternans in isolated rabbit hearts. Circulation, 118(1):17-25.

Morales, A. R., Romanelli, R. E. N. Z. O., & Boucek, R. J. (1980). The mural left anterior descending coronary artery, strenuous exercise and sudden death. Circulation, 62(2), 230-237.

Narayan, S. M., Bode, F., Karasik, P. L., & Franz, M. R. (2002). Alternans of atrial action potentials during atrial flutter as a precursor to atrial fibrillation. Circulation, 106(15), 1968-1973.

Nearing B. D., Huang, A. H., Verrier R. L. (1991). Dynamic tracking of cardiac vulnerability by complex demodulation of the T wave. Science, 252(5004), 437-440.

Nearing, B. D., & Verrier, R. L. (2002). Modified moving average analysis of T-wave alternans to predict ventricular fibrillation with high accuracy. Journal of applied physiology, 92(2), 541-549.

Nei, M., Ho, R. T., & Sperling, M. R. (2000). EKG abnormalities during partial seizures in refractory epilepsy. Epilepsia, 41(5), 542-548.

Nishikii-Tachibana, M., Pargaonkar, V. S., Schnittger, I., Haddad, F., Rogers, I. S., Tremmel, J. A., & Wang, P. J. (2018). Myocardial bridging is associated with exercise-induced ventricular arrhythmia and increases in QT dispersion. Annals of Noninvasive Electrocardiology, 23(2), e12492.

Opherk, C., Coromilas, J., & Hirsch, L. J. (2002). Heart rate and EKG changes in 102 seizures: analysis of influencing factors. Epilepsy research, 52(2), 117-127.

Pahlm, O., Haisty Jr, W. K., Edenbrandt, L., Wagner, N. B., Sevilla, D. C., Selvester, R. H., & Wagner, G. S. (1992). Evaluation of changes in standard electrocardiographic QRS waveforms recorded from activity-compatible proximal limb lead positions. The American journal of cardiology, 69(3), 253-257.

Pang, T. D., Nearing, B. D., Krishnamurthy, K. B., Olin, B., Schachter, S. C., & Verrier, R. L. (2019). Cardiac electrical instability in newly diagnosed/chronic epilepsy tracked by Holter and ECG patch. Neurology, 93(10), 450-458.

Parks, S. E., Lambert, A. B. E., & Shapiro-Mendoza, C. K. (2017). Racial and ethnic trends in sudden unexpected infant deaths: United States, 1995–2013. Pediatrics, 139(6), e20163844.

Patel, R. K., Mark, P. B., Halliday, C., Steedman, T., Dargie, H. J., Cobbe, S. M., & Jardine, A. G. (2011). Microvolt T-wave alternans in end-stage renal disease patients—associations with uremic cardiomyopathy. Clinical Journal of the American Society of Nephrology, 6(3), 519-527.

Pavei, J., Heinzen, R. G., Novakova, B., Walz, R., Serra, A. J., Reuber, M., ... & Marques, J. L. (2017). Early seizure detection based on cardiac autonomic regulation dynamics. Frontiers in physiology, 8, 765.

Pishva, N., & Khosrojerdi, H. (2015). A prospective study on QT dispersion in neonates: A new risk factor. Iranian Journal of Medical Sciences, 28(1), 23-25.

Pulignano, G., Patruno, N., Urbani, P., Greco, C., & Critelli, G. (1990). Electrophysiological significance of QRS alternans in narrow QRS tachycardia. Pacing and Clinical Electrophysiology, 13(2), 144-150.

Qu, Z., Xie, Y., Garfinkel, A., & Weiss, J. N. (2010). T-wave alternans and arrhythmogenesis in cardiac diseases. Frontiers in physiology, 1, 154.

Randall, B., Thompson, P., & Wilson, A. (2019). Racial differences within subsets of Sudden Unexpected Infant Death (SUID) with an emphasis on asphyxia. Journal of Forensic and Legal Medicine, 62, 52-55.

Rashba, E. J., Cooklin, M., MacMurdy, K., Kavesh, N., Kirk, M., Sarang, S., ... & Gold, M. R. (2002). Effects of selective autonomic blockade on T-wave alternans in humans. Circulation, 105(7), 837-842.

Rashba, E. J., Osman, A. F., MacMurdy, K., Kirk, M. M., Sarang, S., Peters, R. W., ... & Gold, M. R. (2002). Influence of QRS duration on the prognostic value of T wave alternans. Journal of cardiovascular electrophysiology, 13(8), 770-775.

Rinkenberger, R. L., Polumbo, R. A., Bolton, M. R., & Dunn, M. (1978). Mechanism of electrical alternans in patients with pericardial effusion. Catheterization and cardiovascular diagnosis, 4(1), 63-70.

Rohana, J., Ishak, S., & Wan Nurulhuda, W. M. Z. (2018). Sudden infant death syndrome: Knowledge and practise in parents of preterm infants. Pediatrics International, 60(8), 710-713.

Rosenbaum, D. S., Albrecht, P., & Cohen, R. J. (1996). Predicting sudden cardiac death from T wave alternans of the surface electrocardiogram: promise and pitfalls. Journal of cardiovascular electrophysiology, 7(11), 1095-1111.

Roukoz, H., & Saliba, W. (2007). Dofetilide: a new class III antiarrhythmic agent. Expert review of cardiovascular therapy, 5(1), 9-19.

Schomer, A. C., Nearing, B. D., Schachter, S. C., & Verrier, R. L. (2014). Vagus nerve stimulation reduces cardiac electrical instability assessed by quantitative T-wave alternans analysis in patients with drug-resistant focal epilepsy. Epilepsia, 55(12), 1996-2002.

Schwartz, P. J., Stramba-Badiale, M., Segantini, A., Austoni, P., Bosi, G., Giorgetti, R., ... & Salice, P. (1998). Prolongation of the QT interval and the sudden infant death syndrome. New England Journal of Medicine, 338(24), 1709-1714.

Secemsky, E. A., Verrier, R. L., Cooke, G., Ghossein, C., Subacius, H., Manuchehry, A., ... & Passman, R. (2011). High prevalence of cardiac autonomic dysfunction and T-wave alternans in dialysis patients. Heart Rhythm, 8(4), 592-598.

Sheng, D., & Cheng, X. (2017). Analysis of the QT dispersion and T wave alternans in patients with epilepsy. Yangtze Medicine, 1(2), 109.

Siniorakis, E., Arvanitakis, S., Tzevelekos, P., Giannakopoulos, N., & Limberi, S. (2017). P-wave alternans predicting imminent atrial flutter. Cardiology Journal, 24(6), 706-707.

Smith, J. M., Clancy, E. A., Valeri, C. R., Ruskin, J. N., Cohen, R. J. (1988). Electrical alternans and cardiac electrical instability. Circulation, 77(1), 110-121.

Stafstrom, C. E., & Carmant, L. (2015). Seizures and epilepsy: an overview for neuroscientists. Cold Spring Harbor perspectives in medicine, 5(6), a022426.

Strzelczyk, A., Adjei, P., Scott, C. A., Bauer, S., Rosenow, F., Walker, M. C., & Surges, R. (2011). Postictal increase in T-wave alternans after generalized tonic–clonic seizures. Epilepsia, 52(11), 2112-2117.

Suorsa, E., Korpelainen, J. T., Ansakorpi, H., Huikuri, H. V., Suorsa, V., Myllylä, V. V., & Isojärvi, J. I. (2011). Heart rate dynamics in temporal lobe epilepsy—a long-term follow-up study. Epilepsy research, 93(1), 80-83.

Suszko, A., Nayyar, S., Labos, C., Nanthakumar, K., Pinter, A., Crystal, E., & Chauhan, V. S. (2020). Microvolt QRS alternans without microvolt T-wave alternans in human cardiomyopathy: A novel risk marker of late ventricular arrhythmias. Journal of the American Heart Association, 9(17), e016461.

Thompson, J. M., & Mitchell, E. A. (2006). Are the risk factors for SIDS different for preterm and term infants?. Archives of disease in childhood, 91(2), 107-111.

Tomson, T., Ericson, M., Ihrman, C., & Lindblad, L. E. (1998). Heart rate variability in patients with epilepsy. Epilepsy research, 30(1), 77-83.

Torp-Pedersen, C., Møller, M., Bloch-Thomsen, P. E., Køber, L., Sandøe, E., Egstrup, K., ... & Camm, A. J. (1999). Dofetilide in patients with congestive heart failure and left ventricular dysfunction. New England Journal of Medicine, 341(12), 857-865.

Tse, G., Wong, S. T., Tse, V., Lee, Y. T., Lin, H. Y., & Yeo, J. M. (2016). Cardiac dynamics: alternans and arrhythmogenesis. Journal of Arrhythmia, 32(5), 411-417.

Tsiaousis, G., & Fragakis, N. (2016). P-wave alternans in a patient with hyponatremia. Hellenic Journal of Cardiology, 57(3), 188-190.

Verrier, R. L., & Nieminen, T. (2010). T-wave alternans as a therapeutic marker for antiarrhythmic agents. Journal of cardiovascular pharmacology, 55(6), 544-554.

Verrier, R. L., Nearing, B. D., Olin, B., Boon, P., & Schachter, S. C. (2016). Baseline elevation and reduction in cardiac electrical instability assessed by quantitative T-wave alternans in patients with drug-resistant epilepsy treated with vagus nerve stimulation in the AspireSR E-36 trial. Epilepsy & Behavior, 62, 85-89.

Verrier, R. L., Pang, T. D., Nearing, B. D., & Schachter, S. C. (2020). The Epileptic Heart: concept and clinical evidence. Epilepsy & Behavior, 105, 106946.

Walker, M. L., & Rosenbaum, D. S. (2003). Repolarization alternans: implications for the mechanism and prevention of sudden cardiac death. Cardiovascular research, 57(3), 599-614.

Wolbrette, D. L., Hussain, S., Maraj, I., & Naccarelli, G. V. (2019). A quarter of a century later: What is dofetilide's clinical role today?. Journal of cardiovascular pharmacology and therapeutics, 24(1), 3-10.

Yu, S., Van Veen, B. D., & Wakai, R. T. (2013). Detection of t-wave alternans in fetal magnetocardiography using the generalized likelihood ratio test. IEEE Transactions on Biomedical Engineering, 60(9), 2393-2400.

Yuan, S. M. (2016). Myocardial bridging. Brazilian journal of cardiovascular surgery, 31(1), 60-62.

Zareba, W., Moss, A. J., le Cessie, S., & Hall, W. J. (1994). T wave alternans in idiopathic long QT syndrome. Journal of the American College of Cardiology, 23(7), 1541-1546.

Zhao, H., Strasburger, J. F., Cuneo, B. F., & Wakai, R. T. (2006). Fetal cardiac repolarization abnormalities. The American journal of cardiology, 98(4), 491-496.

ABBREVIATIONS AND SYMBOLS*

AAm: alternans amplitude (average over all electrocardiogram heartbeats)

A_{AMFM}: local alternans amplitude by adaptive match filter (on each heartbeat)

AAr: alternans area (average over all electrocardiogram heartbeats)

ACI: alternans correlation index

A_{CM}: local alternans amplitude by correlation method (on each heartbeat)

AMFM: adaptive match filter method

APos: position of alternans (average over all electrocardiogram heartbeats)

CM: correlation method

EAMFM: enhanced adaptive matched filter method

ECG: electrocardiogram

ECGA: electrocardiographic alternans

iqr: interquartile range

NHB: number of heartbeats (included in electrocardiographic tracing/window)

NRHB: number of replaced heartbeats (in electrocardiographic tracing/window)

NS: number of seconds (seconds between starting time instants of two consecutive electrocardiographic tracings/windows)

p: statistical significance level

PWA: P-wave alternans

QRSA: QRS-complex alternans

SCD: sudden cardiac death

SIDS: sudden infant death syndrome

SNR: signal to noise ratio

SUDEP: sudden unexpected death in epilepsy

TWA: T-wave alternans

ε: error

* Parameters specifically defined (and quantified) in clinical studies reported in the thesis are not present in this list, which instead explains the meaning of acronyms and symbols used through all the text.